

Effects of chlorpyrifos, an organophosphate pesticide on the intestinal barrier of Atlantic salmon (*Salmo salar*)

Iresha Chavindi Fernando



Master Thesis in Environmental Toxicology

University of Bergen, Norway

Department of Biological Sciences

February 2021

Acknowledgements

First and foremost, I would like to show my uttermost gratitude to my supervisors. A huge thanks my main supervisor Øystein Sæle for giving me the opportunity to take part in the “gut matters” project at IMR. Thanks for your guidance and encouragement throughout the year. A special thanks to my co supervisor Anders Goksøyr for the help and guidance in toxicology.

Also, a huge thanks to Chandru, who was always there for me to answer my questions about my project. I would also like to thank Eva Mykkeltvedt and Hui-Shan Tung for the help and guidance in the molecular lab. Moreover, thanks to Maren hoff Austgulen for helping me in the cell lab with the RTgutGC cell line. Thanks to Hoang Le for sharing your experience and helping me with the in vitro gut sac model.

Thank you to all my fellow study colleagues Ana, Sahar, Angela, Amalie, Madushi, Alice and Kjersti who helped me get the year with tea breaks and many unforgettable memories. I am gonna miss you all.

And I am so thankful to my wonderful boyfriend Andreas Hagen. Thank you for helping me with the statistical analysis and for your incredible knowledge about Python. Writing this thesis would have not been possible without you. You are my rock!

At last, I would also like to thank my parents, parents in law and my awesome friends who have encouraged me and supported me through this journey.

Abbreviations

Abbreviations	Full words
AChE	Acetylcholinesterase
AhR	Aryl hydrocarbon receptor
AJ	Adherens junction
ANOVA	Analysis of Variance
ARNT	Arylhydrocarbon receptor nuclear translocator
ATP	Adenosine triphosphate
BMC	Benchmark concentration
BMR5	Benchmark concentration response 5%
CI	Cell index
CPF	Chlorpyrifos
CPM	Chlorpyrifos-methyl
CYP1A	Cytochrome P450 1A
CYP3A	Cytochrome P450 3A
DMSO	Dimethyl sulfoxide
ER	Endoplasmic reticulum
FITC-D	Fluorescein isothiocyanate–dextran
FM	Fish meal
GST	Glutathione S-transferase
LC50	Lethal concentration 50%
LD	Lipid droplet
LD50	Lethal dose 50%
LOAEL	Lowest-observed-adverse-effect level
LPC	Lysophosphatidylcholine
LPCAT2	Lysophosphatidylcholine acyltransferase
NOAEL	No-observed-adverse-effect level

P _{app}	Apparent permeability
PBS	Phosphate buffered saline
PCB	Polychlorinated biphenyls
PLIN2	Perilipin 2
PPARA	Peroxisome Proliferator Activated Receptor Alpha
PXR	Pregnane X receptor
qPCR	Quantitative polymerase chain reaction
ROS	Reactive oxygen species
RT	Reverse transcriptase
RTCA	xCELLigence Real Time Cell Analysis
RXR	Retinoid x receptor
SBM	Soybean meal
SD	Standard deviation
TAG	Triacylglycerol
TEER	Transepithelial electrical resistance
TJ	Tight junction
UGT	UDP-glucuronosyltransferases
XRE	Xenobiotic response element
ZO	Zonula occludens

Table of Contents

Acknowledgements.....	
Abbreviations	
1. Abstract	
2. Introduction	1
2.1 Aquaculture.....	1
2.1.1 Fish feed and fish nutrition	2
2.2 Pesticides.....	3
2.2.1 Pesticide exposure and toxicity in fish	4
2.2.2 Chlorpyrifos.....	6
2.2.3 Saponin	7
2.3 The intestinal barrier.....	7
2.3.1 Gut permeability	10
2.3.2 Intestinal response to xenobiotics/pesticides	10
2.3.3 Metabolism of xenobiotics	11
2.3.4 Pesticides and lipid metabolism.....	13
2.4 Aims.....	15
3. Materials	17
3.1 Chemicals	17
3.2 Kits.....	18
3.3 Equipment.....	19
3.4 Instruments	19
3.5 Software	20
3.6 Solutions.....	20
3.6.1 Ringer’s solution.....	20
3.6.2 Toluidine Blue Staining.....	21
3.6.3 Cell growth media	21
3.6.4 cDNA reaction mix	21
3.6.5 SYBRGreen reaction mix	22
3.6.6 One step qPCR.....	22
3.7 Primers	23

4. Method.....	24
4.1 Species and maintenance	24
4.2 Exposure design	24
4.3 The gut sac model	25
4.3.1 Apparent permeability.....	27
4.4 Histology	28
4.4.1 Pre infiltration	28
4.4.2 Infiltration	28
4.4.3 Polymerization and embedding.....	29
4.4.4 Mounting.....	29
4.4.5 Microtome sections	29
4.4.6 Staining.....	29
4.5 Cell line.....	30
4.6 Cell culture	30
4.7 Measurement of transepithelial electrical resistance	31
4.7.1 Exposure.....	31
4.8 Real - time quantitative PCR	32
4.8.1 Pesticide exposure	32
4.8.2 RNA extraction	32
4.8.3 Quality of RNA.....	33
4.8.4 cDNA synthesis.....	33
4.8.5 Primer test - One step qPCR.....	34
4.8.6 Agarose gel electrophoresis.....	35
4.8.7 Real time quantitative PCR	35
4.8.8 Primer design	36
4.9 Xcelligence	36
4.10 Statistics	37
5. Results	38
5.1 General health.....	38
5.2 Soya saponin exposure	38
5.3 Apparent permeability.....	39
5.4 Histology	41
5.5 Cytotoxicity assay.....	45

5.6 Transepithelial electrical resistance	48
5.6.1 Effects of chlorpyrifos on the transepithelial electrical resistance	49
5.7 Gene expression.....	51
5.7.1 Transcription of genes involved in detoxification	51
5.6.2 Transcription of genes involved in lipid metabolism	52
6. Discussion.....	54
6.1 Saponin showed no effects on fish intestine	54
6.2 Increased permeability is not seen in guts exposed to chlorpyrifos	56
6.3 Cytotoxicity of chlorpyrifos	58
6.3.1 ANOVA vs Regression model.....	59
6.4 TEER over time	60
6.5 TEER after chlorpyrifos exposure	61
6.6 Effects of chlorpyrifos on the genes involved in detoxification	62
6.6.1 <i>cyp1a</i> expression.....	62
6.6.2 <i>cyp3a</i> expression.....	63
6.6.3 <i>gst</i> and <i>ugt</i> expression	64
6.7 Effects of chlorpyrifos on the genes involved in lipid metabolism	65
7. Conclusion.....	66
8. Further perspectives	66
9. References.....	68
10. Appendix	80

1. Abstract

Aquaculture is the fastest growing food producing sector worldwide. The decline in capture fisheries has led to a decrease in fish oil and fish meal production. Due to this decline, there is a need for alternative lipid and protein sources in fish feed. Lipid and protein sources of plant origin has been increasingly replacing fish ingredients. Today fish feed typically contains about 70 % plant ingredients. Replacement of plant ingredients has reduced hazardous environmental contaminants such as dioxins and polychlorinated biphenyls (PCBs) in fish feed. However, it has also been introduced new undesirable substances, such as chlorpyrifos (CPF) which is an organophosphate pesticide.

In this study the effects of CPF were investigated on intestinal permeability of Atlantic salmon. Apparent permeability was measured on the mid intestinal section of fish injected with 500 μ M CPF for 3 hours, using the gut sac model. Furthermore, an intestinal cell line (RTgutGC) derived from rainbow trout was also used as an in vitro model for Atlantic salmon. The transepithelial electrical resistance (TEER) was measured in cells exposed to 0.5 – 500 μ M CPF for 24 hours. The transcriptional levels of several genes involved in detoxification and lipid metabolism was also quantified with the same dose range of CPF exposed to 24 hours, with real-time PCR. Cytotoxicity was determined by the xCELLigence system in cells exposed to 0.05 – 500 μ M CPF for 24 hours.

Results from the gut sac model showed that CPF had no effect on the intestinal permeability and histological evaluation showed no inflammation in the epithelium. High TEER values indicated increased permeability of cells exposed to high concentrations of CPF. Most of the studied genes did not respond to CPF, but a downregulation of genes was seen when cells were exposed to high concentrations of CPF. xCELLigence system showed that cells exposed to CPF concentrations of 50 μ M and upwards induce cytotoxicity.

In conclusion the gut sac model showed no effects of CPF at 500 μM on the intestinal sac of fish while the RTgutGC cell line model showed the CPF at 500 μM was highly toxic to CPF inducing 100 % cell death. The difference in the CPF toxicity at 500 μM may be explained by duration of the exposure period, differences between the model systems and species differentiation. Further research is required to investigate whether the RTgutGC cell model is good in vitro model for salmon when studying the effects of CPF.

2. Introduction

2.1 Aquaculture

Aquaculture, defined by FAO, 1988 is the farming of aquatic organisms including fish, mollusks, crustaceans and aquatic plants. It is now the fastest growing food-producing sector worldwide. The global fish production is estimated to have reached about 179 million tonnes in 2018 and aquaculture fish production accounted for 46 percent of this total fish production (FAO,2020). Since 1999 the growth of the global aquaculture production has been increasing, while the growth of global capture fisheries has been relatively stable (FAO, 2020). Aquaculture production has been dominated by Asia with an 89% share in the last two decades (FAO,2020). China being the major aquaculture producing country, a significant share of this production also comes from India, Indonesia, Vietnam, Bangladesh, Egypt, Norway and Chile (FAO,2020).

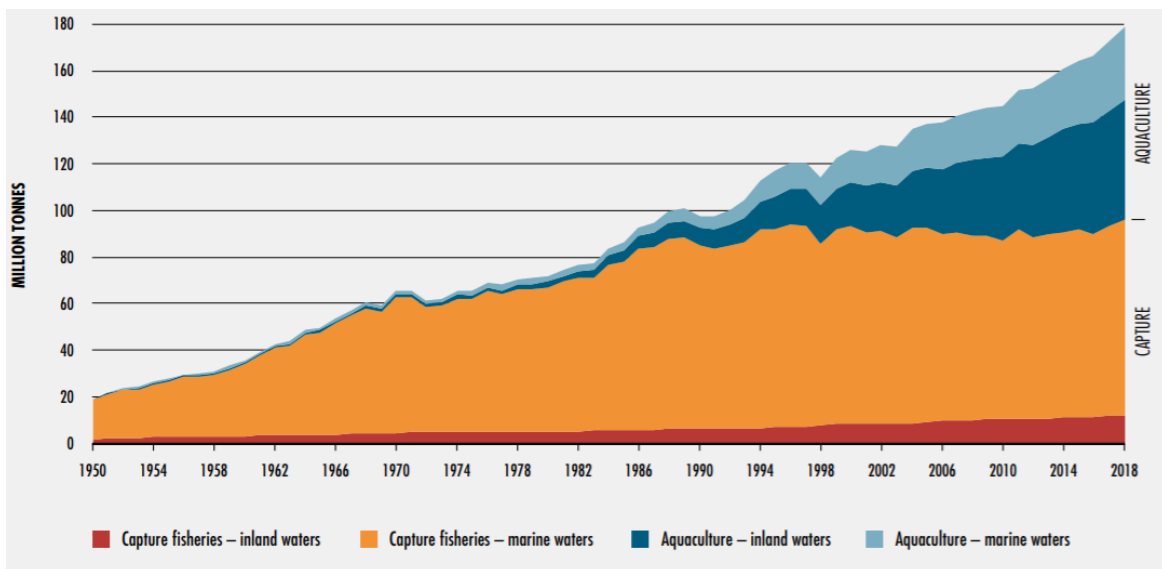


Figure 2.1 Global capture fisheries and aquaculture production, excluding aquatic mammals, crocodiles, alligators and caimans, seaweeds and other aquatic plants (FAO,2020).

Aquaculture plays an important role in food production, economic development, and food security. The growth of aquaculture will have to continue to meet the increasing demand for fish. Growth without proper planning and management would not be sustainable and therefore need to be improved significantly (Lin, 2004). The aquaculture sector is being heavily criticized for alteration or destruction of natural habitats, introduction and transmission of aquatic animal diseases and degrading the aquatic environment through the release of uneaten food, waste products and pharmaceuticals (Bashir et al., 2020). Proper local, national and international planning and management will improve the production, efficiency and environmental sustainability of the sector allowing it to develop (Lin, 2004).

2.1.1 Fish feed and fish nutrition

Fish feed is the most important and the first major step in modern aquaculture production chain (Cho, 1990; Craig, 2009; Maage et al., 2008). In cultured fish where natural food is absent or where they make a small contribution to the nutrition of the fish, the feed should be nutritionally complete. Fish feeds, in the form of granules or pellets provides the sufficient nutrition needed by the fish (Cho, 1990). A good nutritious feed will strengthen the fishes immune defense, health, welfare, and development, producing a healthy high-quality product (Bhosale et al., 2010).

The production of fish feed is mainly targeted at carnivorous species such as salmonids, cod, bass and bream (Maage et al., 2008). These species require a protein rich diet, of which fish meal and fish oil traditionally have been the most important and the main components (Bhosale et al., 2010; Pettersson, 2010). Due to the decline in capture fisheries, fish oil and meal production has been stagnating. For this reason, there is a need for alternative lipid/protein sources to guarantee the future growth of the industry (Yıldız et al., 2018).

Lipid and protein sources of plant origin are increasingly being used in aquaculture feed production. Due to its increased production, low cost and sustainability, plant products make a good candidate for replacing fish ingredients (Ayisi et al., 2019; Sales & Glencross, 2011; Sørensen et al., 2011). Today fish feed typically contains about 70 % plant ingredients (Ytrestøyl et al., 2015). Soybean meal, sunflower meal, pea protein concentrate, wheat and corn gluten are currently

been used as plant protein in Norwegian aquaculture (Sørensen et al., 2011). Rapeseed oil is the main plant oil that is used at present. However palm and soybean oil may also be used (Sørensen et al., 2011).

Vegetable oils contains n-6 and n-9 polyunsaturated fatty acids (PUFA) in abundance (Ayisi et al., 2019; Craig, 2009). In contrast to fish oils, vegetable oils lack n-3 highly unsaturated fatty acids which are known to have a variety of health benefits for humans (Craig, 2009). Replacement of fish oils with vegetable oils has therefore led to the reduction of n-3 fatty acids which reduces the nutritional quality of the fish, which may have a negative impact on human nutrition (Ayisi et al., 2019; Pettersson, 2010; Yıldız et al., 2018).

Plant ingredients in fish feed have not shown negative effects on growth, performance, survival and feed utilization (Menoyo et al., 2005; Ye et al., 2019). Replacement of marine fish oil with plant oil has reduced the levels of hazardous environmental contaminants such as dioxins and PCBs in fish feed (Berntssen et al., 2010). However, this substitution has also introduced new undesirable substances in the feed (Søfteland et al., 2014).

2.2 Pesticides

Pesticides are chemical and biological compounds used mainly on agricultural lands to prevent, destroy, and control unwanted organisms also known as pests (Biscaldi et al., 1986). Pesticides can be categorized into several groups depending on their target organisms. These include insecticides, fungicides, nematocides, molluscicides, rodenticides, plant growth regulators and others (Pang, 2018). Pesticides play an important role in agriculture. Although they prevent large crop losses, enhance economic potential by increasing the production of food and eradicate vector borne diseases, they also disrupt the natural aquatic ecosystem (Aktar et al., 2009). Pesticides enter the aquatic environment unintentionally. They are washed off from land through rain fall, spray drifts, irrigation and drainage into rivers, streams and eventually the ocean (Stanley et al., 2016). Pesticides are designed to be highly specific for undesirable targets. However not all pesticides are highly selective and may be toxic to non-target organisms, including humans

(Casarett et al.,1996). The wide spread use of pesticides have resulted in low levels of pesticide residues in food and drinking water causing increasing concern for the possible treats to human health (Adedeji & Okocha, 2012).

2.2.1 Pesticide exposure and toxicity in fish

Aquatic toxicology is referred to as the study of effects of environmental contaminants on aquatic organisms (Helfrich et al., 2009; Srivastava et al., 2016). In all parts of the world pesticides have been found in the aquatic ecosystem and have become a global problem (Adedeji & Okocha, 2012; Sabra et al., 2015). Unlike other non-target organisms fish and aquatic organisms are being constantly exposed to pesticides, since they live and breathe under water (Stanley et al., 2016). Due to this reason pesticides have been found to be highly toxic to aquatic lifeforms. It is unlikely that pesticides levels in the ocean will exceed those in freshwater, as the dilution in the ocean would likely result in concentrations less than those in rivers and streams (Ernst, 1980; Giesy et al., 1999).

Fish are mainly exposed to pesticides in three primary ways, 1) dermally, direct absorption through skin, 2) inhalation, direct uptake of pesticides through gills or 3) orally, drinking/ingestion of contaminated water/food(Helfrich et al., 2009; Sabra et al., 2015). Some chemicals may be highly toxic by one route but not others. The degree of a toxic response of a substance can vary substantially depending on factors like exposure route, duration, dosage, physiological properties of the compound, species, and individual sensitivity (Helfrich et al., 2009; Sabra et al., 2015). A dose is referred to as the amount of a toxic compound entering an organism, expressed as mg/kg (Helfrich et al., 2009).

The dose causing 50% lethality in a test animal population is called LD50 (lethal dose 50%). The smaller the value of LD50 the more potent (more toxic) is the chemical (Casarett et al., 1996). LC50 stands for lethal concentration 50% is used for the concentration of a chemical in air or in aqueous solution (Casarett et al., 1996). When a chemical causes a defined form of toxicity there exists a dose below which no observable effect occurs, called the threshold. The highest dose at

which no toxic effect is seen is called no observable effect level (NOEL) and the lowest dose at which there was an observed toxic or adverse effect is called lowest observed adverse effect level (LOAEL) (Casarett et al., 1996). These important toxicological concepts are used to derive quantitative estimates of toxicity of chemical substances in dose response curves.

Pesticide toxicity to fish has been investigated in several studies. Pesticides effect on fish may be anything from acute mortality to sublethal effects. Chronic (continuous, long term) exposure to low concentrations of pesticides may cause diverse effects such oxidative damage, inhibition of acetylcholine esterase (AChE) activity, histopathological changes, developmental changes, reproduction, mutagenesis and carcinogenicity (Adedeji & Okocha, 2012; Sunanda et al., 2016).

Pesticide exposure to fish and other aquatic organisms depends on its bioavailability, bioconcentration, biomagnification and persistence in the environment (Helfrich et al., 2009; Sabra et al., 2015; Stanley et al., 2016). Bioaccumulation is defined as the uptake, storage and accumulation of contaminants in organisms from their environment (Segner, 1998), and it occurs when an organism absorbs a substance at a rate faster than that at which the substance is lost. Many pesticides are lipid- soluble and accumulate in fatty tissue of living organisms and biomagnified up the food web (Stanley et al., 2016). Exposure to many pesticides may lead to chemical interactions between them that increase their toxicity (Stanley et al., 2016).

2.2.2 Chlorpyrifos

Chlorpyrifos (O,O-diethyl-O-3,5,6-trichlor-2-pyridyl phosphorothioate, CPF) is an organophosphate insecticide which is used to control a wide range of pests on agricultural and animal farms. CPF was developed by Dow chemicals in 1962 and was first registered for the use in 1965 (Dow & Company, 2011). CPF was banned in the European union since January 2020 due to its harmful effects on the brains of fetus and young children (EFSA, 2019; Hites, 2021) but it's still widely used in other parts of the world (Dow & Company, 2011).

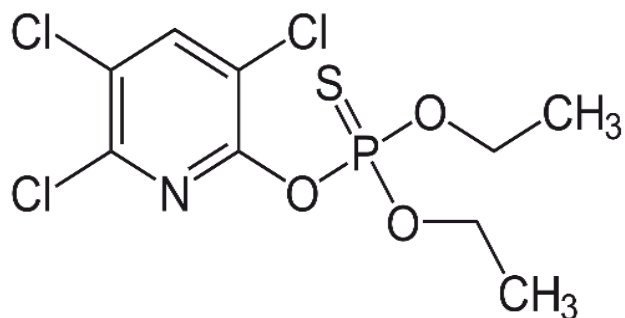


Figure 2.2.2 Chemical structure of Chlorpyrifos

Several studies have shown that waterborne CPF bioaccumulates and is toxic to fish (Schimmel et al., 1983; Yen et al., 2011). The mode of action of CPF is similar for both target and non-target organisms. CPF affects the normal function of the nervous system by inhibiting the breakdown of AChE in nerve cells (Giesy et al., 1999). This leads to an increasing level and duration of action of the ACh action in the central nervous system. The resulting accumulation of ACh causes overstimulation of the neuronal cells, which leads to neurotoxicity and eventually death. Secondary toxic effects of CPF can induce morphological, neurobehavioral, oxidative, biochemical, histopathological, haematological, endocrine disruption, immunotoxicity and developmental alterations (Deb & Das, 2013; Sunanda et al., 2016; Xing et al., 2015; Yen et al., 2011).

Although CPF is readily absorbed by most organisms, they are subjected to rapid metabolism and are easily excreted. Therefore, CPF has a low bioaccumulation and biomagnification potential compared to many persistent organic pollutants (Racke et al., 2002; Varó et al., 2002).

2.2.3 Saponin

The use of plant ingredients in fish feed has introduced a wide variety of antinutritional substances. Antinutrients are naturally occurring compounds that interfere with nutrition absorption in the body (Francis et al., 2001).

Saponins are amphiphilic molecules that consist of a sugar moiety linked to steroid or triterpenoid aglycone (Knudsen et al., 2008). They have the ability to form stable soap like foams in aqueous solutions, hence the name (Francis et al., 2002). They can be found in wild plants and in cultivated crops such as soybean, pea and lupin (Min Gu et al., 2014; Krogdahl et al., 2010). Saponins are considered to be involved in plants defense system against microbial and insect attack (Knudsen et al., 2008; Sparg et al., 2004). Previous studies have showed saponins from soybean meal are responsible for inducing enteritis in the distal intestine of Atlantic salmon (Knudsen et al., 2007, 2008).

2.3 The intestinal barrier

The intestinal tract forms the largest and the most important barrier that separates the external environment from the internal (Groschwitz & Hogan, 2009; Martin et al., 2016).

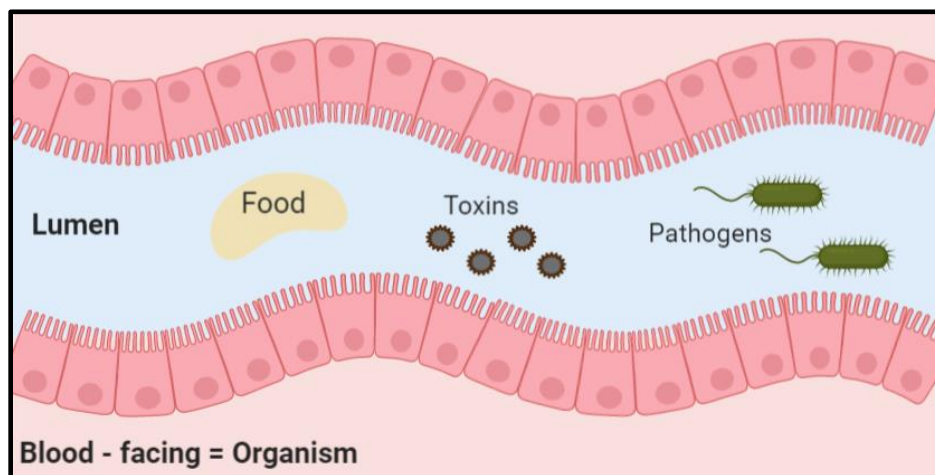


Figure 2.3.1 The intestinal epithelium barrier, that separates the external environment (luminal contents) from the internal. (Created in Biorender)

The mucosal barrier can be roughly divided into three components: mucus layer, intestinal epithelium and the immunological barrier (Camilleri et al., 2019; Jutfelt, 2011). The mucus layer is composed of glycoproteins called mucins secreted by goblet cells (Jutfelt, 2011). Mucus aids the transport of small molecules and prevents the entry of microbiota and large molecules into the epithelium (Farré et al., 2020). It also protects the epithelium from digestive enzymes and serves as a lubricant (Farré et al., 2020).

The intestinal epithelium lies beneath the mucus layer which forms a continuous and polarized barrier. It is composed of different types of specialized cells such as enterocytes, goblet cells, immune and endocrine cells (Jutfelt, 2011). Enterocytes are the most abundant cell type in the epithelium, where they maintain the epithelial barrier integrity and plays a major role in nutrient uptake (Jutfelt, 2011).

The intestinal epithelium allows the permeability of essential dietary nutrients, electrolytes, and water (Martin et al., 2016; Peterson & Artis, 2014). Apart from nutrients, the mucosa also faces exterior antigens such as, pathogen and toxins. Uncontrolled passage of these harmful substances across the epithelium can cause inflammatory responses (Ašmonaite et al., 2018; Groschwitz & Hogan, 2009; Knudsen et al., 2008; Sundh & Sundell, 2015). Thus, the intestinal epithelium also maintains an effective defense against these by limiting the permeation (Martin et al., 2016).

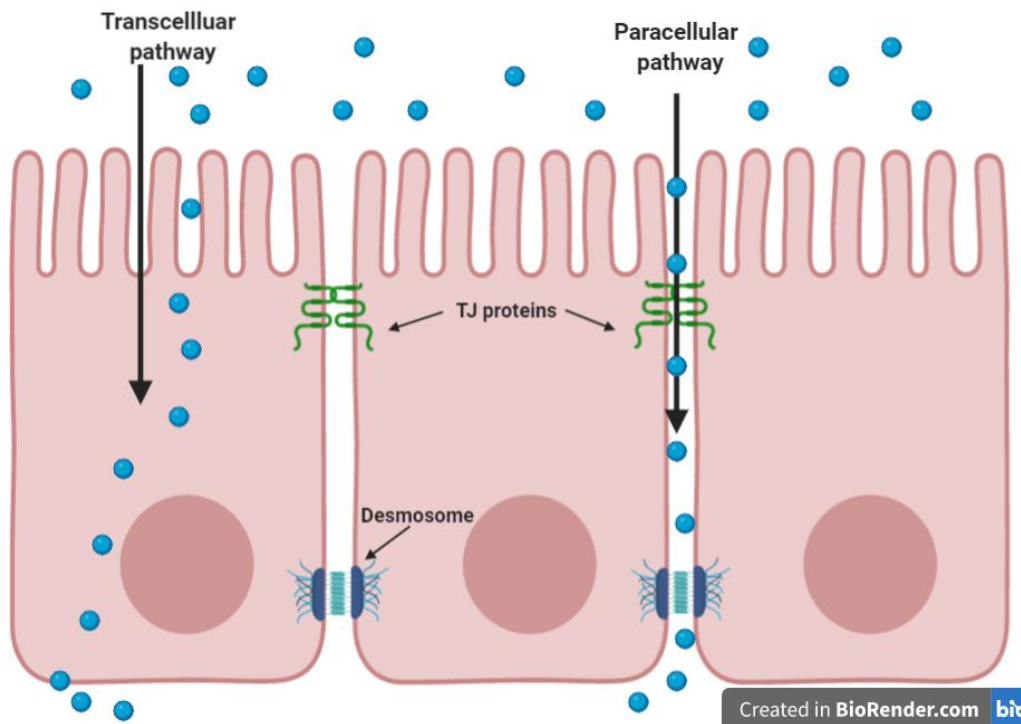


Figure 2.3.2 Paracellular and transcellular transport in the intestinal epithelium. The enterocytes form a polarized single cell layer. The apical side, characterized with villi, is in contact with the intestinal lumen. The epithelial cells are tied together by the TJ, AJ (not shown) and desmosomes. Transcellular transport is mediated by solute transport across the membrane and paracellular pathway is mediated by transport of compounds through the intercellular epithelial cell spaces. (Created in Biorender)

Permeation of luminal products across the epithelial barrier has several pathways depending on the size, hydrophobicity, and other chemical characteristics (Martin et al., 2016). Transcellular pathway is associated with the transport of small hydrophilic and lipophilic compounds across the plasma membrane of the enterocyte (Chelakkot et al., 2018). The paracellular pathway is associated with the transport of compounds through the intercellular epithelial cell spaces, regulated by apical junctional complex made up of adherens junctions (AJ) and tight junctions (TJ) (Stewart et al., 2017). AJs and desmosomes provide strong connective bonds between the epithelial cells (De Santis et al., 2015; Groschwitz & Hogan, 2009). TJs provide mechanical links

between cells whose function is to prevent free passage of ions and small solutes through the space between the cells (Groschwitz & Hogan, 2009).

2.3.1 Gut permeability

Increased gut permeability results in the translocation of luminal contents to the inner layers of the intestinal wall (Bischoff et al., 2014). Increased permeability can occur through increased tight junction permeability, or through disruption of the epithelial monolayer (Jutfelt, 2006; Knudsen et al., 2008).

Tight junctions consist of transmembrane proteins including occludens, claudins and junctional adhesion molecules. They link adjacent cells to actin cytoskeleton through scaffolding proteins like zonula occludens (ZO) (Groschwitz & Hogan, 2009; Stewart et al., 2017). Structural abnormalities or disruption to these proteins may cause severe leakage (Bischoff et al., 2014; Stewart et al., 2017).

Numerous factors can alter intestinal permeability such as gut microbiota modifications, mucus layer alterations and epithelial damage (Bischoff et al., 2014). Other evidences indicates that various chemicals, including food contaminants and additives may disrupt the epithelial barrier and increase permeability (Gillois et al., 2018).

2.3.2 Intestinal response to xenobiotics

Xenobiotics are chemical compounds (such as drugs, pesticides) that are foreign to a living organism (Grace et al., 2012). In order to be absorbed and transferred to the whole body xenobiotics must first pass through the epithelium (Grace et al., 2012). Xenobiotics are not absorbed through any special transport process but share the same transport process as nutrition absorption (Grace et al., 2012). Xenobiotics cross the luminal membrane through various mechanisms that involve passive diffusion or active transport (Gelberg, 2018; Grace et al., 2012).

Transport facilitated by passive diffusion is the major route of xenobiotic absorption (Gelberg, 2018; Grace et al., 2012). The rate of passive diffusion is determined by the concentration gradient across the cell membrane, lipid solubility, molecular size and the electrical charge associated with the molecule (Brock & Hobson, 2007; Gelberg, 2018). Xenobiotics with high lipid solubility are readily absorbed and non-ionized molecules diffuse more readily across the cell membrane than highly ionized substances (Brock & Hobson, 2007; Gelberg, 2018).

Active transport is the movement of substance through the membrane against the concentration gradient. This process requires cellular energy from ATP. Active transport mainly exists for transfer of natural substances such as amino acids, sugars, bile acids etc (Grace et al., 2012). Xenobiotics that are structurally similar to these natural substances compete for a transporter protein, to be transported across the cell membrane. For example 5-fluorouracil and 5-bromouracil are actively transported across the rat intestinal epithelium by the process through which natural pyrimidines, uracil and thymine are absorbed (Brock & Hobson, 2007).

Large molecules that cannot enter the cell via passive or active transport may still enter by a process known as endocytosis (phagocytosis and pinocytosis) (Brock & Hobson, 2007; Gelberg, 2018; NIH & NLM, 2016). In this process the cell surrounds the molecule by invagination to form a vesicle which then will be moved to the interior of the cell.

2.3.3 Metabolism of xenobiotics

Xenobiotic metabolism is the process of converting lipophilic compounds into excretable hydrophilic compounds. Detoxification enzyme activities are highest in the liver and are higher in terrestrial than in aquatic organisms (Nikinmaa, 2014). The reason for this is because free diffusion of molecules out of the organism is possible for aquatic but not for the terrestrial organisms. (Nikinmaa, 2014). Biotransformation of xenobiotics are classified in to two essential phases known as phase I and phase II (Beiras, 2018). Phase I reactions transform lipophilic xenobiotics to more polar products via oxidation, reduction, and hydrolysis reactions (Brock & Hobson, 2007). Small polar groups are either exposed (“unmasked”) or added to the xenobiotic,

during phase I biotransformation (Gerba, 2019). Xenobiotics that have undergone phase I biotransformation will either be transported out of the cell (phase III) and excreted from the body or undergo further biotransformation by phase II reactions (Beiras, 2018; Gerba, 2019).

Cytochrome P450s (CYP) are the most important group of enzymes in the liver that catalyze the oxidative metabolism of a wide range of foreign compounds (Meucci & Arukwe, 2006; Topic Popovic et al., 2012). Specially CYP1A, which is a subfamily of CYP has attracted particular attention because of its role in biotransformation (Meucci & Arukwe, 2006). The transcriptional activation of *cyp1a* is mediated through the aryl hydrocarbon receptor (AhR). AhR is a ligand-activated transcription factor that resides in the cytosol along with its associated proteins. When a xenobiotic binds to AhR it dissociates its proteins and translocate into the nucleus, where it forms a dimer with aryl hydrocarbon receptor nuclear translocator (ARNT). This AhR/ARNT dimer binds to the xenobiotic-response element (XRE) in the promoter region of the DNA where it induces the transcription of *cyp1a*. The *cyp1a* mRNA travels to the cytoplasm and induces translation of CYP1A (Beiras, 2018; Nikinmaa, 2014).

However, it has been established that CYP3A is the major phase I enzyme in the intestine of most mammals and other species, including fish (Husoy et al., 1994; Schlenk et al., 2008). In contrast to *cyp1a*, *cyp3a* induction by xenobiotics is largely dependent on the pregnane X receptor PXR, which regulates the *cyp3a* expression by binding as a heterodimer with retinoid X receptor (RXR) to several promoter regions of DNA (Istrate et al., 2010; Willson & Kliewer, 2002).

Occasionally, detoxification of xenobiotics through the phase I pathway does not occur. One possible reason might be that the toxic compound has a high molecular weight (> 800) (Nikinmaa, 2014). In some cases, biotransformation produced metabolites are more toxic than the parent compound, a process called bioactivation (Gerba, 2019). Another possibility is that reactive oxygen species (ROS) are produced in phase I biotransformation reactions, that may react with cellular macromolecules like DNA (Nikinmaa, 2014; Sabra et al., 2015). This can lead to serious health effects such as cancer or birth defects.

Xenobiotics that have undergone phase I reactions produce new intermediate metabolites that contain a reactive chemical group such as hydroxyl, —OH; amino, —NH₂; or carboxyl, —COOH (Gerba, 2019; NIH & NLM, 2016). These metabolites do not possess sufficient hydrophilic properties to permit elimination from the body and therefore undergoes Phase II biotransformation (Gerba, 2019).

Phase II reactions are referred to as conjugation reactions that add polar functional groups to phase I metabolites (Beiras, 2018). The resulting conjugate metabolite is more water soluble than the original toxicant or phase I metabolite, thus facilitating excretion. In some cases, the xenobiotic already has a functional group that can be conjugated, and it can be bio transformed by a Phase II reaction without going through a Phase I reaction (NIH & NLM, 2016). There are three major conjugation pathways and the conjugating enzymes that are involved in these pathways are UDP-glucuronosyltransferases (UGT) , sulfotransferases (SULT), and glutathione- S-transferases (GST) (Gerba, 2019). These enzymes are normally located in close proximity to phase I enzymes, which speeds up the whole biotransformation (Nikinmaa, 2014).

2.3.4 Pesticides and lipid metabolism

One major nutrient group that gets absorbed by enterocytes, are lipids. Dietary fat comprises a variety of lipids such as non-polar lipids, triacylglycerols (TAGs) and cholesterol esters, and phospholipids(PL) (Ko et al., 2020). Triacylglycerol is a major lipid class in the diet of marine fish and is generally the predominant lipid class in the diet of freshwater fish (Tocher, 2003). In many fish species TAG is hydrolyzed by bile salt activated lipase (BAL), to free fatty acids and monoacylglycerols (Sæle et al., 2018). These digested lipids are taken up by enterocytes, mostly by passive diffusion but also by transporters (Beilstein et al., 2016). For example long chained fatty acids are transported via the active transport and short fatty acid chains are absorbed by diffusion (Sæle et al., 2018).

Inside the enterocyte, the digested lipids are resynthesized to TAGs and phospholipids at the endoplasmic reticulum (ER) (Beilstein et al., 2016). In mammals the resynthesized lipids in the ER

membrane have two fates. They can either be stored as lipid droplets in the cytosol or be packaged into chylomicrons (Beilstein et al., 2016; Ko et al., 2020; Mahmood, 2014). However the fate of this process is still unknown in fish (Sæle et al., 2018).

Chylomicrons are large spherical triglyceride-rich lipoprotein formed in the lumen of ER (Mahmood, 2014). The surface of the chylomicrons is formed by a phospholipid monolayer which is surrounded by apolipoprotein B (apoB) and the core is rich in triacylglycerols and cholesteryl esters (Sæle et al., 2018). Chylomicrons are secreted through the basolateral membrane out of the cell into the blood circulation in fish. In the circulation, chylomicrons are metabolized by lipoprotein lipase, which provides fatty acids to cells (Beilstein et al., 2016).

Cytosolic lipid droplets are large spherical particles, consisting of a core of neutral lipids surrounded by a phospholipid monolayer (Ko et al., 2020; Mahmood, 2014; Olzmann & Carvalho, 2019; Welte & Gould, 2017). The phospholipid monolayer is mainly composed of phosphatidylcholine (PC). PC is subjected to remodeling, where it loses an acyl chain to generate lyso-phosphatidylcholine (LPC). LPC is resynthesized to PC by the enzyme LPC acyltransferases (Ipcat), where it gains an acyl chain from acyl-CoA (reacylation) (Cotte et al., 2018).

The formation of lipid droplets involves the budding of newly synthesized TAGs between the two leaflets of the ER membrane (Ko et al., 2020; Mahmood, 2014; Olzmann & Carvalho, 2019; Wang, 2016). The LD budding is facilitated by perilipins (PLIN), that regulate lipid droplet stability and turnover (Ko et al., 2020). Lipid droplets are now being recognized as highly dynamic organelles with various functions (Ko et al., 2020; Mahmood, 2014; Olzmann & Carvalho, 2019; Welte & Gould, 2017). The primary function of LDs is storage of lipids. During the fasting state of the enterocytes or during cell growth, which requires membrane expansion and high phospholipid biosynthesis, neutral lipids stored in LD are broken down to fatty acids which are used for energy production and membrane biosynthesis (Beilstein et al., 2016; Olzmann & Carvalho, 2019; Welte & Gould, 2017).

Peroxisome proliferator-activated receptor- alpha (PPAR α) is a transcription factor belonging to the nuclear receptor superfamily that is stimulated by small lipophilic ligands such as eicosanoids and fatty acids. For transcriptional regulation, PPAR α forms heterodimers with the retinoid-X-receptor (RXR). When the PPAR α /RXR heterodimer is activated by an agonist, it binds to specific DNA sequences called PPAR response element (PPRE), which stimulates the transcription of target genes (Decara et al., 2020; Ibabe et al., 2002). PPAR α is highly expressed in the liver, heart, kidney, and small intestine; however, its function has been exclusively studied in liver (Ibabe et al., 2002). In liver PPAR α plays a crucial role in peroxisomal fatty acid oxidation, mitochondrial beta oxidation, fatty acid transport and apolipoprotein synthesis (Pawlak et al., 2015).

2.4 Aims

As discussed earlier, plant ingredients have been increasingly replacing fish ingredients in fish feed. Plant based feeds not only change the dietary balance of essential nutrients in fish, but it also has introduced harmful agricultural pesticides. Previous studies have documented the presence of CPF residues in fish feed (Sun & Chen, 2008).

CPF residue levels have been reported in products from plants such as soy or maize, that are commonly used as ingredients in salmon feed (Søfteland et al., 2014). Norwegian fish feed manufacturers are currently the largest importers of soya, for example from Brazil into Norway (Lundeberg & Leifsdatter Grønland, 2017). Since Brazil has the highest rate of pesticide use in the entire world (Lundeberg & Leifsdatter Grønland, 2017), farmed salmon in Norway are exposed to CPF through the feed ingredients imported from Brazil. Documentation of CPF residue levels in salmon feeds has raised concern about their potential toxicity in salmonids species.

The main aim of this study was to investigate the oral effects of CPF on the intestinal epithelium of Atlantic Salmon. We hypothesized that CPF disrupts the gut barrier by increasing its permeability. It was also hypothesized that CPF affects the lipid metabolism and detoxification genes in enterocytes by downregulating these at high concentrations of CPF.

The study was divided into two experiments. In the first part, the intestinal permeability of the gut, exposed to CPF and saponin, was measured using the gut sac model. Gut tissue samples were also collected for histological evaluation to detect the effects of CPF on intestinal segments. For the second experiment, an intestinal cell line, RTgutGC, derived from rainbow trout was used as an in vitro model for salmon. The transepithelial electrical resistance (TEER) was measured to assess the barrier function of the epithelial cells. Cells were exposed to different concentrations of CPF, and the TEER was measured again after 24 hours. Gene expression analysis on selected genes involved in detoxification and lipid metabolism were conducted to examine the expression of these genes exposed to different concentrations of CPF. Lastly, the xCELLigence system was applied for cytotoxicity assessment.

3. Materials

3.1 Chemicals

Table 3.1 List of chemicals utilized in this thesis

Name	Supplier
Calcium chloride	Sigmaaldrich
Chlorpyrifos	Sigmaaldrich
Dimethyl sulfoxide (DMSO)	Sigmaaldrich
Entellan® (mounting medium)	Merck Millipore
Ethanol	Antibac
Fetal bovine serum (FBS)	Sigmaaldrich
Fluorescein isothiocyanate–dextran	Sigmaaldrich
Hanks' Balanced Salt Solution	Sigmaaldrich
Leibovitz' L-15 medium (LB-15)	Sigmaaldrich
Magnesium chloride	Sigmaaldrich
Magnesium chloride	Sigmaaldrich
Phosphate-buffered saline (PBS)	Sigmaaldrich
Potassium chloride	Sigmaaldrich
Sodium chloride	Sigmaaldrich
Sodium bicarbonate	Sigmaaldrich
Monosodium phosphate	Sigmaaldrich
Technovit® 3040	Kulzer
Technovit® 7100	Kulzer
Technovit® 7100 liquid and powder	Kulzer
Toluidine blue	Sigma
Trypsin	Sigmaaldrich
Triton X- 100	Cayman
Buffer RLT Plus	Qiagen

Buffer RW1	Qiagen
Buffer RPE	Qiagen
SYBR Green I Master	Roche
Magnesium Chloride	Applied Biosystems
Multiscribe Reverse Transcriptase (RT)	Applied Biosystems
Oligo d(T)16 primer	Applied Biosystems
RNA Nano dye concentrate	Agilent
RNA Nano gel matrix	Agilent
RNA Nano marker	Agilent
RNA ladder	Agilent
TE buffer	PanReac AppliChem ITW Reagents
TaqMan Reverse Transcription Reagents	Thermo Fisher
SYBR GREEN Master	Roche-Norge
TAE buffer	Bio-rad
Gelred	Biotium
One Step RT-PCR buffer	Qiagen
Q solution	Qiagen
dNTP mix	Qiagen
RNase inhibitor	Qiagen
One Step RT-PCR Enzyme Mix	Qiagen

3.2 Kits

Table 3.2 List of Kits utilized in this thesis

Kits	Supplier
OneStep RT-PCR Kit	Qiagen
RNA 6000 Nano Kit	Agilent
TaqMan Reverse Transcriptase reagents	Applied Biosystems

Technovit 7100	Kulzer
Technovit 3040	Kulzer

3.3 Equipment

Table 3.3 List of equipment utilized in this thesis

Instrument	Application	Provider
Bürker haemocytometer	Cell counting	Kova international
Chip priming station	Load gel matrix to nano chip	Agilent
E-plate 96-well	Cell plate for xCelligence	Agilent
Histobloc	Block for mold	Kulzer
Histoform	Mold	Kulzer
RNA nano chip	Separate nuclear acid fragments	Agilent
Transparent PET membrane 0.4 µm	Cell culture insert	Falcon®

3.4 Instruments

Table 3.4 List of instruments utilized in this thesis

Instrument	Application	Provider
2100 Bioanalyzer	Quality control of RNA	Agilent
Biomek 4000	Pipetting robot	Beckman coulter
BX51 microscope	Microscope	Olympus
Centrifuge 5804R	Centrifuge	Eppendorf™
Chemidoc xrs+	Gel Doc	Bio-Rad
EVOM2	Measurement of TEER	World precision instrument
GeneAmp PCR 9700	cDNA synthesis	Termo fisher
IKA MS 3 S36 Basic Chip Vortex	Shaker	Sigma
Leica RM2165	Rotary Microtome	Leica Biosystems
Light cycler 480 Instrument	qPCR analysis	Roche

MICRO STAR 17R	Microcentrifuge	VMR
Nanodrop	Spectrophotometer	Termo fisher
Nikon DS Fi1 camera	Photography	Nikon instruments
VICTOR X5 2030 Multilabel reader	Plate reader	PerkinElmer
xCELLigence® RTCA MP	Monitor cells	Agilent

3.5 Software

Table 3.5 List of software utilized in this thesis

Software	Provider
Agilent 2100 Bioanalyzer	Agilent Technologies
Bio render	Bio render
Bio-Rad CFX Maestro	Bio-Rad
Excel	Microsoft
GraphPad Prism 8	GraphPad Software Inc
Image lab 6.0.1	Pictures of gel
Nanodrop	Isogen Life Science
NIS elements	Nikon
PerkinElmer 2030 Software version 4.00	PerkinElmer
Pycharm community edition 2020	JetBrains
Rstudio 1.3.1056	Rstudio
RTCA Software	Agilent

3.6 Solutions

3.6.1 Ringer's solution

Table 3.6.1 Components for Ringer's solution

Component	Concentration (mM)
Magnesium chloride	0.47

Potassium chloride	2.5
Sodium bicarbonate	20.2
Monosodium phosphate	0.42
Calcium chloride	1.5
Sodium chloride	129

3.6.2 Toluidine Blue Staining

Table 3.6.2 Components for Toluidine Blue staining for histologi

Component	Amount/ Volume
Toluidine Blue O	1 g
Sodium Borate (Borax)	1 g
Distilled water	100 ml

3.6.3 Cell growth media

Table 3.6.3 Components for growth media for RTgutGC cells

Component	Volume (Concentration)
Leibovitz's L-15	445 ml
Fetal bovine serum 10 %	50 ml (10 %)
Antibiotics	5 ml (1%)

3.6.4 cDNA reaction mix

Table 3.6.4 cDNA reaction mix for 30 ul cDNA reaction (20 µl mix + 10 µl RNA)

	Reagents	30 µl	Final concentration
	H ₂ O free from RNase	1.3	
Non	10X TaqMan RT buffer	3.0	1X
enzymatic	25 mM MgCl ₂	6.6	5.5 mM

reagents	10mM deoxyNTPs Mixture (2.5 mM of each dNTP)	6.0	500 µM per dNTP
	50 µM oligo d(T) ₁₆ /random hexamers/	1.5	2.5 µM
Enzymes	RNase Inhibitor (20U/µl)	0.6	0.4 U/µl
	Multiscribe Reverse Transcriptase (50U/ µl)	1.0	1.67 U/µl

3.6.5 SYBRGreen reaction mix

Table 3.6.5 SYBRGreen reaction mix for Light Cycler 480

Reagent	Volume per sample (µl)	Final concentration
ddH ₂ O	2.8	
Primer I (50µM)	0.1	500 nM
Primer II (50µM)	0.1	500 nM
SYBR GREEN PCR Master Mix (2X)	5	1X

3.6.6 One step qPCR

Table 3.6.6 Components for one step qPCR

Components	25 µl rxn	Final concentration
5x QIAGEN One Step RT-PCR buffer	5	1x
Q solution	5	5x
dNTP mix (10 mM of each dNTP)	1	400µM of each
Primer forward	0.3	0.6 µM
Primer revers	0.3	0.6 µM
RNase inhibitor	0.25	
QIAGEN One Step RT-PCR Enzyme Mix	1	
RNase free H ₂ O	X	Up to 25 µl incl. template RNA
Template RNA	Y	1,0 µg RNA

3.7 Primers

Table 3.7 Primers used for the qPCR analysis

Gene	Accession nr.	Forward	Reverse
<i>cyp3a27</i>	U96077.1	ACAACCAGGGTCTGCTGATG	GGTAGGGTGCTCCTGCATTT
<i>cyp1a</i>	AF015660.1	CATCATCCCACACTGCACGAT	GCACTCAGGAAACGGTCAGG
<i>gstr</i>	NM_001160559.2	GGGACCCCAGTTGATTCTCTG	CGGGGACACGGTAGTTGTAG
<i>ugt2a2</i>	XR_002468865	CCACCTGCGAACAGAGTCTT	TGGGTTTACGCTTCCTGCAT
<i>lpcat2</i>	XM_021586592.1	ATGCTATGCTCCGTGAGTCTG	GAGCAGTGGTGGGGTGAAC
<i>plin2-1</i>	CB494091.p.om. Tinant et al., 2020	GATGGCAATGAGGCAGAGAACA	AGGCAGAGTGGCTAAGGGACAG
<i>pparab</i>	NM_001197211.1	CTACCGGCCCGCCGTC	CTGGGACAGGTACTCAGGGA
<i>actb</i>	NM_001124235 Wang et al.,2019	CAAAGCCAACAGGGAGAAGATGA	ACCGGAGTCCATGACGATAC
<i>rps20</i>	NM_001124235 Wang et al.,2019	AGCCGCAACGTCAAGTCT	GTCTTGGTGGGCATACGG
<i>eEF2</i>	-	TGCCCTGGACACAGAGATT	CCCACACCACAGCAACAA

4. Method

4.1 Species and maintenance

This study was a feeding trial conducted for 69 days at Nofima research station at Sunndalsøra, Norway. Mixed gender groups of Atlantic salmon (*Salmo salar*) were distributed into six 1.5 m² tanks, with 24 – 27 fish per tank, containing 500 L seawater flowing at 20 L min⁻¹. The average ambient water temperature during the feeding trial was 11.2 C°. Oxygen content of the water was monitored and maintained at above 80% saturation.

During the feeding trial salmon in three of the tanks were fed a fish meal-based control diet, whereas the others were fed a high protein soya bean meal (SBM). Formulations of the diets are presented in Table 10.1 in appendix and both diets are supplied with essential nutrients. A total of 24 fishes were used for this experiment, where 12 of them were randomly selected fish from the SBM fed tanks and 12 randomly selected from the control tanks.

4.2 Exposure design

For this experiment four different experimental groups were created, where intestinal sacs from six fish from each diet group were injected with either 500 µM or a control without CPF (Table 4.1.2).

Table 4.2.1: Exposure design for each diet groups

Diet	Treatment group 1	Treatment group 2
SBM	500 µM CPF	0 µM CPF
Control	500 µM CPF	0 µM CPF

Stock solutions of CPF were prepared by dissolving 17.53 g of CPF in 400 µl of DMSO. The stock solution for fluorescence, was prepared by dissolving 26.6 mg and 25 mg of FITC-D in 50 ml of

Ringer's solution for day 1 and day 2, respectively. For the bolus with the pesticide and the fluorescence, 80 μl of CPF solution was dissolved in 14.92 ml of fluorescence solution. For the control diet, without CPF, 80 μl of DMSO was dissolved in 14.92 ml of fluorescence solution. Lastly the standard curve for FITC-D molecule ranging from 10^{-1} to 10^{-8} was constructed by diluting the stock solution for fluorescence in ringer solution as shown in figure 4.2.

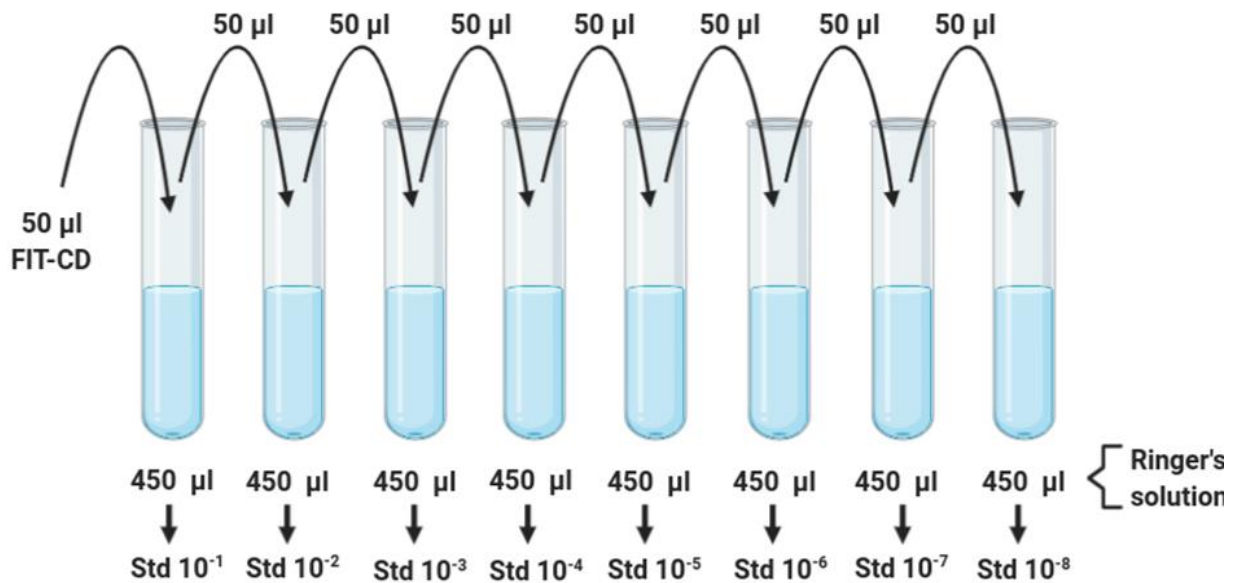


Figure 4.2: Serial standard dilution of FITC-D sample.

4.3 The gut sac model

Gut sacs were prepared according to Mateer et al., 2016 with slight modifications. Fish were killed by blow to the head. A horizontal incision was made in the middle of the abdomen exposing the gut and the gastrointestinal tract was then removed. An intestinal section, the mid gut after pyloric caeca, of approximately 5 - 8 cm, was dissected out and immersed in Ringer's solution (Table 3.6.1). Before preparing the intestinal sacs the luminal content of the intestinal segment was flushed out.

One opening of the intestinal segment was tied and securely closed with a suture loop. A pre-tied suture loop was gently placed around the second opening of the segment. The intestinal sections were then filled with either medium containing both CPF and FITC-D, or just FITC-D(control), before closing the ends. The filled gut sacs were rapidly mounted in individual glass tubes. Twelve glass tubes were placed in a cold-water bath set to 12 °C. Each of these tubes were filled with 45 ml Ringer’s solution and aerated with 95% O₂ and 5% CO₂ by an air tube (figure 4.3).

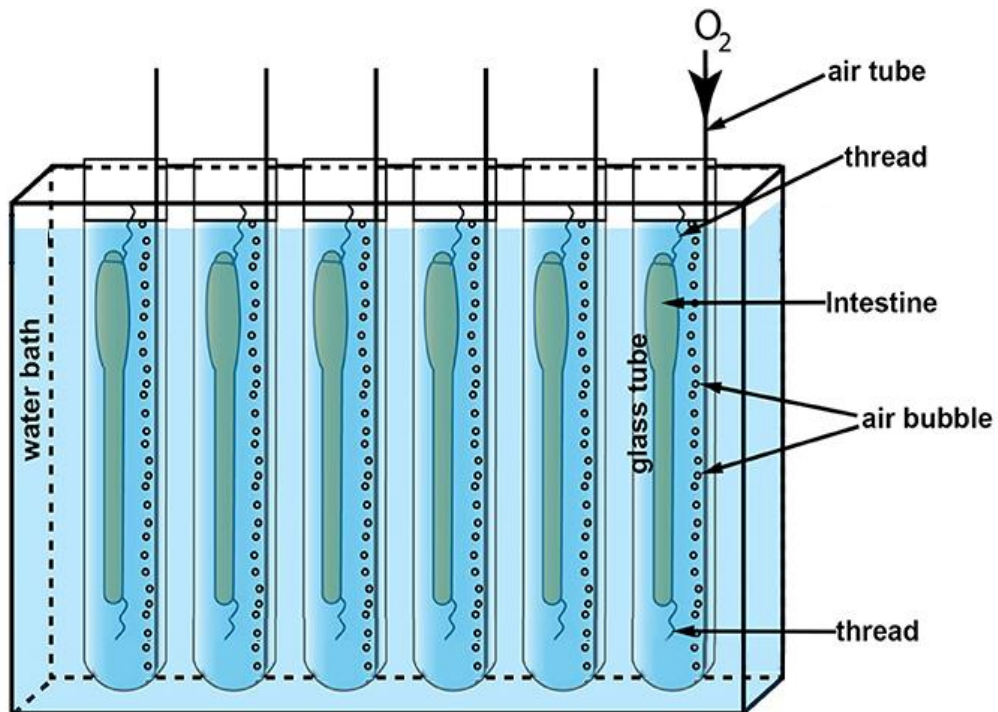


Figure 4.3: In vitro experimental setup. The prepared intestinal sacs were placed in glass tubes containing Ringer’s solution and immersed in a cold-water bath. In intestinal sacs were filled with ringer solution containing both FITC-D and CPF or just FITC-D (control). Oxygen was supplied to each solution with an individually mounted air tube.

At 20-minute time intervals for 3 hours, triplicates of 100 µl of sample were taken from the glass tubes and transferred to a 96 well black plate. The volume was replaced with 300 µl (3x 100 µl) fresh Ringer's solution at each time. Triplicates of 100 µl from each standard curve were also transferred to a 96 well black plate.

At the end of the experimental period the intestinal sacs were cut open exposing the mucosal surface. The length and the width of each intestinal segment was measured. Intestinal tissue samples of approximately 1 cm dimension, from all the fish were also collected for histological evaluation. Each tissue was placed in 1.5 ml of 4 % phosphate buffered (PBS) formaldehyde solution for 24 hours. The tissues were later stored in 70 % ethanol until further processing.

The fluorescence of the samples and the standards for FITC-D were measured at excitation wavelength 493 nm and emission wavelength of 518 nm by PerkinElmer's Multilable plate reader. The samples were centrifuged for one minute at 1000 rpm before the measuring the FITC-D counts.

4.3.1 Apparent permeability

The average FITC-D counts for the standard were calculated and the concentration was found for each sample absorbance on the standard curve. The sample FITC-D concentration was determined by plotting the FITC-D counts of the standard versus the concentration of the FITC-D standards. For each time point the sample FITC-D concentration was converted to cumulative concentration (Q_t) from the equation below.

$$Q_t = C_t \times V_r + \sum Q_t \times V_s$$

Where:-

Q_t = Cumulative concentration at time t

C_t = Concentration of the sample FITC-D at time t

V_r = Volume at the receiver side (external medium)

Q_t sum = Sum of all previous Q_t s

V_s = Volume sampled

The slope of the, dQ/dt , was calculated by plotting the cumulative concentration Q_t versus the time(s). At last, the apparent permeability was calculated for each intestinal sac from the following equation.

$$P_{app} = \frac{\delta Q}{\delta t} \times \frac{1}{A \times C_0}$$

Where :

P_{app} = Apparent permeability

A = Area of the tissue

C_0 = Initial concentration of FITC-D inserted in sacs

4.4 Histology

The intestinal tissue samples were stored in 70 % ethanol. The ethanol was later replaced with 80 % and then 96 %. Tissues were incubated in each solvent for an hour. They were carefully embedded in histoform molds afterwards.

4.4.1 Pre infiltration

Equal parts of ethanol 96% and base liquid Technovit 7100 were mixed. Approximately 1.5 ml of this solution was added to each mold containing the tissue samples. Samples remained in the solution for an hour.

4.4.2 Infiltration

1 g of hardener (bag) was dissolved in 100 ml of base liquid Technovit 7100. The pre

infiltration solution was replaced by approximately 1.5 ml of infiltration solution and the samples remained in the solution overnight.

4.4.3 Polymerization and embedding

1 ml of hardener (bottle) was added to 15 ml of the prepared infiltration solution. The infiltration solution was replaced by ca. 1.5 ml of the prepared solution. The samples were covered in transparent plastic sheet to avoid oxygen contamination and left for 24 hours to harden.

4.4.4 Mounting

Two parts of Technovit 3040 powder was mixed with 1-part Technovit 3040 liquid to obtain a viscous liquid. The liquid and the histoblocs were placed into the mold one after the other. After 10 – 15 min the histoblocs together with the fixed specimen were removed from the histoform.

4.4.5 Microtome sections

The resin blocks were inserted to a microtome and trimmed (10 – 12 μm thickness) to expose the tissue surface. Once the tissues were exposed, sections at a thickness of 1 μm were trimmed. The ribbons of sections were placed delicately on the surface water in a water bath to flatten out. These sections were then transferred on to microscopic slides and the slides were then placed on a hot plate at 50 °C allowing the sections to dry.

4.4.6 Staining

After the sections were completely dried, they were stained with borax-buffered toluidine blue solution for about 3-5 minutes until color developed. Slides were gently rinsed with distilled water 2-3 times to remove excess stain and then air dried. A couple of drops of mounting medium was added on the slide and a coverslip was gently placed over the slide preventing air bubbles. Once again, the slides were air dried overnight. The sections were then photographed using an Olympus microscope with a Nikon camera.

4.5 Cell line

RTgutGC is a cell line established from a primary culture derived from the distal portion of the gut of a female rainbow trout *Oncorhynchus mykiss* (Minghetti et al., 2017). These cells are heteroploid and possess an epithelial like morphology. It has also been reported that RTgutGC cells express alkaline phosphatase activity which is an indication of enterocyte differentiation (Minghetti et al., 2017). In previous studies, RTgutGC cells have been grown as monolayers on permeable supports, leading to a two-compartment intestinal barrier model consisting of a polarized epithelium (J. Wang et al., 2019). The idea behind this is to mimic the *in vivo* intestinal lumen. RTgutGC is a physiologically adequate fish intestinal barrier model equivalent to the Caco-2 human intestinal epithelial cell line, which is used to study fish intestinal immune and barrier functions (Wang et al., 2019).

4.6 Cell culture

The RTgutGC cell line were aseptically cultured in L-15 medium containing 10% FBS and incubated at 19 °C. The cells were grown in 75 cm² cell culture flasks for 5-7 days, until they were harvested for experimental purposes. Cells were harvested by discarding the culture medium from the flask followed by rinsing the cell layer twice with 8-10 ml PBS. The cells were enzymatically detached from the flask by adding 1-2 ml of trypsin for 2 minutes in room temperature. The trypsin reaction was stopped by adding 10 ml of fresh culture medium and the detached cells were aspirated gently by pipetting. The resulting cell suspension was centrifuged at 1000 rpm, 19 °C for 3 minutes. Cells were resuspended in 1-2 ml growth medium, after discarding the supernatant. The density of the cells was determined by loading 10 µl of cell suspension on to a haemocytometer and the number of cells were counted manually. The cells were diluted to required volume in culture media and seeded in wells prior to experiments. Cells were split in 1:2 ratio for maintenance, after reaching confluency.

4.7 Measurement of transepithelial electrical resistance

To evaluate the epithelial integrity of the RTgutGC barrier, transepithelial electrical resistance (TEER) was measured. Cells were seeded in transwell membrane inserts with 0.4 μm pore size at a density of 150,000 cells/ml per insert. Membrane inserts were plated in a 12-well plate filled with 1 ml of L-15 in each basolateral compartment, figure 4.7.1. Cells were incubated at 19 °C, with a change of medium, allowing the cells to form a barrier. For the control (blank) empty (cell-free) membranes were filled with 1 ml of media in both apical and basolateral chamber. TEER levels were measured over time by using an EVOM voltmeter meter with STX2 chopstick electrodes according the EVOM instruction manual. The unit area resistance ($\Omega \text{ cm}^2$) was calculated by subtracting the values obtained from membranes containing cells from the blank and by multiplying by the growth area of the insert.

4.7.1 Exposure

Cell were grown for at least 10 days at 19 °C before pesticide exposure experiments. Cells were exposed to CPF concentrations of 0.5, 5, 50, 100, 500 μM and DMSO 0.2% (control). The TEER was then measured 24 hours after exposure.

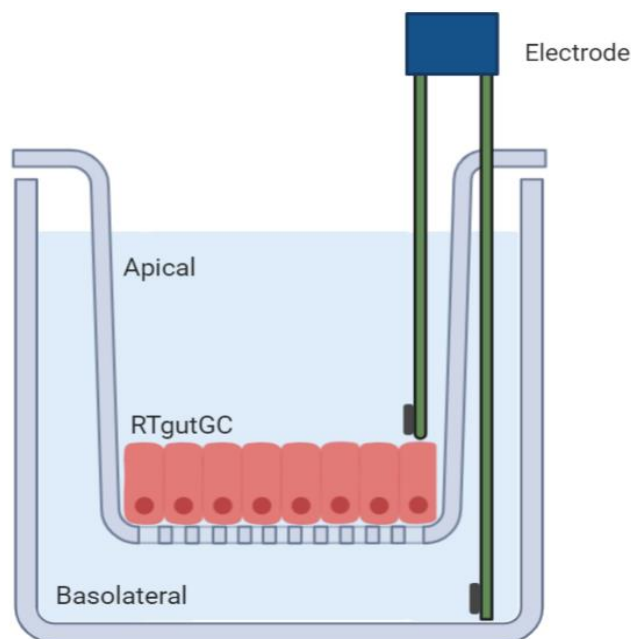


Figure 4.7.1: Outline of *in vitro* intestinal barrier model based on intestinal epithelial cell line, RTgutGC. Cells are seeded in transwell membrane inserts with pore size 0.4 μm separating the apical media compartment from the basolateral media compartment. The TEER levels were measured using an EVOM voltmeter with STX2 chopstick electrodes.

4.8 Real - time quantitative PCR

4.8.1 Pesticide exposure

Cells were seeded in six-well plates in 3 ml complete L-15 medium at a density of 600,000 cells/well and incubated at 19 °C for 3-4 days prior to exposure with a change of medium. The cells were then exposed to 0.5, 5, 50, 100, 500 μM CPF and 0.2% DMSO (control) in triplicates for 24 hours. After 24 hours of pesticide exposure, cells were washed twice with PBS. For lysing of cells 600 μl of RLT Plus buffer was added to each well and mixed well by pipetting up and down a few times. The lysate was transferred to individual 1.5 ml tubes and stored at - 80 °C until further processing.





4.8.2 RNA extraction

The RNA lysate was thawed on ice before proceeding with the RNA extraction. The homogenized lysate was transferred to gDNA eliminator spin columns placed in 2 ml collection tube and centrifuged for 30 s at 9000 g. The column was discarded and the flow-through was saved. One volume (460 – 480 μl) of 70 % ethanol was added to each flow-through and was mixed well by pipetting. Samples were transferred to RNeasy spin column placed in 2 ml collection tubes and centrifuged for 30 s at 9000 g and the flow-through was discarded. 700 μl of RW1 was added to the spin columns and centrifuged for 30 s at 9000 g and the flow-through was discarded. 500 μl of RPF was added to the RNeasy spin column and centrifuged for 30 s at 9000 and the flow through was discarded. Another 500 μl of RPF was added to the spin columns and centrifuged for 2 min at 9000 and the flow-through was discarded. Spin columns were placed in new 2 ml collection tubes and centrifuged for 1.6 x g for 1 minutes. RNeasy spin columns were placed in new 1.5 ml collection tubes and 20 μl of ddH₂O was directly added to the spin column membrane

and centrifuged for 1 min at 9000 x g to elute the RNA. RNA concentrations of the samples were later determined by the Nanodrop.

4.8.3 Quality of RNA

For the quality control of RNA, 12 random samples were selected for integrity analysis. From each sample, 2 µl was transferred to microcentrifuge tubes and placed on a heating block at 70 °C for 2 minutes for denaturation. All the reagents were equilibrated to room temperature for 30 minutes before use. For the gel dye mix, 0.5 µl of RNA 6000 Nano dye concentrate was added to a 32.5 µl of filtered gel (RNA 6000 Nano gel matrix). The gel dye mix was vortexed and spinned for 10 minutes at 13000 g and stored at 4 °C in the dark.

RNA chip was placed on the priming station and 9 µl of gel-dye mix were pipetted in the well-marked . The plunger was positioned at 1 ml before closing the chip priming station. The plunger was pressed until it was held by the clip and it was released after 30 s. The plunger was slowly pulled back to its 1 ml position after 5 s. After opening the chip priming station, 9 µl of gel-dye mix was pipetted to the wells marked . In all the sample wells and the well marked “ladder” , 5 µl of RNA marker was loaded. 1 µl of prepared ladder was then loaded in the well marked “ladder”  and 1 µl of samples (previously denatured by heat) were added in each of the sample wells. The chip was vortexed for 1 min at 2400 rpm in the IKA vortexer before running it in the Agilent 2100 Bioanalyzer.

The Bioanalyser provides an objective measurement of RNA quality with RNA integrity number, RIN. RIN number is based on a numbering system from 1 – 10, where 1 being the most degraded and 10 being the most intact RNA.

4.8.4 cDNA synthesis

RNA samples were thawed on ice. The samples were diluted individually with ddH₂O to a final resulting concentration of 50 ng/µl in a total volume of 30 µl. RNA concentrations were measured

using the Nanodrop. The RNA volume was adjusted either by adding RNA or adding ddH₂O for samples not within the range of 50 ± 5 % ng/ μ l.

For the RNA pool 2 μ l from each undiluted RNA samples were pooled together in a RNA mix to create a standard curve. The concentration of the RNA mix was adjusted to 100 ± 5 % ng/ μ l with ddH₂O. From this tube, total of six serial dilutions was made by mixing 40 μ l sample and 40 μ l ddH₂O, giving a series of the following concentrations: 100 ng/ μ l, 50 ng/ μ l, 25 ng/ μ l, 12.5 ng/ μ l, 6.25 ng/ μ l and 3.125 ng/ μ l.

The Reverse Transcriptase reaction mix was prepared for 63 wells (3x number of samples +3x number of concentrations in std + 2 negative controls), Table 3.6.4. The two negative control utilized: “ntc” (non-template control) and “nac” (non-amplification control). All reagents were added to make the RT reaction mix except for the multiscribe enzymes. The “nac” control was prepared by removing 20 μ l from the RT reaction mix and transferring it to a 96-well plate. The multiscribe enzyme was then added to the mix and 20 μ l of this mix was distributed to rest of the wells. 10 μ l of diluted standards and RNA samples were then added to their respective wells and mixed carefully by pipetting up and down a couple of times. To the “nac” control, 10 μ l of excess RNA from 50 ng/ μ l was added and 10 μ l of ddH₂O was added to the “ntc” control.

The plate was then covered by a 96-well plate cover and centrifuged at 50 g for 1 minute. The PCR was then performed by GeneAmp PCR 9700 (Applied biosystem). The steps in the PCR were 10 min incubation (25 °C), 60 min elongation (48 °C) and 5 min reverse transcriptase inactivation (95 °C). The plate was left in the instrument until the next day at 4 °C. The cDNA plate was later sealed with a tape pad and stored at -20°C until further processed for real-time quantitative PCR.

4.8.5 Primer test - One step qPCR

The quality control of the primers of all the target genes were done by a one-step PCR using the QIAGEN OneStep RT-PCR Kit. Primers were diluted in 1 x TE buffer to a final concentration of 50 μ M and incubated in room temperature for 2 minutes and vortexed for 15 seconds. RNA samples and reagents were thawed on ice and the enzyme mix was placed on a -20 °C block prior to one

step qPCR. Based on the sample RNA concentrations, the volume needed for 1 µg RNA was calculated, and the volume of ddH₂O was adjusted according to a total reaction volume of 25 µl. All the reagents were mixed in a master mix, table 3.6.6, except for the primers, RNA and ddH₂O, which were added after distributing the master mix into separate 1.5 ml tubes. Each solution was mixed properly by pipetting up and down for several times. The PCR was run in the GeneAmp PCR system 9700 (Applied Biosystems).

4.8.6 Agarose gel electrophoresis

Agarose gel electrophoresis was performed to check the expression levels of the products from One Step RT-PCR. According the size of the fragments (150 – 200 bp), a 2 % agarose gel was chosen. A gram of agarose was added to 100 ml 1x TAE buffer. The solution was heated in a microwave oven for about 1 minute until everything was dissolved. The solution was then cooled before adding 10 µl of Gel red Nucleic Acid Stain. The melted agarose was poured into a tray and a comb was placed in and the gel was left to solidify for 30 minutes. The gel was then placed in a electrophoresis tray filled with running buffer (1xTAE). The comb was then removed carefully. The PCR products were mixed with 6x loading dye in the ratio 1:6 (1 µl 6x loading dye and 5 µl sample). The samples were then added to the wells. The lid was placed on the unit and the gel was run at 86V until the bands had moved into the gel, and then at 50V for 45 min. For photographing of the gel, the gel was placed on the glass plate on the bottom drawer of Gel Doc. The program, Image lab was utilized to take a picture of the gel.

4.8.7 Real time quantitative PCR

The cDNA plate was thawed on ice and centrifuged at 1200 x g for 1 minute and spun at 1500 rpm for 5 minutes. The samples were then diluted 1:2 by adding 30 µl ddH₂O to each well using a pipetting robot. The cDNA plate is only diluted once before the first qPCR run. It was then centrifuged at 1200 x g for 1 minute and vortexed at 1500 rpm for 5 minutes and placed on ice. Regents for the SYBR Green PCR Master Mix and the primers were thawed on ice prior to making the solution. The reaction mix was made for each gene according to the number of reactions, (Table 3.6.5). 112µl of from this mix were added to wells of an 8 - well stripe. Using a pipetting

robot 8 μ l of the reaction mix and 2 μ l of cDNA from each well were transferred to a 384-well plate. The plate was then covered with an optical adhesive cover and centrifuged at 1500 g for 2 minutes. The plate was placed into the light cycler 480 Real Time PCR System for the analysis of the real time PCR quantification. Genes used for the qPCR analysis is listed in Table 3.7.

4.8.8 Primer design

Totally of 6 relevant genes were selected for primer design. Primers were designed for the mRNA sequence of four genes associated with detoxification, *cyp1a*, *cyp3a*, *ugt* and *gst* and two genes associated with lipid metabolism, *lpcat2* and *ppara*. *Plin2*, (lipid metabolism gene) was selected according to Tinant et al., 2020. *Actb* and *rps20*, according to (Wang et al., 2019), and *eEF2* were selected as reference genes. Primers were designed using NCBI data base and its primer design tool.

4.9 Xcelligence

xCELLigence Real Time Cell Analysis (RTCA) instruments use biosensors to continuously monitor cell behavior in a label-free manner (Kho et al., 2015). The xCELLigence system uses an E-plate 96-well plate that is coated with gold microelectrode sensor arrays at the bottom surface which measures the electron flow transmitted between the electrodes in the presence of an electrically conductive solution such as culture media. This electrical impedance across the electrodes allows to monitor and detect physiological changes of the cells (Hamidi et al., 2017).

The E96 xCELLigence plate was prepared by adding 50 μ l of culture media to each well and by incubating in xCELLigence for 30 minutes. After 30 minutes the background impedance was measured to ensure that all wells and connections were working within acceptable limits. After the background check, all the media was removed from the wells and cells were seeded at a density of 20,000 cells/well in 100 μ l culture media. The plate was placed back in the xCELLigence and the adhesion, growth and proliferation of the cells were monitored every 15 min for 24 hours. 24 hours after seeding, the cells were exposed to a dose range of 0.05 - 500 μ M CPF. Controls

received medium with 0.2% DMSO and some wells were treated with 10% triton as a positive control. After exposure, the experiment was run for approximately 40 hours.

4.10 Statistics

All statistical analyses were performed in R (v.3.6.1) with RStudio (v. 1.2.5019) and Pycharm 2020.2. GraphPad Prism 8.0, RStudio and Pycharm were utilized to create all statistical figures. One-way analysis of variance (ANOVA) was performed to examine the effects of the saponin exposure on weight loss of the fishes. Two-way ANOVA was performed to examine the effect of diet and treatment on apparent permeability of each intestinal sac. Data of TEER values, qPCR and cytotoxicity were analyzed using a one-way ANOVA followed by a Tukey's multiple comparison test. The NOAEL and LOAEL values were determined by ANOVA followed by a Tukey's test on the xCelligence system data. The LC50 was determined by linear interpolation. The data from xCelligence system was also fitted to a three-parameter sigmoid curve and the sigmoid curve equation was used to calculate the LC50 and BMC5 values. All the data were tested for homogeneity of variances and data normality using Levene's test and Shapiro Wilk's test respectively.

5. Results

5.1 General health

No mortality related to dietary treatment was observed. Fish used for the experiment displayed no external changes and looked healthy. Two fishes out of 26 fishes were discarded from the experiment, where one was used as a trial and therefore discarded from the results. The second fish was starved and therefore was not used for the experiment. None of the fish were sexually matured.

5.2 Soya saponin exposure

Before the feeding trial the initial body weight of the control and the SBM fed fish were 178.5 ± 1.0 g and 177 ± 2.1 g respectively. After 67 – 69 days of the feeding trial the final average weight for the control group was 571 ± 21 g and 555 ± 17 g for the SBM group. Replacement of fish meal (control) with soya bean meal resulted in slight decrease in fish growth, figure 4.2, but not statistically significant ($p=0.6$).

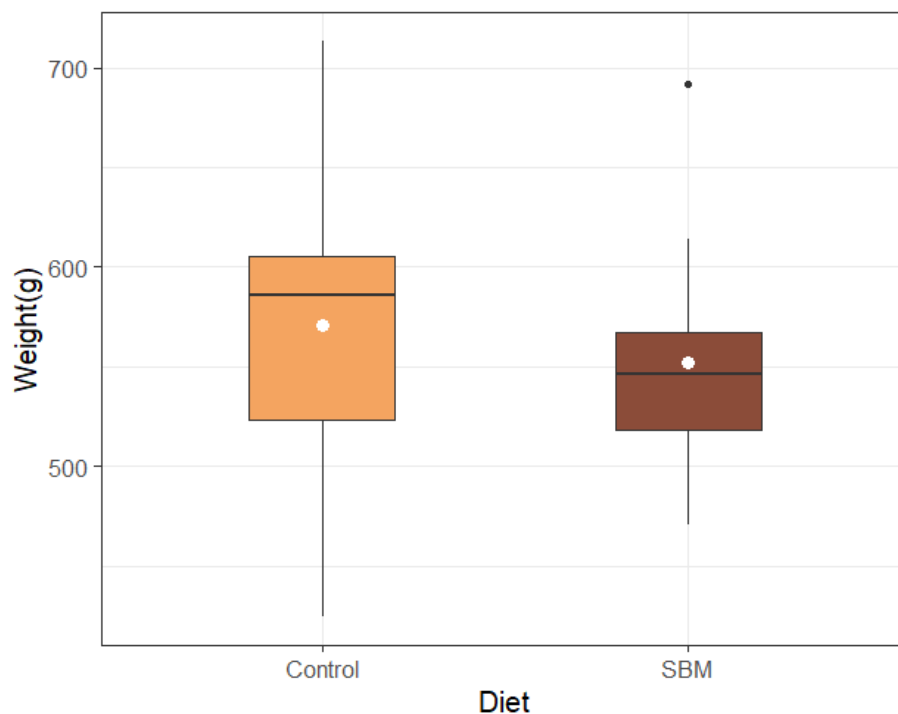


Figure 5.2.1: - Final weight (g) of Atlantic salmon fed fish meal (control) and soya bean meal (SBM). Whiskers represent the minimum and maximum values. The Lower box limit represents Q1 (lower quartile), middle – median and upper limit - Q3 (upper quartile). White circle - mean, black dots – outliers.

5.3 Apparent permeability

None of the intestinal sacs seemed damaged and the ends were properly closed. The cumulative concentration of FITC-D of all the intestinal sacs were low at 0 t indicating that none of the sacs were leaking. The cumulative concentration of each point for every intestinal sac generally increased as the time increased, and all the trend lines had a positive slope (appendix figures 10.1 – 10.24).

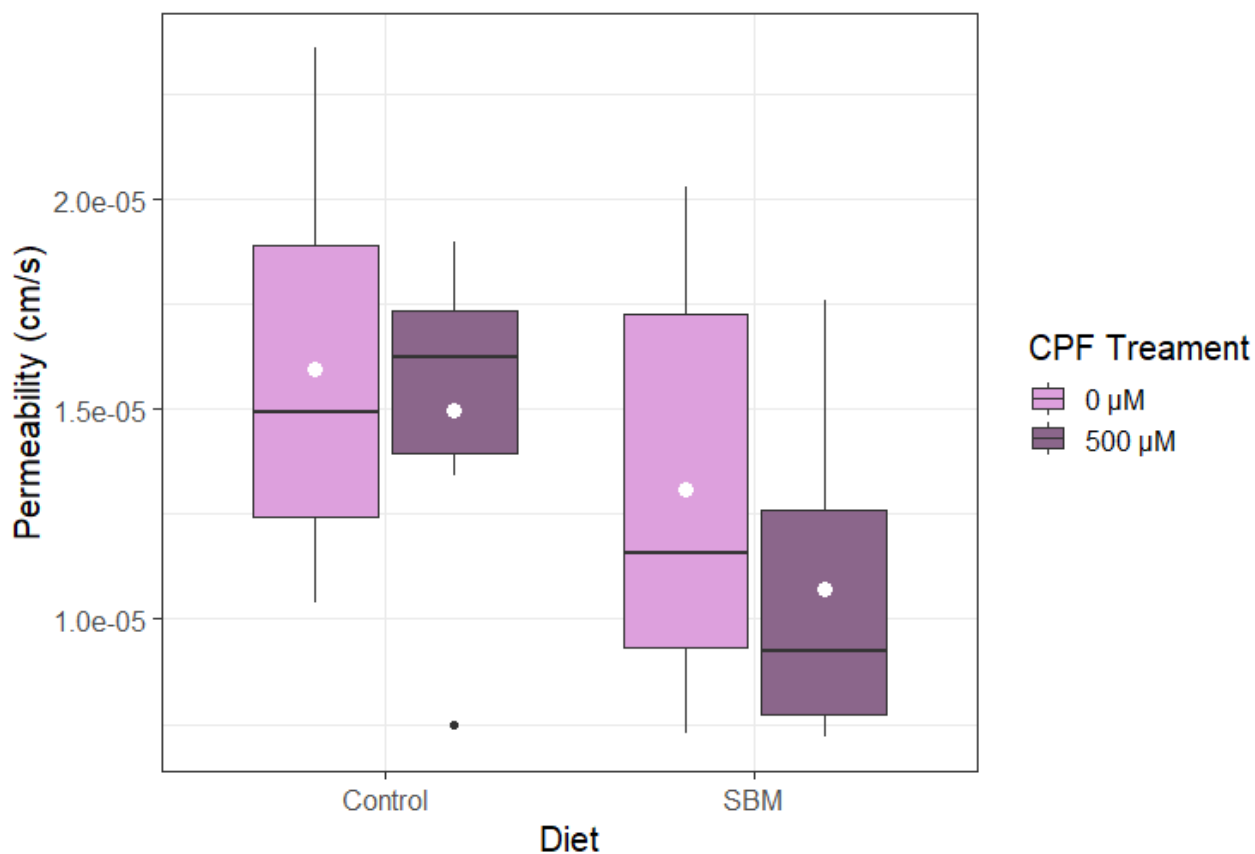


Figure 5.3.1: Apparent permeability of Atlantic salmon intestinal sacs of each experimental group and the effect of CPF treatment. Control 0 μM and Control 500 μM represents fish fed with fish meal later injected 0 and 500 μM CPF in the intestinal sac, respectively. SBM 0 μM and SBM 500 μM represents fish fed with soybean meal later injected with 0 and 500 μM CPF in the intestinal sac, respectively. The Lower box limit represents Q1 (lower quartile), middle – median and upper limit - Q3 (upper quartile). White circle - mean, black dots – outliers.

The apparent permeability values for each intestinal segment for different experimental groups are plotted in figure 5.3.1. The average apparent permeability of the mucosa for fish fed with SBM diet injected with 500 μM CPF and 0 μM CPF are $1.01 \times 10^{-5} \text{ cms}^{-1}$ and $1.31 \times 10^{-5} \text{ cms}^{-1}$ respectively. The average permeability for the FM fed group (control) injected with 500 μM CPF and 0 μM CPF are $1.50 \times 10^{-5} \text{ cms}^{-1}$ and $1.60 \times 10^{-5} \text{ cms}^{-1}$ respectively.

The highest intestinal permeability value was observed in the control group with zero CPF exposure. There were no statistical differences between the permeabilities in each experimental group. Although there appeared to be a trend of decreasing permeability in CPF exposed intestinal segments in both groups.

Output from ANOVA showed that the effect of the diet ($p=0.07$) and treatment ($p= 0.4$) alone were not statistically significant. The interaction of the diet and treatment ($p =0.71$) was also not statistically significant. This concludes that the diet and treatment together and alone did not affect the intestinal apparent permeability.

5.4 Histology

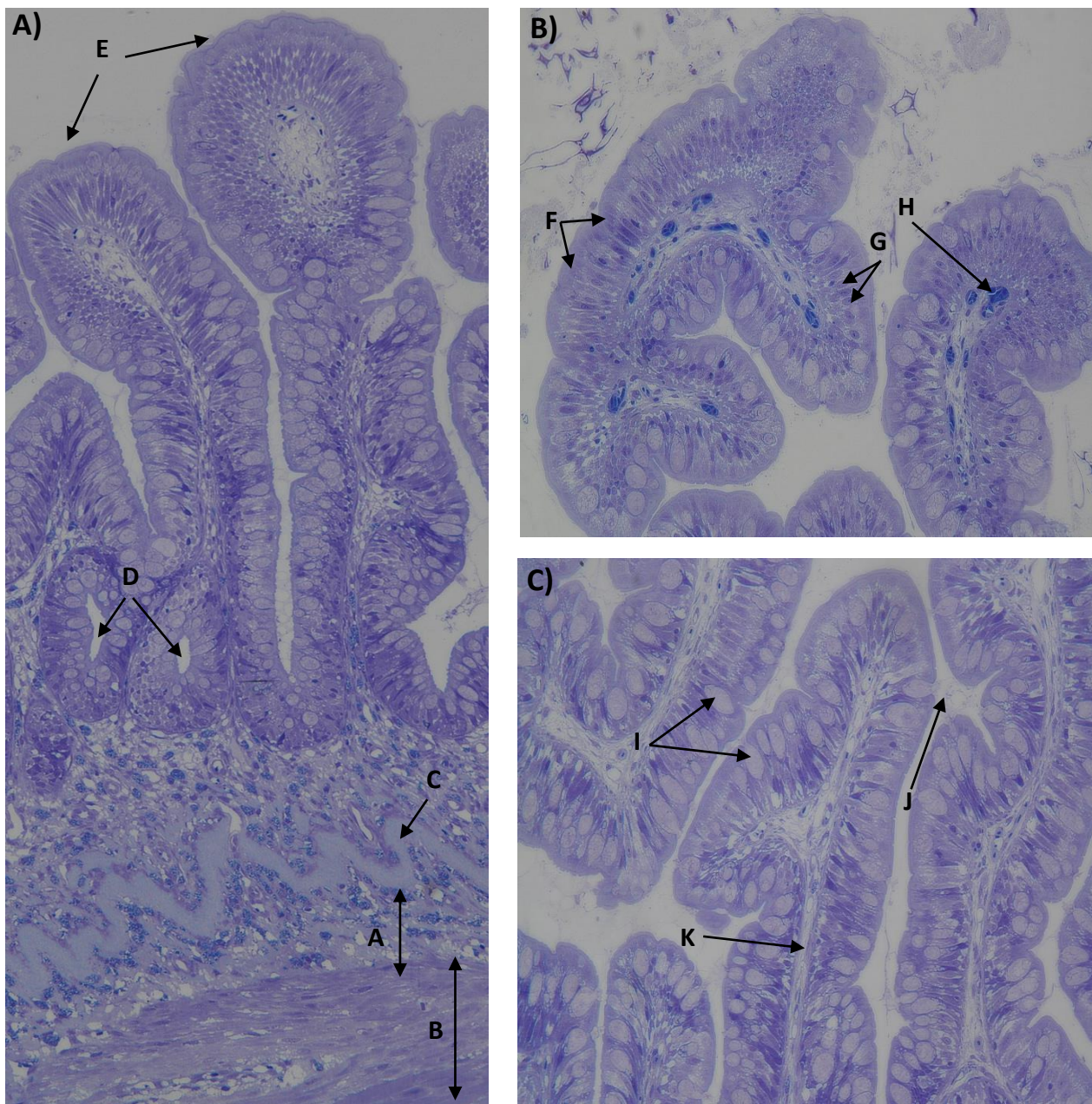


Figure 5.4.1: Histological appearance of intestinal tissue of fish fed with fish meal(control). A – Submucosa, B - *Muscularis externa*, C- *Muscularis Mucosae*, D – Crypts, E - Villi, F – Enterocytes, G- Nuclei, H – Blood vessel, I – Goblet cells, J – Mucus, K- Lamina propria. Scale bar A) = 100 μm, B) & C) = 50 μm

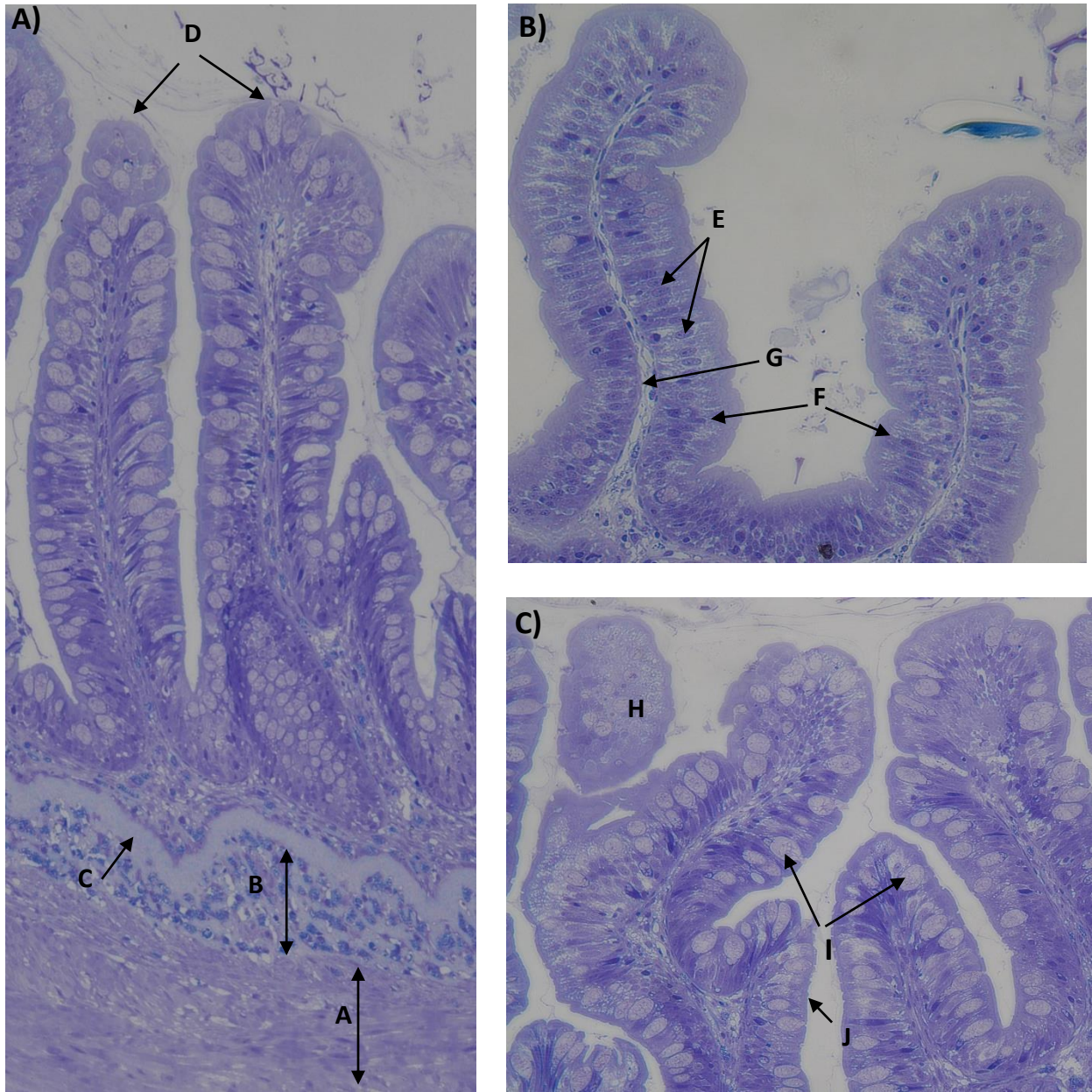


Figure 5.4.2: Histological appearance of intestinal tissue of fish fed with SBM. A - *Muscularis externa*, B – Submucosa, C- *Muscularis Mucosae*, D – Villi, E - Nuclei, F – Enterocytes, G- Lamina propria, H – Horizontal plane of segment, I – Goblet cells, J – Brush border. Scale bar A) = 100 μ m, B) & C) = 50 μ m

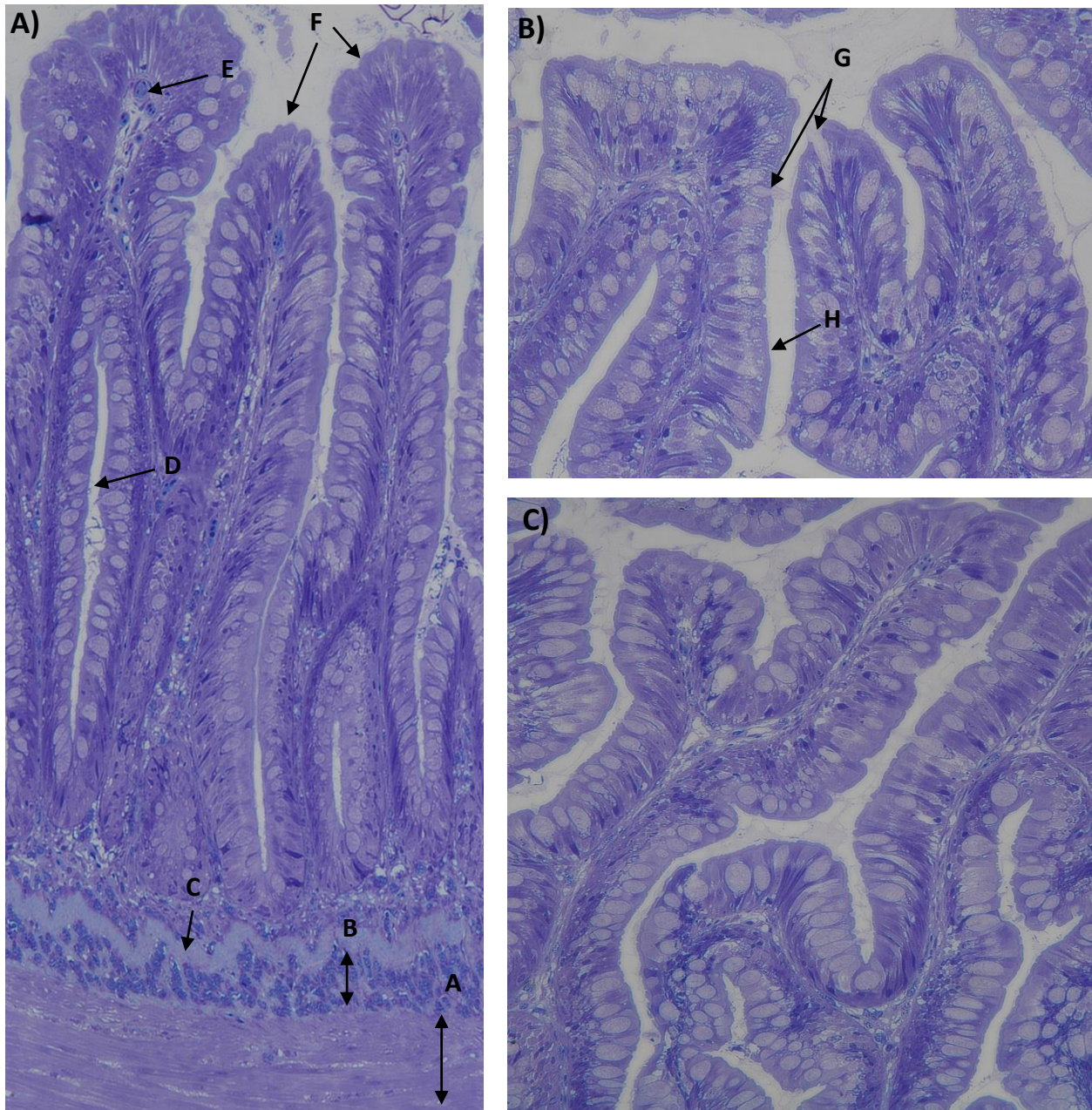


Figure 5.4.3: Histological appearance of intestinal tissue of fish fed with fish meal (control) and later injected with 500 μM CPF. A - *Muscularis externa*, B – Submucosa, C- *Muscularis Mucosae*, D – Crypts, E - Blood vessel, F - Villi, G- Secretion of mucus from goblet cells, H – brush border. Scale bar A) = 100 μm , B) & C) = 50 μm

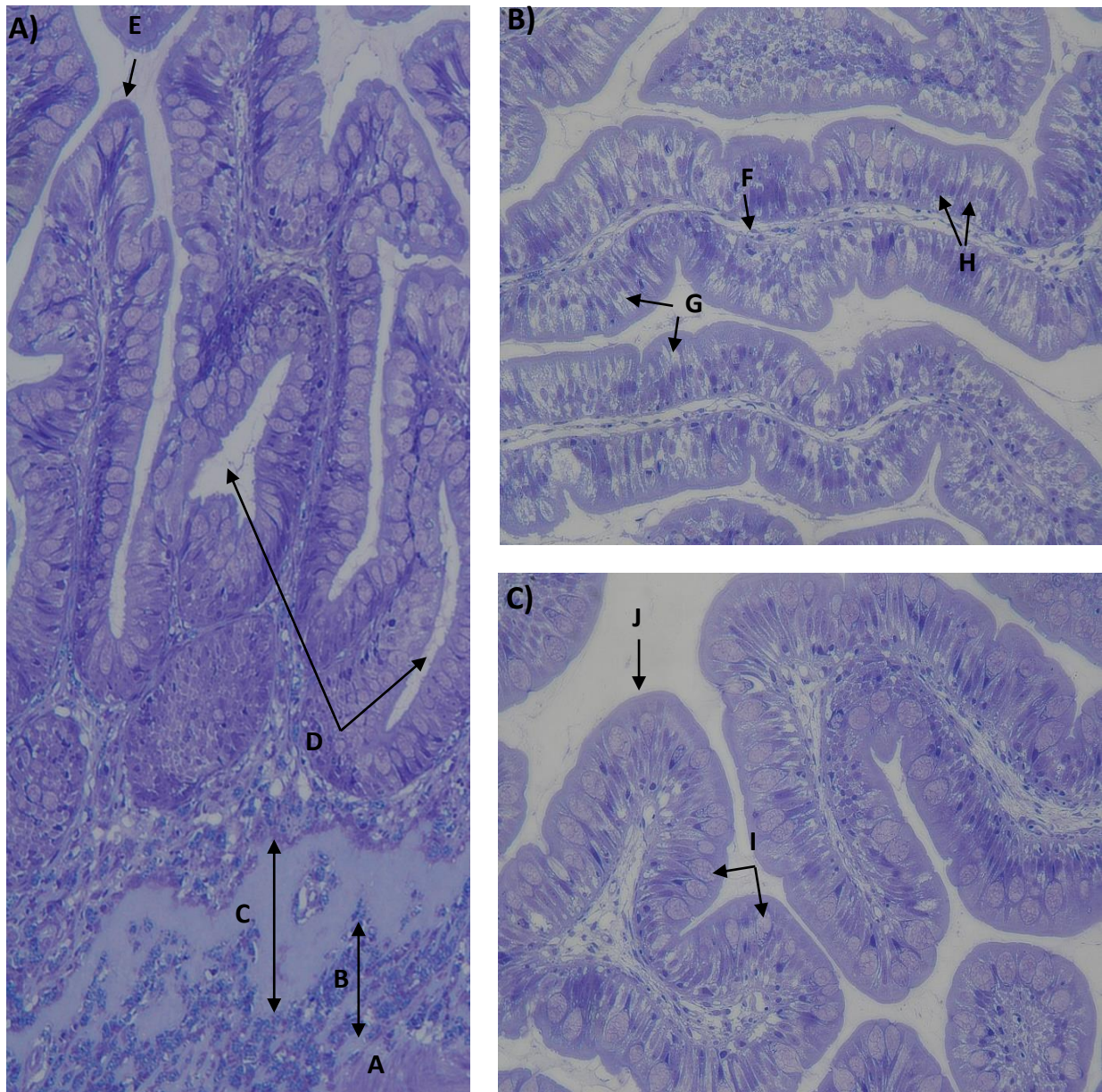


Figure 5.4.4: Histological appearance of intestinal tissue of fish fed with SBM and later injected with 500 μM CPF. A - *Muscularis externa*, B - Submucosa, C- *Muscularis Mucosae*, D – Crypts, E - Villi, F – Lamina propria, G- Enterocytes, H – Nuclei, I – Goblet cells, J – Brush border. Scale bar A) = 100 μm , B) & C) = 50 μm

Results from the histological evaluation of the intestinal segments of fish fed with different diets are shown in figures 5.4.1 – 5.4.4. Intestinal segments of fish fed with SBM and FM exposed to 0 μM and 500 μM displayed normal morphology with no inflammatory response and no histological alteration. Intestinal segments showed normal structures of the intestine, which consists of *muscularis externa*, submucosa, *muscularis mucosae*, lamina propria, enterocytes etc.

Histological observations of intestinal segments from the gut sac experiment showed no infiltration of lamina propria and submucosa, no shortened of mucosal fold, no fusion of villi and/or flattened villi and no loss of supranuclear vacuoles were seen in the enterocytes, in any of the exposure groups. Numerous goblet cells scatted among the absorptive cells (enterocytes) are seen in all the exposed intestinal segments, including the control. These cells are specialized for secretion of mucus which lubricates the intestine. Figure 5.4.3 B) shows the secretion of mucus into the lumen by a goblet cell. Some regions of the intestinal segments displayed few goblet cells comparing to other regions of the intestine of some fishes, figure 5.4.4 B) and C).

5.5 Cytotoxicity assay

The cytotoxicity test was performed after the qPCR and TEER analysis. Due the down regulation of *cyp1a* mRNA expression at 5 μM CPF compared with the 0.5 μM CPF (see figure 5.7.1) a dose range from 0.05 – 500 μM CPF was chosen for this experiment.

The strength of cell adhesion is represented as the Cell Index (CI) which is a unit-less measurement. The cell index of cells beginning from 20,000 cells/well increased as the cell number increased. The CI made a sharp increase up to 10-12 hours and remained stable thereafter (appendix figure 10.27). The CI was normalized at the time point before CPF addition by dividing through by the value at this time point.

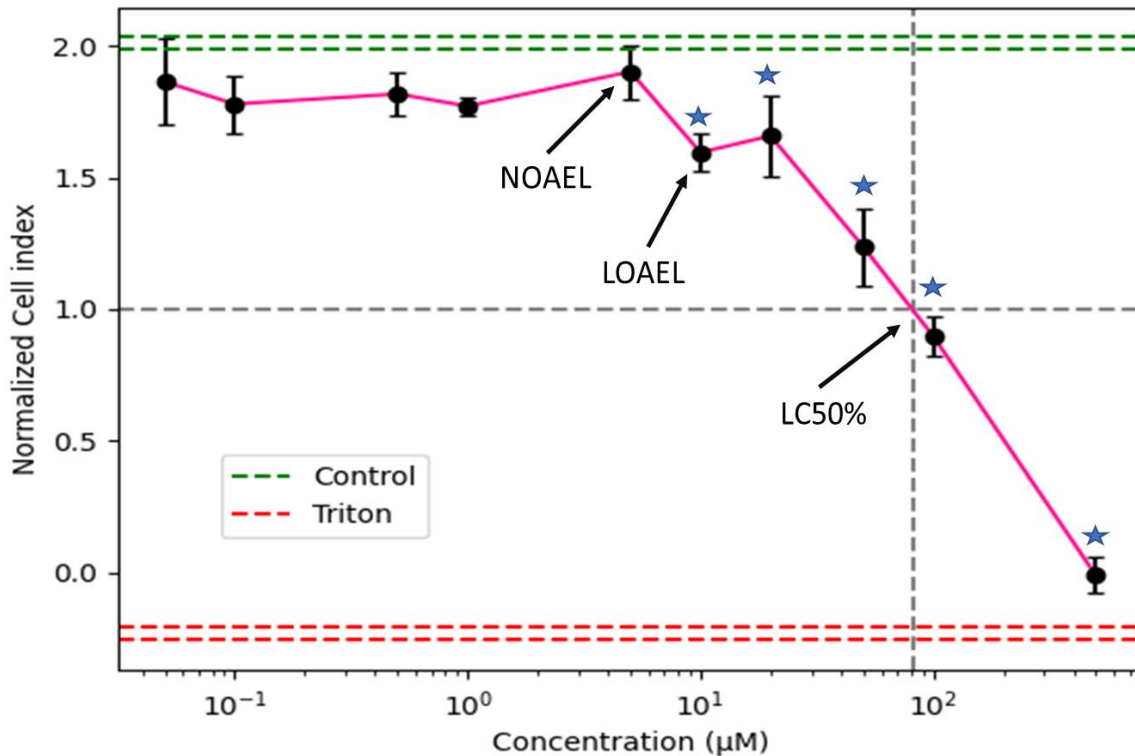


Figure 5.5.1: Response curve of the cell index of RTgutGC cells upon CPF exposure. Cells were seeded at a density of 20,000 cells/well in a 96-well E-plate allowing the cells to adhere and proliferate for 24 hours. Cells were then exposed to CPF in the dose range of 0.05 – 500 µM for 24 h using an xCELLigence system. xCELLigence data shows cell adhesion as mean cell index ± SD of three replicates. Significant difference observed between the control and the exposed group by one-way ANOVA is indicated by ★ ($p > 0.05$). NOAEL = No observed adverse effect level, LOAEL = Lowest observed adverse effect level, Green lines = ± SD interval of the Control, Red lines = ± SD interval of the Triton 20%, Grey line = LC50% (Lethal concentration 50%).

The response to CPF exposure (0.05 - 500 µM) of RTgutGC cells after 24 hours is shown in figure 5.5.1 (linear fit), and 5.5.2 (logistic regression). Controls (DMSO 0.2%) reached a mean cell index (CI) value of 2 ± 0.02 . RTgutGC cells exposed to CPF up to 5 µM showed no significant difference compared with the controls. Cells exposed to 10, 20, 50, 100 and 500 µM was significantly different compared with the controls, based on ANOVA. All the cells exposed to 500 µM CPF had undergone cell death, giving a mean CI value around 0. CI of all positive controls (n=3) treated

with 20% triton dropped down to negative values and a similar observation was made in one well of cells exposed to 500 μM CPF. Based on ANOVA analysis, cells exposed to 5 μM CPF is the highest concentration not significantly different from the control, indicating the NOAEL value; and cells exposed to 10 μM CPF, being the lowest concentration significantly different from the control, indicating the LOAEL value. The LC50 of CPF in RTgutGC cells, as determined by linear interpolation, was 84 μM (figure 5.5.1).

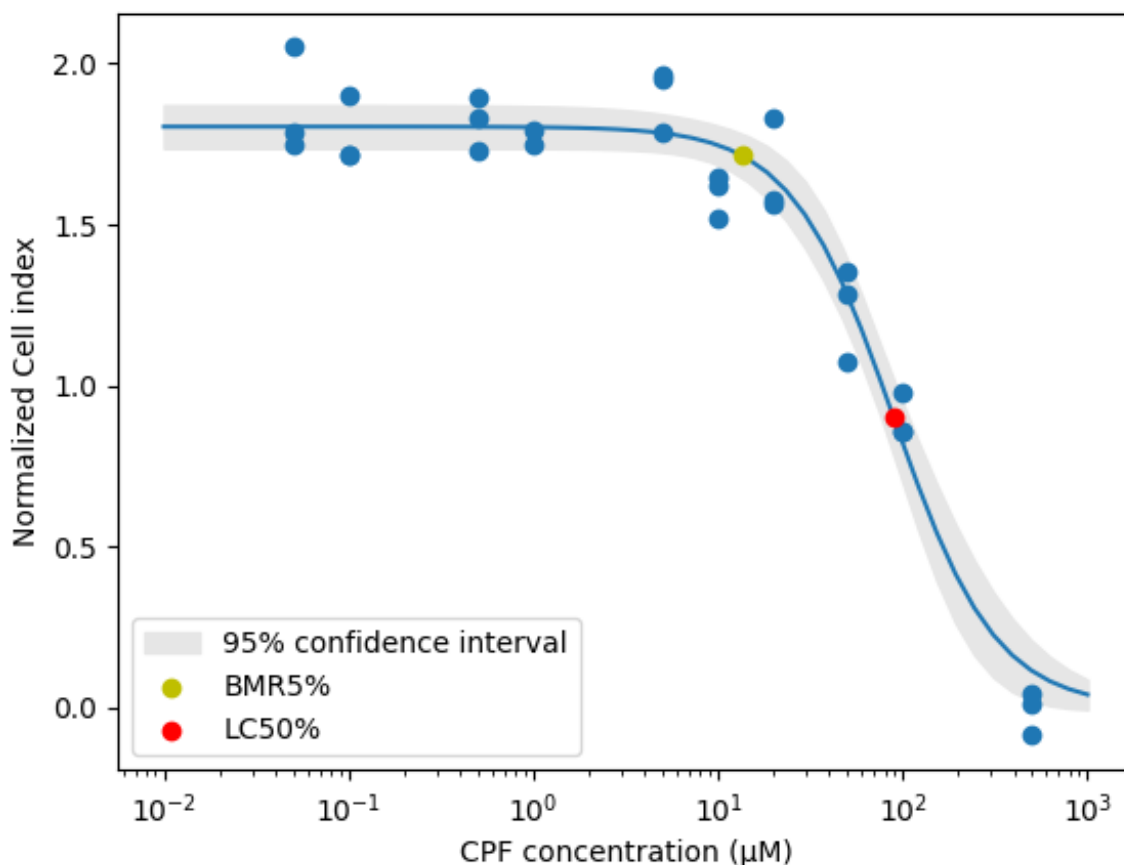


Figure 5.5.2 Sigmoid curve fit of the exposure response curve for CPF and Cell Index of RTgutGC cells. Cells were exposed to CPF in the dose range of 0.05 – 500 μM for 24 h using a xCELLigence system. Control and 20% Triton is not included in this analysis. Blue line = sigmoid curve, Blue dots = raw data, Yellow dot = Benchmark response 5% (BMR5), Red dot = Lethal concentration 50% (LC50), Grey line = 95% confidence interval.

According to the logistic regression plot there is little or no effect in the adhesion of cells at low concentrations of CPF. Beyond the concentration of 5 μM CPF the regression line starts to decline indicating a high adhesion of cells. From concentrations beyond 10 μM there is a clear decline in the adhesion of cells both in the data in the regression and the slope of the regression is steep. At the highest concentration tested the adhesion of cell is a fraction of the adhesion at low concentrations. The measured BMR5 and LC50 for CPF in RTgutGC cell in this analysis are 13.5 ± 0.06 and 89 ± 0.12 μM at 95% confidence, respectively.

5.6 Transepithelial electrical resistance

A cell density of 150,000 cells/ml and a culture period of 10 days with symmetrical culture conditions, consistently yield a dense, single epithelial monolayer on the permeable membranes. The cells were seeded and left in culture allowing it to attach overnight prior to the TEER experiment, Figure 5.6.1. On the first day cells developed an average TEER of 33 ± 10 $\Omega \cdot \text{cm}^2$. Over time TEER levels increased and reached an average of 65 ± 5.2 $\Omega \cdot \text{cm}^2$ after 10 days of culture with significant difference observed over time ($p = 3.983\text{e-}09$). TEER values reached a stable plateau at around 6-10 days. Cells seemed to have stopped proliferating but remained viable. Formation of a double cell layer, especially in the center of the membrane, was observed in the RTgutGC cell layer after 8-10 days of culture.

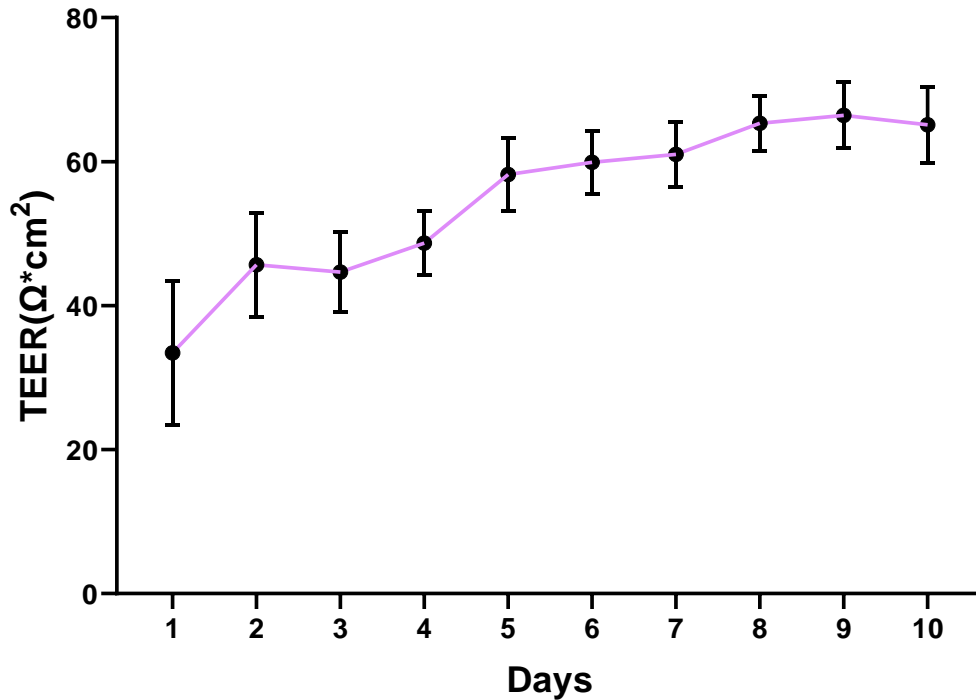


Figure 5.6.1: Transepithelial electrical resistance (TEER) of RTgutGC cells. Cells were seeded at a density of 150,000 cells/ml on transwell membrane inserts (0.4 μm pore size) and grown for up to 10 days. Cells were cultured continuously under symmetrical conditions in L-15/FBS in both apical and basolateral compartment. Data represent the mean \pm standard deviation (SD) from three independent replicates. Significant difference was observed over time (One-way ANOVA $p > 0.05$)

5.6.1 Effects of chlorpyrifos on the transepithelial electrical resistance

The effect of CPF on membrane integrity and permeability of the RTgutGC cell monolayer after 24 hours is shown in figure 5.6.2. As described in the method section cultures were treated with CPF in the dose range of 0.5 – 500 μM . The TEER values are shown in percent, where the TEER values measured 24 hours after the addition of CPF divided by the TEER values measured before the addition of CPF multiplied by 100. The average baseline TEER values of the monolayers (on day 10) varied from 59 -76 $\Omega\cdot\text{cm}^2$. Cell cultures in L-15 media containing 0.2% DMSO (control) did not significantly alter the initial TEER values after 24 hours. CPF caused a dose dependent decrease in TEER values. TEER levels of cells exposed to low concentrations of CPF were not

affected, however TEER levels exposed to higher concentrations of CPF (50 – 500 μM) were significantly lower than those of control cells. Cell death was induced in all wells exposed to 500 μM CPF, decreasing the TEER values close to background levels.

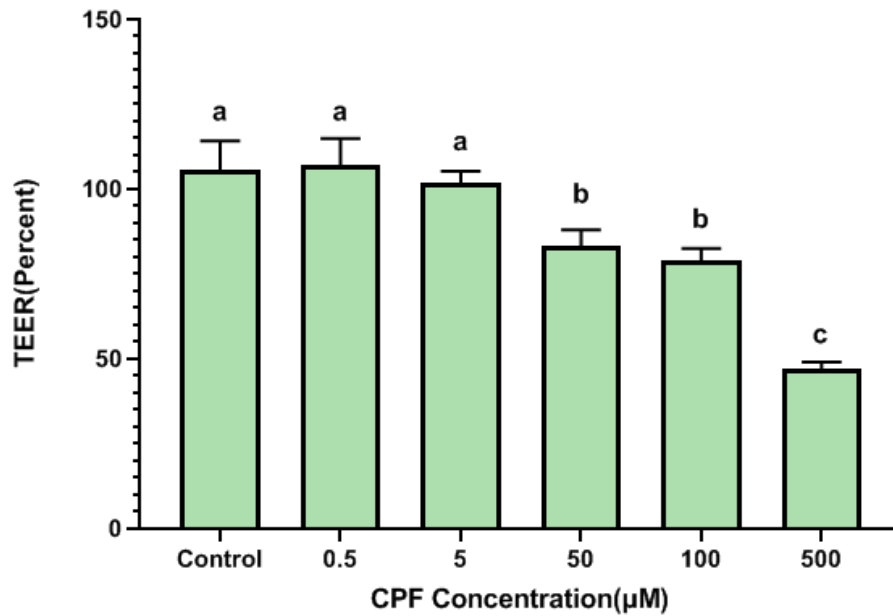


Figure 5.6.2: Transepithelial electrical resistance (TEER) values in RTgutGC cells after treatment with different concentrations of chlorpyrifos (CPF) for 24 h compared with the initial value. Results are expressed as the mean \pm SD of three independent experiments. Different letters (a,b,c) indicate significant differences in TEER (One - way ANOVA, $p < 0.05$).

5.7 Gene expression

5.7.1 Transcription of genes involved in detoxification

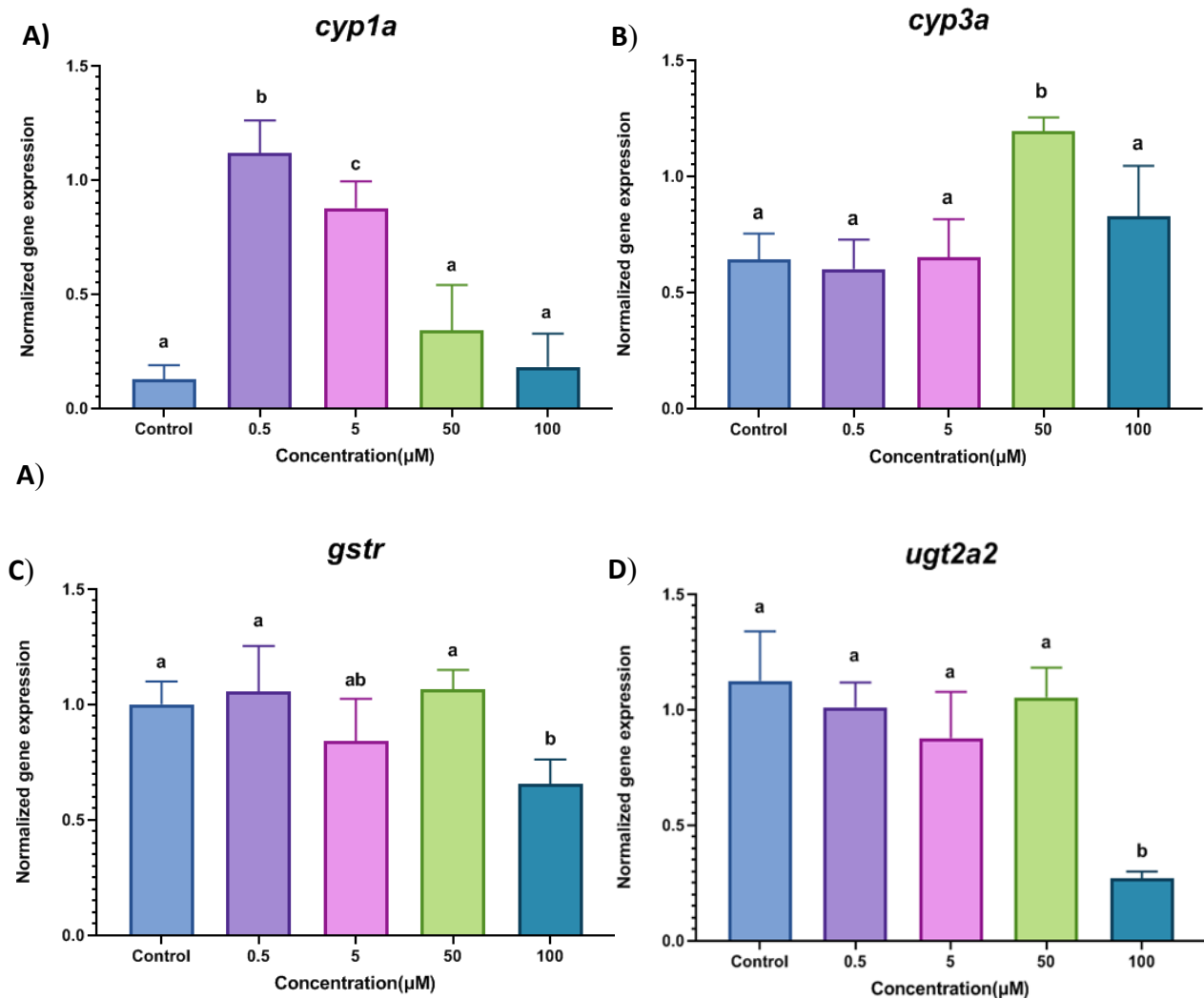


Figure 5.7.1: Expression of genes involved in detoxification, A) *cyp1a*, B) *cyp3a*, C) *gstr*, D) *ugt2a2* in rainbow trout gut cells (RTgutGC) exposed to chlorpyrifos (CPF) and DMSO control (0.2%) for 24 hours. mRNA expressions are represented as mean normalized expression and the values represent mean \pm SD of six replicates (n=6). Different letters indicate statistical differences in mean values between treatments (One-way ANOVA, $p < 0.05$)

Cell death was induced in all cell cultures exposed to 500 μM CPF and this exposure was therefore excluded from the gene expression experiment. Figure 5.7.1 shows the induction of the *cyp1a*, *cyp3a*, *gstr* and *ugt2a2* mRNA in RTgutGC cells 24 hours after exposed to 0.5 – 100 μM CPF. All four genes, *cyp1a* ($p = 2.07\text{e-}12$), *cyp3a* ($p = 8.23\text{e-}07$), *gstr* ($p = 0.000113$) and *ugt2a2* ($p = 2.16\text{e-}09$) were significantly affected by the exposure. *cyp1a* was significantly up regulated at 0.5 and 5 μM CPF with a fold change of 8.8 and 6.9, respectively. *cyp1a* seemed to downregulate with the increasing CPF concentration. *cyp3a* expression was significantly upregulated at 50 μM CPF with a fold change of 1.86. Both *gstr* and *ugt2a2* mRNA expression was significantly downregulated at 100 μM CPF, but was not significantly altered in cells exposed to CPF lower concentrations of CPF.

5.7.2 Transcription of genes involved in lipid metabolism

The expression of genes involved in the lipid metabolism in RTgutGC cells 24 hours after exposed to 0.5 – 100 μM CPF are shown in figure 5.7.2. All three genes, *lpcat2* ($p = 0.00545$), *pparab* ($p = 0.000662$) and *plin2* ($p = 3.1\text{e-}13$) were significantly affected by CPF exposure. The mRNA expression levels of *lpcat2* significantly decreased at 100 μM CPF. *lpcat2* expression slightly increased at 50 μM but was not significantly different compared to the control. Similar to *lpcat2*, the expression of *pparab* was significantly downregulated at 100 μM CPF and the *pparab* expression of cells treated with 0.5 – 50 μM CPF was not significantly different compared with the controls. The mRNA expression of *plin2* was low in the controls compared with the controls of *lpcat2* and *pparab*. Expression levels were also low in cells exposed to low concentrations of CPF (0.5 and 5 μM). However, the expression levels significantly peaked at 50 and 100 μM CPF compared with the controls. *plin2* mRNA levels of the cells exposed to 50 and 100 μM CPF had a fold change of 9.8 and 4.8 respectively.

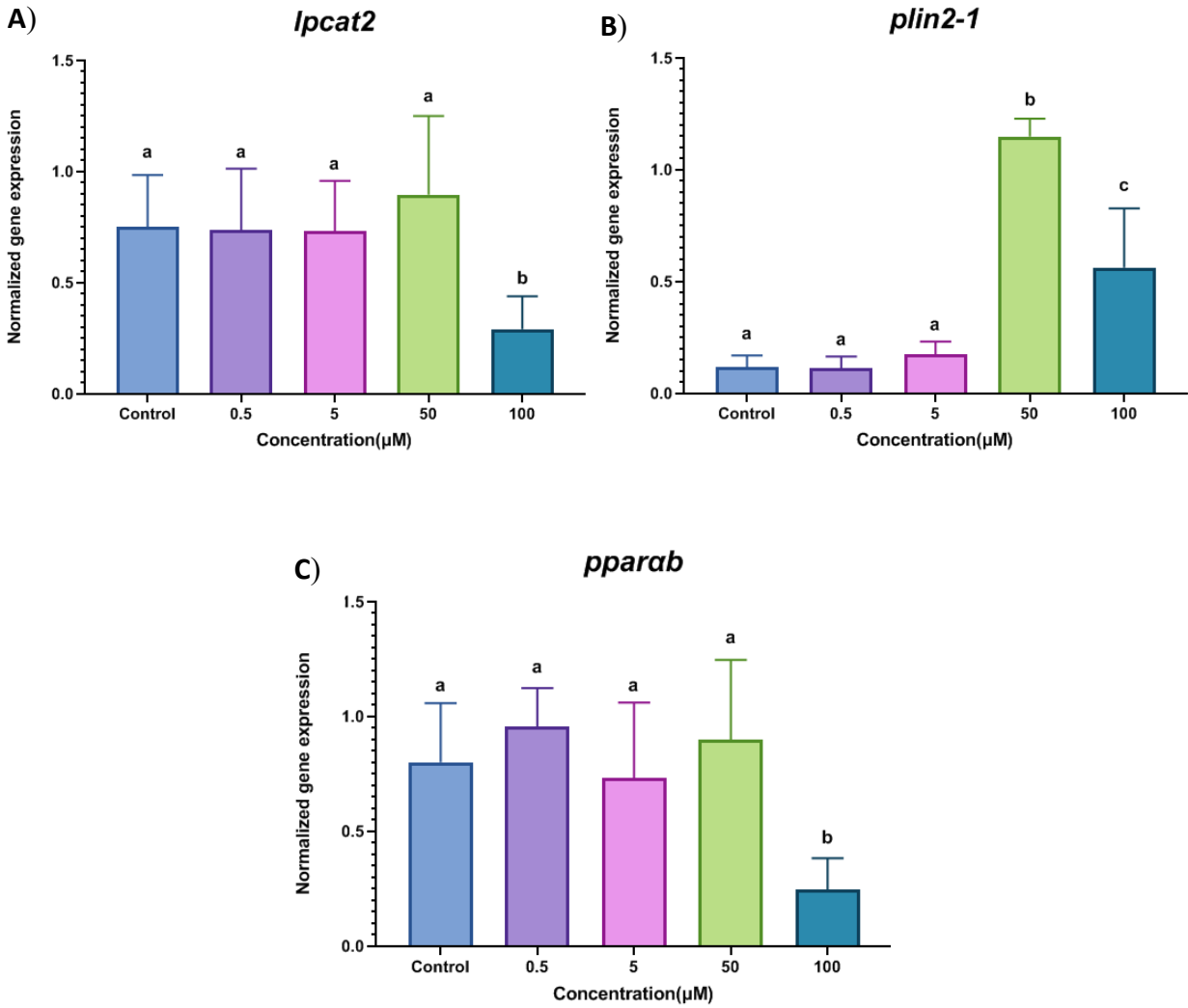


Figure 5.7.2: Expression of genes involved in lipid metabolism, A) *lpcat2*, B) *plin2-1*, C) *pparab* in rainbow trout gut cells (RTgutGC) exposed to chlorpyrifos (CPF) and DMSO control (0.2%) for 24 hours. mRNA expressions are represented as mean normalized expression and the values represent mean \pm SD of six replicates (n=6). Different letters indicate statistical differences in mean values between treatments (One-way ANOVA, $p < 0.05$)

6. Discussion

This study aimed to assess how oral exposure to, chlorpyrifos (CPF), an organophosphate pesticide, affects the intestinal health in Atlantic salmon. A two-month feeding trial was conducted where the fish were fed with a fish meal diet (control) and a soybean meal diet. At the end of the feeding trial, the intestinal sac of fish from the different feeding groups were excised. The effect of CPF on intestinal permeability of these intestinal sacs was measured using a gut sac model. Histological assessment on the intestinal tissue samples were performed to examine the effects of the CPF and saponin (a natural toxin from soybean). Results from the gut sac model indicated that permeability of intestinal sacs was not affected by saponin and CPF exposure. Histological evaluation observed no inflammation on intestinal segments exposed to both CPF and saponin. Furthermore, an intestinal cell line, RTgutGC, derived from rainbow trout was used as an in vitro model for salmon. TEER, qPCR analysis and xCELLigence cytotoxicity analysis were performed on cell cultures exposed to different concentrations of CPF. Results showed that as the CPF concentration increased the cell viability/ integrity of the cell monolayer decreased.

6.1 Saponin showed no effects on fish intestine

Atlantic salmon exposed to soya saponin over a period of two months had little effect on its body weight (Figure 5.2.1). Studies have shown that saponins inhibit the activities of digestive enzymes, reduce overall growth rate, and reduce intestinal absorption of nutrient through binding of saponins to the epithelium (Francis et al., 2001; Kregiel et al., 2017; Samtiya et al., 2020).

According to Knudsen et al., 2008 and Sahlmann et al., 2015, Atlantic salmon that received a SBM diet did not significantly differ in growth compared to fish that received a FM diet, which agrees with our results. A possible reason for this could be that the effects of the soy saponin could have been less severe with the prolonged experimental period through a compensatory growth after the fish adapted to these unfavorable toxins (Chen et al., 2011). Complex formations between saponin together with other soybean components could also lead to inactivation of the toxic

effects of the saponins (Francis et al., 2001; Makkar et al., 1995). Olli et al., 1995 and Sørensen et al., 2011 showed that dietary SBM often had a negative impact on growth rate in Atlantic salmon. However, M. Gu et al., 2015 showed that Atlantic salmon fed with SBM showed a significantly higher body weight than those fed FM. The varying effects of saponin observed in different studies maybe due the varying doses of saponins in the diets, differences in sensitivity in different/induvial species and the exposure period (Gu et al., 2015) .

According to Chikwati et al., 2013; Knudsen et al., 2008; Sørensen et al., 2011 and Krogdahl et al., 2015 Atlantic Salmon fed SBM displayed severe enteritis in the distal intestine. SBM containing diet is known to cause inflammation in the distal intestine but not in other parts of the intestinal region (Chikwati et al., 2013; van den Ingh et al., 1991). Histological analysis from our results showed no entities in the mid intestine of fish fed with SBM; However, an increased amount of goblet cells was observed.

The mucus layer is normally impermeable to microbes, toxins and other environmental irritants thus protecting the underlying epithelium (Johansson & Hansson, 2014). Evidence from both clinical and animal studies have indicated that inflammation can be caused by impaired goblet cell function which in turn affects the mucin quality and quantity (Grondin et al., 2020). The increased goblet cell density may have been the result of hypertrophic mucus production when subjected to irritation by saponins (Francis et al., 2001). This might be also true for intestinal segments exposed to CPF, since an increased amount of goblet cells were also seen in intestinal segments exposed to CPF. Increased goblet cells in the controls could be due to stressed fish before the experiment.

The gut sac model from our study showed no effect of soya saponins on gut permeability in the mid intestine. (Knudsen et al., 2008) showed that dietary soya saponins increased gut permeability in the distal intestine in Atlantic salmon. Inflammatory reactions in the gut are secondary effects of increased intestinal permeability (Knudsen et al., 2007). Increased intestinal

permeability could expose the underlying mucosa to gut microflora that can promote inflammatory responses (Knudsen et al., 2007).

The posterior part of the intestine (proximal and mid) is considered to be the main site of nutrition absorption, and therefore contains less microbes than the distal intestine (Jutfelt, 2011). This might be the explanation to why we see inflammation in the distal intestine, and not in the mid intestine. The binding and the lower dissociation constant of soya saponin to the intestinal brush border membranes might also be higher in the distal intestine than the mid intestine, which may also lead to increased intestinal permeability and therefore inflammation (van den Ingh et al., 1991).

6.2 Increased permeability is not seen in guts exposed to chlorpyrifos

The gut sac technique has proven to be an excellent *ex vivo* model for studying the intestinal transport process (Mateer et al., 2016; Whittamore et al., 2016). The gut sac model was used to study the apparent permeability (P_{app}) of the FITC-D molecule across the intestinal barrier in our experimental setup. Our results showed that the permeability of intestinal segments exposed to 500 μ M CPF was no different than the control.

To our knowledge no studies have been done on intestinal permeability of CPF in teleost fish. However, numerous studies have been done on this subject in rodents (Condette et al., 2014; Liang et al., 2019; Zhao et al., 2016). Zhao et al., 2016 showed that mice fed with CPF diet over 30 days caused broken integrity of the gut barrier which resulted in intestinal inflammation and a high intestinal permeability. Condette et al., 2014 also observed increased intestinal permeability of rats exposed to daily ingestion of CPF. In our study the intestinal segments were exposed to CPF for a total of 3 hours, collecting samples at 20-minute time intervals. Possible reasons for the lack of effect of CPF on gut permeability could mainly be the duration of the exposure period, dosage, and the size of the fish. Intestinal permeability may also vary greatly in different regions of the intestine. However an unpublished study by Le Bideau et al, 2019, figure

6.2.1 showed that intestinal segments exposed to 500 μM CPF increased gut permeability in Atlantic salmon, but there was a significant difference in fish size compared with our study .

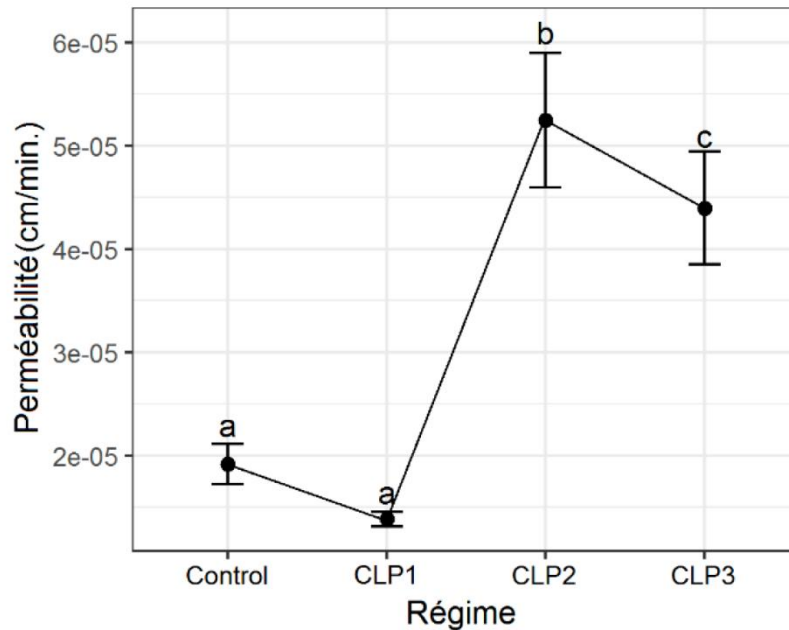


Figure 8 : Moyennes des Papp en fonction des régimes de CLP administrés. CLP1, CLP2, CLP3 : 250 μM , 500 μM , 1000 μM ; 6 échantillons par régime ; Control : 2 échantillons. Barres d'erreurs : écart-types standards ; Comparaison des moyennes : ANOVA puis test de Tukey ($p < 0.05$).

Figure 6.2.1 Intestinal permeability in the mid intestinal sacs of Atlantic salmon exposed to CPF. CLP1, CLP2, CLP3: 250 μM , 500 μM , 1000 μM chlorpyrifos, respectively. From Le Bideau (2019).

Cook & Shenoy, 2003 investigated the intestinal transport of CPF, using the single-pass intestinal perfusion (SPIP) technique on rats and the results showed that the duodenum and ileum exhibit a decrease in permeability at the highest CPF concentration, which is in line with our results. The low permeability of the FITC-D molecules on the intestinal segments exposed to CPF in our experiment could suggest that CPF is transported primarily via a passive, transcellular mechanism across the intestinal epithelium with a saturable process, potentially via a membrane transport protein (Cook & Shenoy, 2003).

It is important that each intestinal sac is cut in equal length and the sac is filled with the correct volume to avoid unequal distension of the mucosa. Under-distension of the intestinal segment may reduce the exposure of luminal contents to the mucosal surface and increase the thickness of the tissue through which the marker (FITC-D) must travel (Mateer et al., 2016). Over-distension of the segment may damage or activate stress-responses in the tissue, potentially confounding results (Mateer et al., 2016). Permeability also largely depends on size, hydrophobicity and quality of the probe (Mateer et al., 2016; Trapani et al., 2004).

The lack of effects observed in the gut sac model can be confirmed from the histological analysis. The exposed and the non-exposed intestinal segments (control) to CPF, induced no inflammation. Khatun et al., 2016 and Stalin et al., 2019 carried experiments on *H.fossilis* and *Channa punctatus* respectively, and were exposed to CPF for 30 days. The histopathological alteration of both species had shown continuous damage to the intestine. The histological alterations were found to be dose and time dependent as the cellular alterations were more pronounced with the higher concentration and exposure duration period of CPF.

6.3 Cytotoxicity of chlorpyrifos

As mentioned before, the xCELLigence RTCA system measures the net adhesion of cells. In the absence of cells, the impedance is mainly determined by the electron flow between the electrodes in the presence of a bulk solution. Adhering cells disrupt the interaction between the electrodes and the bulk solution, leading to an increase in impedance. Impedance is mainly dependent on cell number, cell morphology and cell size and on the strength of cell attachment to the substrate coating the plate (Hamidi et al., 2017).

Normally cell plates are coated with extra cellular matrix (ECM) proteins where cells bind using transmembrane proteins called integrins, thus increasing the efficiency of cell adhesion (Hamidi et al., 2017). Higher concentrations of CPF induce cell detachment by disrupting these proteins resulting in low impedance values.

According to the international standard for in vitro cytotoxicity testing (ISO, 2009), the reduction of cell viability to contaminants by more than 30% is considered a cytotoxic effect. Based on the ANOVA analysis the xCelligence system showed 38%, 55% and 100% cell viability reduction, from the controls, in cells exposed to 50, 100, 500 μM CPF, respectively. The regression model showed 34%, 52% and 100% cell viability reduction from the baseline. Therefore, we can confirm that RTgutGC cells exposed to CPF concentrations of 50 μM and upwards induce cytotoxicity.

Babín & Tarazona, 2005 found CPF to be the most potent compound of out of six pesticides tested in rainbow trout liver (RTL-W1) and rainbow trout gonadal (RTG 2) cell lines in a Neural red and FRAME KB protein assay and the inhibition of EROD activity was observed at the lowest tested concentration 0.02 mg/L for CPF. Sjøfteland et al., 2014 and Olsvik & Sjøfteland, 2020 observed that Atlantic salmon hepatocytes exposed up to 1000 μM CPF and chlorpyrifos-methyl (CPM) were not cytotoxic, which is not in line with our results. These studies have used primary hepatocyte cell cultures and the reason for the differences in sensitivity between salmonid primary hepatocytes and cell lines to CPF is unknown (Sjøfteland et al., 2014).

6.3.1 ANOVA vs Regression model

The NOAEL and the LOAEL values for CPF in RTgutGC cells from the exposure response curve determined by the ANOVA model were 5 and 10 μM respectively. The LC50 value was 84 μM determined by linear interpolation. The LC50 and BMC5 values of CPF for the cells, determined by the sigmoid curve equation were 89 ± 0.12 and 13.5 ± 0.06 μM , respectively.

The regression from the sigmoid curve is based upon the fit to the entire dataset and the line is generated by an assumed modeled relationship between all these points. NOAEL and LOAEL values are not applicable in this context as the regression yields a continuous function. However, a benchmark concentration (BMC) method is more applicable to use in a regression model. The BMC method was proposed as an alternative by Crump, 1984 to address many limitations of the NOAEL/LOAEL method. The BMC is more reliable than NOAEL/LOAEL since it is less dependent on dose selection, dose spacing and sample size (Crump, 1984; EPA, 2012). It also takes into account

the shape of the dose–response curve and other related information (EPA, 2012). BMC is a the concentration level associated with a specified change in the response called, benchmark response (BMR) (EFSA, 2016). BMR5 used in this study is the 5% decrease in cell adhesion compared with the base line cell adhesion.

Traditionally, NOAEL and LOAEL have been used to determine the point of departure (POD), which is a point on a dose/exposure response curve corresponding to estimated low effect or no effect level (EFSA, 2016). Since this approach has limitations, the BMD approach provides a promising method for calculating the POD (Crump, 1984; EFSA, 2016). NOAELs and LOAELs are based upon a hypothesis testing approach and provides a less detailed visualization and quantitative description of a toxic response than a regression model (Landis et al,2017). Therefore, the BMC5 and LC50 determined from the regression model in this study would yield more accurate values.

6.4 TEER over time

TEER is a rapid, non- invasive method for measuring the electrical resistance across a cellular monolayer and is very sensitive and reliable method to confirm the integrity and permeability of the monolayer (Hickman, 2016; Shuler & Hickman, 2016). TEER indicates the integrity of the tight junction where it reflects the ionic conductance of the paracellular pathway in the epithelial monolayer (Hickman, 2016).

The RTgutGC cell line established a single monolayer on permeable insert membranes which led to a formation of functional epithelium that accommodated TEER levels up to $65 \pm 5.2 \Omega \cdot \text{cm}^2$. According to Loretz, 1995, Claude & Goodenough, 1973 and Sundell et al., 2003 our low TEER values can be characterized as a leaky epithelia. The increasing TEER value overtime is probably due to the growth and proliferation of the RTgutGC which can be attributed to the increase in tightening of cell – cell contacts (Schug et al., 2018). TEER values reach a plateau when the cells form a confluent monolayer.

The TEER values obtained from the RTgutGC cell line appears to be closely related to the TEER values obtained from the distal intestinal segments of Atlantic salmon adapted to fresh water (Sundell et al., 2003). Thus the RTgutGC cell line appears to closely reflect the in vivo transepithelial resistance in salmonids (Minghetti et al., 2017). Higher TEER values were observed in Atlantic salmon and Rainbow trout in the distal compared to the proximal intestine (Sundell et al., 2003; Sundell & Sundh, 2012). This is due to the need for a tighter barrier increases as the bacterial levels peaks in the distal intestine (Jutfelt, 2011; K. S. Sundell & Sundh, 2012).

Although TEER measurements are very powerful they can also be subjected to variability. In addition to the cell monolayer, the medium, the permeable membrane and the electrode/medium interface all contribute to the final TEER values and subtracting these values from a blank removes much of the variability (Hickman, 2016). Temperature is known to affect the TEER measurement (Hickman, 2016; Shuler & Hickman, 2016). For the RTgutGC cell line, the TEER measurements should be conducted in 19 °C room temperature to obtain consistent values. The position of the chopstick electrodes can also introduce variability between measurements and therefore it is important to maintain the same vertical holding position to obtains consistent read outs (Shuler & Hickman, 2016). Other factors such as cell passage number, cell culture medium composition and shear stress could also influence the TEER values (Shuler & Hickman, 2016).

6.5 TEER after chlorpyrifos exposure

Exposure of CPF to RTgutGC cells for 24 hours led to a concentration dependent decrease in the TEER values. Reasons for the reduction of TEER values could be the increase in paracellular permeability to ions due to the disruption to the tight junctions, changes in transcellular ion flux through altered plasma membrane channels or pumps or uncontrolled cell death within the monolayer (Gao et al., 2018). From this angle the decreased TEER of cells exposed to low concentrations of CPF (0.5 and 5 µM) could be due to the increase in paracellular permeability and low TEER of cells exposed to high concentrations of CPF is due to cell membrane disruption and cell death.

Numerous studies have been conducted on the intestinal integrity of Caco2 cells (Gao et al., 2018; Okada et al., 2000). Tirelli et al., 2007 investigated the effects of CPF on the intestine and the integrity of the epithelial barrier using Caco-2/TC7 cells. Results showed that the TEER values of the cells exposed to the highest concentration of CPF (250 μ M) decreased, indicating a leaky gut, which agrees with our results. Similar results have been seen in caco-2 monolayers exposed to other contaminants (Gao et al., 2018). Considering the fact that Caco-2 cells are known to develop a much tighter epithelium, indicated by higher TEER values (150 - 400 Ω cm²) (Shuler & Hickman, 2016), the RTgutGC cell line seem to have a similar physiological response to CPF.

6.6 Effects of chlorpyrifos on the genes involved in detoxification

6.6.1 *cyp1a* expression

Our study investigated four key genes related to xenobiotic biotransformation. The mRNA expression of *cyp1a* increased in cells treated with 0.5 CPF and then decreased in a concentration dependent manner. Normally *cyp1a* expression is low in cells that has not been exposed to contaminants (Goksøyr et al., 1991). Our results from the xCelligence analysis showed that CPF concentrations over 50 μ M were cytotoxic to the RTgutGC cells. This could explain the low expression levels of *cyp1a* in cells exposed to 50 and 100 μ M CPF. As the CPF concentration increased, the expression capacity of *cyp1a* was possibly overwhelmed and inhibited, which counteracted the effects of induction (Liguori et al., 2012). The decreased *cyp1a* expression at 5 μ M CPF was not due to cytotoxicity, which can be confirmed from the xCelligence cytotoxicity test. The mechanism behind the low expression at non cytotoxic concentrations is unclear.

The AhR receptor, which regulates transcription of the *cyp1a* gene, can be activated by ligands to induce transcription of its target genes. It is possible that some ligands may regulate the effects of AhR differently between tissue / cell types (Liguori et al., 2012). CPF can undergo bioactivation by CYP1A to a more toxic metabolite called CPF-oxon, which is more active and less stable than the parent compound (Sams et al., 2004). The sulfur ion released in CPF activation is highly reactive and is believed to bind immediately to the heme iron of the CYP protein inhibiting its

activity (Tang et al., 2002; Neal, 1980). It is also possible that CPF-oxon may inhibit the AhR receptor or other enzymes that involve in the AhR pathway or increase the AhR repressor proteins, resulting in decreasing *cyp1a* expression levels.

Several studies have shown the upregulation of *cyp1a* mRNA expression after CPF exposure in different fish species (Jeon et al., 2016; Sjøfteland et al., 2014; Xing et al., 2014), which agrees with our results. This indicates that chlorpyrifos induces *cyp1a* expression, but that the expression may be inhibited at higher concentrations.

6.6.2 *cyp3a* expression

CYP3A are major phase I enzymes that are mainly expressed in the intestine (Lee & Buhler, 2003). Our results showed that cells exposed to low concentrations of CPF had no effect on the *cyp3a* expression levels. However, the mRNA expression of *cyp3a* was significantly upregulated in RTgutGC cells exposed to high concentration of CPF indicating that it is a weak *cyp3a* inducer (Sjøfteland et al., 2014). This might possibly be due to a low affinity of CPF to the salmonid PXR receptor, the main transcription factor involved in CYP3A regulation, although studies with human PXR has shown a moderately strong affinity (Lemaire et al., 2004). In humans, several different CYP isoforms have been shown to be involved in CPF metabolism, including CYP3A (Tang et al., 2001).

Atlantic salmon hepatocytes exposed to CPF showed no significant effects on *cyp3a* expression (Olsvik et al., 2019). Jeon et al., 2016 showed up regulation and Ma et al., 2013 showed downregulation of *cyp3a* in zebrafish and gold fish exposed to CPF, respectively. These conflicting results demonstrate that alteration of *cyp3a* genes after CPF exposure is dependent on the species analyzed.

6.6.3 *gst* and *ugt* expression

Glutathione *S*-transferase (*gst*) and UDP-glucuronosyl-transferase (*ugt*) are genes coding for enzymes involved in the phase II of xenobiotic detoxification. In the present study *gst* and *ugt* did not responded to the treatment of CPF, except in the cells exposed to 100 μ M CPF, which was significantly downregulated compared to the control.

I propose several possible explanations for the *gst* observation. Transcription of certain *gst* isomers are tissue specific and expressed differently in different organs and the abundance of different isoforms of GST within the organ is also variable (Coles et al., 2002; Hao et al., 2008; Xing et al., 2012). CPF or CPF - oxon might also influence the transcription-regulating factors that bind to the promoter region of the *gst* gene and inhibit the transcription of *gst* (Xing et al., 2012). These explanations might also be true for *ugt* since few studies have been conducted on the effects of pesticides on *ugt* gene expression in fish.

According to Bonifacio et al., 2017 the activity of GST was not detected in any of the studied organs in *C. interruptus* exposed to CPF. The hepatic GST activity was also not affected by CPF in juvenile spiny damsel fish (Botté et al., 2012). However, Olsvik et al., 2019 showed that four transcripts encoding GST proteins were significantly different compared with the control in Atlantic cod exposed to medium (4.2 mg CPM/kg) and high (23.2 mg CPM/kg) doses of CPM, supporting GST-mediated conjugation of CPM and CPF-oxon, in fish.

Although no significant difference was observed in the *gst* and *ugt* expression in our study, these enzymes may still play an important role in the detoxification of CPF. However, the response of *gst* and *ugt* to toxicants is most likely dependent on the type of xenobiotics, concentration and time of exposure and the species involved (Botté et al., 2012).

6.7 Effects of chlorpyrifos on the genes involved in lipid metabolism

CPF exposure had no effect on the *ppara* and *lpcat2* gene expressions, except for the highest concentration of CPF (100 μ M). Normally *ppara* expression is high in hepatocytes where it has important roles in fatty acid oxidation, triglyceride clearance, cholesterol homeostasis, and lipoprotein production (Decara et al., 2020; Kersten, 2008). Various chemicals are known to alter the *ppara* gene expression (Intrasuksri et al., 1998; Taxvig et al., 2012)

Takeuchi et al., 2006 characterized mouse *ppara* and *ppary* agonistic activities in an *in vitro* reporter gene assay screening study with 200 pesticides, including CPF. This study showed that only three (diclofop-methyl, pyrethrins, and imazalil) could activate *ppara* and none of them could activate *ppary*. Taxvig et al., 2012 also showed that CPF had no effect on mRNA *ppara* activation in nih-3t3 cells. These studies are in line with our results suggesting that CPF might not interact with PPARs. Less information is available about the effects of pesticides on *lpcat2* gene expression. It is clear from our results that CPF does not affect the *lpcat2* expression.

We observed an increase in mRNA levels of *plin2* in cells exposed to cytotoxic concentrations of CPF. *Plin2* is involved in the formation of lipid droplets and regulates lipid storage and hydrolysis. The increased *plin2* expression might be due to increased lipid droplet accumulation and TAG storage (Jin et al., 2018). Lipid droplets accumulate in cells exposed to oxidative stress in order to protect membranes from peroxidation reactions, maintain membrane saturation and organelle homeostasis, protect cells against reactive oxygen species (ROS) and enable a long-term supply of lipids for energy production and cell survival (Jarc & Petan, 2019; Olzmann & Carvalho, 2019). Thus, high expression of *plin2* in cells exposed to cytotoxic concentrations of CPF enhance the lipid droplet formation that are essential for the cellular response to metabolic stress. Our results are in close agreement with those previously reported in trout treated with colchicine (Seiliez et al., 2016) and bafilomycin A1 (Seite et al., 2019) that led to a similar increasing effect on *plin2* expression.

7. Conclusion

In conclusion, this study showed that CPF exposure using the gut sac model did not increase the intestinal permeability in Atlantic salmon. Fish fed with SBM exposed to saponin also showed no effect on the intestinal permeability. Furthermore, no inflammation was seen in the mid-gut exposed to both CPF and saponin. From the gut sac experiment we can conclude that CPF at 500 μM were not able to induce any effects on the intestinal epithelium of Atlantic salmon.

Higher concentrations of CPF led to a decrease in the TEER in the RTgutGC cell line. This indicated that CPF may interfere with the TJ proteins altering the barrier integrity increasing gut permeability. Results from the expression of genes involved in detoxification revealed that *cyp3a*, *gst* and *ugt* were not affected by the CPF exposure, except for the higher doses with *cyp3a*. CPF did not seem to influence the lipid metabolism genes, *ppara* and *lpcat2*, expression. However, CPF clearly upregulated *plin2* expression at high concentrations. Furthermore, this study showed that CPF is cytotoxic at 50 μM in the RTgutGC cell line.

8. Further perspectives

The work presented in this thesis showed that CPF and saponin had no effect on the mid intestinal epithelium of Atlantic salmon in the gut sac model. Further experiments should be done with the same experimental setup by increasing the exposure time period for CPF. For future experiments, a feeding trial with a daily dose of CPF together with SBM and FM (control) should be conducted to see how this would affect the results. Furthermore, samples from both distal and mid gut should also be collected for histological evaluation.

No relevant intestinal cell lines from fish have been available until recently. We have used the intestinal cell line RTgutGC derived from rainbow trout as a substitute for Atlantic salmon. More

research is required in the future for establishing a gut cell line derived from salmon, for more accurate results for this species.

To understand the role between CPF and intestinal permeability, the gene expression of TJ proteins (claudins and occludins) should be studied. A direct measurement of the protein activity of TJ proteins would also provide a more detailed impression on how these are affected by CPF. Furthermore, it would be also interesting to study the paracellular flux of fluorescent tracers across the cell layer in the presence of different concentrations of CPF.

Farmed fish are constantly being exposed to, not just CPF, but a cocktail of pesticides through fish feed. Pesticide mixtures can be more harmful than individual chemicals (Relyea, 2009). It is therefore important to do further research to determine the types of pesticide residues that can be found in fish feed, and how these alone or together affect the gut health of Atlantic salmon.

9. References

- Adedeji, O. B., & Okocha, R. O. (2012). Overview of pesticide toxicity in fish. *Advances in Environmental Biology*, 6(8), 2344–2351.
- Aktar, W., Sengupta, D., & Chowdhury, A. (2009). Impact of pesticides use in agriculture: Their benefits and hazards. *Interdisciplinary Toxicology*, 2(1), 1–12. <https://doi.org/10.2478/v10102-009-0001-7>
- Ašmonaite, G., Sundh, H., Asker, N., & Carney Almroth, B. (2018). Rainbow Trout Maintain Intestinal Transport and Barrier Functions Following Exposure to Polystyrene Microplastics. *Environmental Science and Technology*, 52(24), 14392–14401. <https://doi.org/10.1021/acs.est.8b04848>
- Ayisi, C., Zhao, J., & Apraku, A. (2019). Consequences of Replacing Fish Oil with Vegetable Oils in Fish. *Journal of Animal Research and Nutrition*, 4(1), 1–11. <https://doi.org/10.21767/2572-5459.100053>
- Babín, M. M., & Tarazona, J. V. (2005). In vitro toxicity of selected pesticides on RTG-2 and RTL-W1 fish cell lines. *Environmental Pollution*, 135(2), 267–274. <https://doi.org/10.1016/j.envpol.2004.11.001>
- Bashir, I., Lone, F. A., Bhat, R. A., Mir, S. A., Dar, Z. A., & Dar, S. A. (2020). Concerns and threats of contamination on aquatic ecosystems. *Bioremediation and Biotechnology: Sustainable Approaches to Pollution Degradation Concerns and Threats of Contamination on Aquatic Ecosystems*, 1–26. https://doi.org/10.1007/978-3-030-35691-0_1
- Beilstein, F., Carrière, V., Leturque, A., & Demignot, S. (2016). Characteristics and functions of lipid droplets and associated proteins in enterocytes. *Experimental Cell Research*, 340(2), 172–179. <https://doi.org/10.1016/j.yexcr.2015.09.018>
- Beiras, R. (2018). Biotransformation. *Marine Pollution*, 205–214. <https://doi.org/10.1016/b978-0-12-813736-9.00012-x>
- Berntssen, M. H. G., Julshamn, K., & Lundebye, A. K. (2010). Chemical contaminants in aquafeeds and Atlantic salmon (*Salmo salar*) following the use of traditional- versus alternative feed ingredients. *Chemosphere*, 78(6), 637–646. <https://doi.org/10.1016/j.chemosphere.2009.12.021>
- Bhosale, S. V., Bhilave, M., & Nadaf, S. (2010). Formulation of Fish Feed using Ingredients from Plant Sources. *Research Journal of Agricultural Sciences*, 1(3), 284–287.
- Biscaldi, G. P., Fonte, R., & Candura, S. (1986). Toxicology of pesticides. *Medecine Biologie Environnement*, 14(1), 231–238. <https://doi.org/10.1136/oem.34.2.152>
- Bischoff, S. C., Barbara, G., Buurman, W., Ockhuizen, T., Schulzke, J. D., Serino, M., Tilg, H., Watson, A., & Wells, J. M. (2014). Intestinal permeability - a new target for disease prevention and therapy. *BMC Gastroenterology*, 14(1), 1–25. <https://doi.org/10.1186/s12876-014-0189-7>
- Bonifacio, A. F., Ballesteros, M. L., Bonansea, R. I., Filippi, I., Amé, M. V., & Hued, A. C. (2017). Environmental relevant concentrations of a chlorpyrifos commercial formulation affect two neotropical fish species, *Cheirodon interruptus* and *Cnesterodon decemmaculatus*. *Chemosphere*, 188(August), 486–493. <https://doi.org/10.1016/j.chemosphere.2017.08.156>

- Botté, E. S., Jerry, D. R., Codi King, S., Smith-Keune, C., & Negri, A. P. (2012). Effects of chlorpyrifos on cholinesterase activity and stress markers in the tropical reef fish *Acanthochromis polyacanthus*. *Marine Pollution Bulletin*, *65*(4–9), 384–393. <https://doi.org/10.1016/j.marpolbul.2011.08.020>
- Brock, W. J., & Hobson, D. W. (2007). Intestinal absorption and metabolism of xenobiotics in humans. *Toxicology of the Gastrointestinal Tract*, *33*(December), 321–344. <https://doi.org/10.1201/9781420004267.ch12>
- Camilleri, M., Lyle, B. J., Madsen, K. L., Sonnenburg, J., Verbeke, K., & Wu, G. D. (2019). Role for diet in normal gut barrier function: Developing guidance within the framework of food-labeling regulations. *American Journal of Physiology - Gastrointestinal and Liver Physiology*, *317*(1), G17–G39. <https://doi.org/10.1152/ajpgi.00063.2019>
- Casarett, Louis J, Curtis D. Klaassen, Mary O. Amdur, and J. D. (1996). Casarett and Doull's Toxicology: The Basic Science of Poisons. In *Journal of Environmental Pathology, Toxicology and Oncology* (Vol. 15, Issues 2–4).
- Chelakkot, C., Ghim, J., & Ryu, S. H. (2018). Mechanisms regulating intestinal barrier integrity and its pathological implications. *Experimental and Molecular Medicine*, *50*(8). <https://doi.org/10.1038/s12276-018-0126-x>
- Chen, W., Ai, Q., Mai, K., Xu, W., Liufu, Z., Zhang, W., & Cai, Y. (2011). Effects of dietary soybean saponins on feed intake, growth performance, digestibility and intestinal structure in juvenile Japanese flounder (*Paralichthys olivaceus*). *Aquaculture*, *318*(1–2), 95–100. <https://doi.org/10.1016/j.aquaculture.2011.04.050>
- Chikwati, E. M., Gu, J., Penn, M. H., Bakke, A. M., & Kroghdahl, Å. (2013). Intestinal epithelial cell proliferation and migration in Atlantic salmon, *Salmo salar* L.: Effects of temperature and inflammation. *Cell and Tissue Research*, *353*(1), 123–137. <https://doi.org/10.1007/s00441-013-1631-9>
- Cho, C. Y. (1990). Fish nutrition, feeds, and feeding: With special emphasis on salmonid aquaculture. *Food Reviews International*, *6*(3), 333–357. <https://doi.org/10.1080/87559129009540876>
- Claude, P., & Goodenough, D. A. (1973). Fracture faces of zonulae occludentes from “tight” and “leaky” epithelia. *Journal of Cell Biology*, *58*(2), 390–400. <https://doi.org/10.1083/jcb.58.2.390>
- Coles, B. F., Chen, G., Kadlubar, F. F., & Radominska-Pandya, A. (2002). Interindividual variation and organ-specific patterns of glutathione S-transferase alpha, mu, and pi expression in gastrointestinal tract mucosa of normal individuals. *Archives of Biochemistry and Biophysics*, *403*(2), 270–276. [https://doi.org/10.1016/S0003-9861\(02\)00226-6](https://doi.org/10.1016/S0003-9861(02)00226-6)
- Condetto, C. J., Khorsi-Cauet, H., Morlière, P., Zabijak, L., Reygnier, J., Bach, V., & Gay-Quéheillard, J. (2014). Increased gut permeability and bacterial translocation after chronic chlorpyrifos exposure in rats. *PLoS ONE*, *9*(7), 1–10. <https://doi.org/10.1371/journal.pone.0102217>
- Cook, T. J., & Shenoy, S. S. (2003). Intestinal permeability of chlorpyrifos using the single-pass intestinal perfusion method in the rat. *Toxicology*, *184*(2–3), 125–133. [https://doi.org/10.1016/S0300-483X\(02\)00555-3](https://doi.org/10.1016/S0300-483X(02)00555-3)
- Cotte, A. K., Aires, V., Fredon, M., Limagne, E., Derangère, V., Thibaudin, M., Humblin, E., Scagliarini, A., De Barros, J. P. P., Hillon, P., Ghiringhelli, F., & Delmas, D. (2018).

- Lysophosphatidylcholine acyltransferase 2-mediated lipid droplet production supports colorectal cancer chemoresistance. *Nature Communications*, 9(1).
<https://doi.org/10.1038/s41467-017-02732-5>
- Craig, S. (2009). Understanding Fish Nutrition, Feeds, and Feeding. *Fisheries*.
- Crump, K. S. (1984). A new method for determining allowable daily intakes. *Toxicological Sciences*, 4(5), 854–871. <https://doi.org/10.1093/toxsci/4.5.854>
- De Santis, S., Cavalcanti, E., Mastronardi, M., Jirillo, E., & Chieppa, M. (2015). Nutritional keys for intestinal barrier modulation. *Frontiers in Immunology*, 6(DEC).
<https://doi.org/10.3389/fimmu.2015.00612>
- Deb, N., & Das, S. (2013). Chlorpyrifos toxicity in fish: A Review. *Current World Environment Journal*, 8(1). <https://doi.org/10.12944/cwe.8.1.17>
- Decara, J., Rivera, P., López-Gambero, A. J., Serrano, A., Pavón, F. J., Baixeras, E., Rodríguez de Fonseca, F., & Suárez, J. (2020). Peroxisome Proliferator-Activated Receptors: Experimental Targeting for the Treatment of Inflammatory Bowel Diseases. *Frontiers in Pharmacology*, 11(May), 1–18. <https://doi.org/10.3389/fphar.2020.00730>
- Dow, T., & Company, C. (2011). 3 *The Chemical Industry in 2010*. 23–47.
<https://doi.org/10.1016/B978-1-4377-7842-7.00003-9>
- EFSA. (2019). Statement on the available outcomes of the human health assessment in the context of the pesticides peer review of the active substance chlorpyrifos. *EFSA Journal*, 17(8). <https://doi.org/10.2903/j.efsa.2019.5809>
- EFSA, 2016. (2016). *GUIDANCE DOCUMENT Use of the benchmark dose approach in risk assessment BMD approach in risk assessment*. December, 1–51.
<https://doi.org/10.2903/j.efsa.20YY.NNNN>
- Epa, U. S. (2012). *Benchmark Dose Technical Guidance/Risk Assessment Forum*. June, 1–99.
http://www.epa.gov/raf/publications/pdfs/benchmark_dose_guidance.pdf%5Cpapers3://publication/uuid/368C9919-510C-4DF4-8DB7-118B49D7F4CA
- Ernst, W. (1980). Effects of pesticides and related organic compounds in the sea. *Helgoländer Meeresuntersuchungen*, 33(1–4), 301–312. <https://doi.org/10.1007/BF02414756>
- FAO (1988). Definition of aquaculture, *Seventh Session of the IPFC Working Party of Experts on Aquaculture*, IPFC/WPA/WPZ, p.1-3, RAPA/FAO, Bangkok
- FAO (2020). (2020). *The State of World Fisheries and Aquaculture 2020*.
<https://doi.org/https://doi.org/10.4060/ca9229en> The
- Farré, R., Fiorani, M., Rahiman, S. A., & Matteoli, G. (2020). Intestinal permeability, inflammation and the role of nutrients. *Nutrients*, 12(4), 1–18.
<https://doi.org/10.3390/nu12041185>
- Francis, G., Kerem, Z., Makkar, H. P. S., & Becker, K. (2002). The biological action of saponins in animal systems: a review. *British Journal of Nutrition*, 88(6), 587–605.
<https://doi.org/10.1079/bjn2002725>
- Francis, G., Makkar, H. P. S., & Becker, K. (2001). Antinutritional factors present in plant-derived alternate fish feed ingredients and their effects in fish. In *Aquaculture* (Vol. 199, Issues 3–4). [https://doi.org/10.1016/S0044-8486\(01\)00526-9](https://doi.org/10.1016/S0044-8486(01)00526-9)
- Gao, Y., Li, S., Wang, J., Luo, C., Zhao, S., & Zheng, N. (2018). Modulation of intestinal epithelial permeability in differentiated caco-2 cells exposed to aflatoxin M1 and ochratoxin a individually or collectively. *Toxins*, 10(1), 1–19. <https://doi.org/10.3390/toxins10010013>

- Gelberg, H. (2018). Pathophysiological Mechanisms of Gastrointestinal Toxicity. In *Comprehensive Toxicology: Third Edition* (Third Edit, Vols. 3–15, Issue July 2016). Elsevier. <https://doi.org/10.1016/B978-0-12-801238-3.10923-7>
- Gerba, C. P. (2019). Chapter 28 - Environmental Toxicology. In *Environmental and Pollution Science (Third Edition)* (3rd ed.). Elsevier Inc. <https://doi.org/10.1016/B978-0-12-814719-1.00028-8>
- Giesy, J. P., Solomon, K. R., Coats, J. R., Dixon, K. R., Giddings, J. M., & Kenaga, E. E. (1999). Chlorpyrifos: Ecological risk assessment in North American aquatic environments. *Reviews of Environmental Contamination and Toxicology*, *160*, 1–129. https://doi.org/10.1007/978-1-4612-1498-4_1
- Gillois, K., Lévêque, M., Théodorou, V., Robert, H., & Mercier-Bonin, M. (2018). Mucus: An Underestimated Gut Target for Environmental Pollutants and Food Additives. *Microorganisms*, *6*(2), 53. <https://doi.org/10.3390/microorganisms6020053>
- Goksøyr, A., Andersson, T., Buhler, D. R., Stegeman, J. J., Williams, D. E., & Förlin, L. (1991). Immunochemical cross-reactivity of β -naphthoflavone-inducible cytochrome P450 (P450IA) in liver microsomes from different fish species and rat. *Fish Physiology and Biochemistry*, *9*(1), 1–13. <https://doi.org/10.1007/BF01987606>
- Grace, D., Abraham, S., Varghese, A., & Sathianarayanan, S. (2012). Absorption And Metabolism Of Xenobiotics: An Overview. *The Internet Journal of Nutrition and Wellness*, *7*(1), 1–4. <https://doi.org/10.5580/6b7>
- Grondin, J. A., Kwon, Y. H., Far, P. M., Haq, S., & Khan, W. I. (2020). Mucins in Intestinal Mucosal Defense and Inflammation: Learning From Clinical and Experimental Studies. *Frontiers in Immunology*, *11*(September), 1–19. <https://doi.org/10.3389/fimmu.2020.02054>
- Groschwitz, K. R., & Hogan, S. P. (2009). Intestinal barrier function: Molecular regulation and disease pathogenesis. *Journal of Allergy and Clinical Immunology*, *124*(1), 3–20. <https://doi.org/10.1016/j.jaci.2009.05.038>
- Gu, M., Gu, J. N., Penn, M., Bakke, A. M., Lein, I., & Krogdahl. (2015). Effects of diet supplementation of soya-saponins, isoflavones and phytosterols on Atlantic salmon (*Salmo salar*, L) fry fed from start-feeding. *Aquaculture Nutrition*, *21*(5), 604–613. <https://doi.org/10.1111/anu.12187>
- Gu, Min, Kortner, T. M., Penn, M., Hansen, A. K., & Krogdahl, Å. (2014). Effects of dietary plant meal and soya-saponin supplementation on intestinal and hepatic lipid droplet accumulation and lipoprotein and sterol metabolism in Atlantic salmon (*Salmo salar* L.). *British Journal of Nutrition*, *111*(3), 432–444. <https://doi.org/10.1017/S0007114513002717>
- Hamidi, H., Lilja, J., & Ivaska, J. (2017). Using xCELLigence RTCA Instrument to Measure Cell Adhesion. *Bio-Protocol*, *7*(24). <https://doi.org/10.21769/bioprotoc.2646>
- Hao, L., Xie, P., Fu, J., Li, G., Xiong, Q., & Li, H. (2008). The effect of cyanobacterial crude extract on the transcription of GST mu, GST kappa and GST rho in different organs of goldfish (*Carassius auratus*). *Aquatic Toxicology*, *90*(1), 1–7. <https://doi.org/10.1016/j.aquatox.2008.07.006>
- Helfrich, L., Weigmann, D., Hipkins, P., & Stinson, E. (2009). Pesticides and Aquatic Animals: A Guide to Reducing Impacts on Aquatic Systems | VCE Publications | Virginia Tech. *VCE Publications*. <https://www.pubs.ext.vt.edu/420/420-013/420-013.html>
- Hickman, J. (2016). Transepithelial/endothelial Electrical Resistance (TEER) theory and

- applications for microfluidic body-on-a-chip devices. *Journal of Rare Diseases Research & Treatment*, 1(3), 46–52. <https://doi.org/10.29245/2572-9411/2016/3.1026>
- Hites, R. A. (2021). The Rise and Fall of Chlorpyrifos in the United States. *Environmental Science & Technology*, 55(3), 1354–1358. <https://doi.org/10.1021/acs.est.0c06579>
- Husoy, A. M., Myers, M. S., Willis, M. L., Collier, T. K., Celander, M., & Goksoyr, A. (1994). Immunohistochemical Localization of CYP1A-Like and CYP3A-like Isozymes in Hepatic and Extrahepatic Tissues of Atlantic Cod (*Gadus morhua* L), a Marine Fish. In *Toxicology and Applied Pharmacology* (Vol. 129, Issue 2, pp. 294–308). <https://doi.org/10.1006/taap.1994.1254>
- Ibabe, A., Grabenbauer, M., Baumgart, E., Fahimi, D. H., & Cajaraville, M. P. (2002). Expression of peroxisome proliferator-activated receptors in zebrafish (*Danio rerio*). *Histochemistry and Cell Biology*, 118(3), 231–239. <https://doi.org/10.1007/s00418-002-0434-y>
- Ibrahim, M., Oldham, D., & Minghetti, M. (2020). Role of metal speciation in the exposure medium on the toxicity, bioavailability and bio-reactivity of copper, silver, cadmium and zinc in the rainbow trout gut cell line (RTgutGC). *Comparative Biochemistry and Physiology Part - C: Toxicology and Pharmacology*, 236(February), 108816. <https://doi.org/10.1016/j.cbpc.2020.108816>
- Intrasuksri, U., Rangwala, S. M., O'Brien, M., Noonan, D. J., & Feller, D. R. (1998). Mechanisms of peroxisome proliferation by perfluorooctanoic acid and endogenous fatty acids. *General Pharmacology*, 31(2), 187–197. [https://doi.org/10.1016/S0306-3623\(98\)00029-9](https://doi.org/10.1016/S0306-3623(98)00029-9)
- ISO, 2009. Biological evaluation of medical devices Part 5: Tests for in vitro cytotoxicity. International standard, ISO 10993-5:2009, pp. 1–34.
- Istrate, M. A., Nussler, A. K., Eichelbaum, M., & Burk, O. (2010). Regulation of CYP3A4 by pregnane X receptor: The role of nuclear receptors competing for response element binding. *Biochemical and Biophysical Research Communications*, 393(4), 688–693. <https://doi.org/10.1016/j.bbrc.2010.02.058>
- Jarc, E., & Petan, T. (2019). Lipid droplets and the management of cellular stress. *Yale Journal of Biology and Medicine*, 92(3), 435–452.
- Jeon, H. J., Lee, Y. H., Kim, M. J., Choi, S. D., Park, B. J., & Lee, S. E. (2016). Integrated biomarkers induced by chlorpyrifos in two different life stages of zebrafish (*Danio rerio*) for environmental risk assessment. *Environmental Toxicology and Pharmacology*, 43, 166–174. <https://doi.org/10.1016/j.etap.2016.03.010>
- Jin, Y., Tan, Y., Chen, L., Liu, Y., & Ren, Z. (2018). Reactive oxygen species induces lipid droplet accumulation in hep2 cells by increasing perilipin 2 expression. *International Journal of Molecular Sciences*, 19(11), 1–19. <https://doi.org/10.3390/ijms19113445>
- Johansson, M. E. V., & Hansson, G. C. (2014). Is the intestinal goblet cell a major immune cell? *Cell Host and Microbe*, 15(3), 251–252. <https://doi.org/10.1016/j.chom.2014.02.014>
- Jutfelt, F. (2006). *The Intestinal Epithelium of Salmonids: Transepithelial Transport, Barrier Function & Bacterial Interactions* (Issue January 2006). <https://gupea.ub.gu.se/handle/2077/4724>
- Jutfelt, F. (2011). Barrier Function of the Gut. *Encyclopedia of Fish Physiology: From Genome to Environment*, 2(January 2011), 1322–1331. <http://dx.doi.org/10.1016/B978-0-12-374553-8.00068-X>
- Kersten, S. (2008). Peroxisome proliferator activated receptors and lipoprotein metabolism.

- PPAR Research*, 2008. <https://doi.org/10.1155/2008/132960>
- Khatun, N., Rahman, T., & Mahanta, R. (2016). Histopathological Studies of Chlorpyrifos. *Global Journal of Medical Research*, 16(3).
- Kho, D., MacDonald, C., Johnson, R., Unsworth, C. P., O'Carroll, S. J., du Mez, E., Angel, C. E., & Graham, E. S. (2015). Application of xCELLigence RTCA biosensor technology for revealing the profile and window of drug responsiveness in real time. *Biosensors*, 5(2), 199–222. <https://doi.org/10.3390/bios5020199>
- Knudsen, D., Jutfelt, F., Sundh, H., Sundell, K., Koppe, W., & Frøkiær, H. (2008). Dietary soya saponins increase gut permeability and play a key role in the onset of soyabean-induced enteritis in Atlantic salmon (*Salmo salar* L.). *British Journal of Nutrition*, 100(1), 120–129. <https://doi.org/10.1017/S0007114507886338>
- Knudsen, D., Urán, P., Arnous, A., Koppe, W., & Frøkiær, H. (2007). Saponin-containing subfractions of soybean molasses induce enteritis in the distal intestine of Atlantic salmon. *Journal of Agricultural and Food Chemistry*, 55(6), 2261–2267. <https://doi.org/10.1021/jf0626967>
- Ko, C. W., Qu, J., Black, D. D., & Tso, P. (2020). Regulation of intestinal lipid metabolism: current concepts and relevance to disease. *Nature Reviews Gastroenterology and Hepatology*, 17(3), 169–183. <https://doi.org/10.1038/s41575-019-0250-7>
- Kregiel, D., Berłowska, J., Witonska, I., Antolak, H., Proestos, C., Babic, M., Babic, L., & Zhang, B. (2017). Saponin-Based, Biological-Active Surfactants from Plants. *Application and Characterization of Surfactants*. <https://doi.org/10.5772/68062>
- Krogdahl, Å., Gajardo, K., Kortner, T. M., Penn, M., Gu, M., Berge, G. M., & Bakke, A. M. (2015). Soya Saponins Induce Enteritis in Atlantic Salmon (*Salmo salar* L.). *Journal of Agricultural and Food Chemistry*, 63(15), 3887–3902. <https://doi.org/10.1021/jf506242t>
- Krogdahl, Å., Penn, M., Thorsen, J., Refstie, S., & Bakke, A. M. (2010). Important antinutrients in plant feedstuffs for aquaculture: An update on recent findings regarding responses in salmonids. *Aquaculture Research*, 41(3), 333–344. <https://doi.org/10.1111/j.1365-2109.2009.02426.x>
- Landis, W.G., Sofield, R.M., & Yu, M.-H. (n.d.). *Analysis of exposure-response*. 79–107.
- Le Bideau, Paul. 2019. Étude ex vivo de la toxicité du chlorpyrifos et du pyrimiphos-méthyle sur la paroi intestinale de *Salmo salar* L. Report from Research traineeship as part of Ingénieur Agrosup Dijon
- Lee, S. J., & Buhler, D. R. (2003). Cloning, tissue distribution, and functional studies of a new cytochrome P450 3A subfamily member, CYP3A45, from rainbow trout (*Oncorhynchus mykiss*) intestinal ceca. *Archives of Biochemistry and Biophysics*, 412(1), 77–89. [https://doi.org/10.1016/S0003-9861\(03\)00029-8](https://doi.org/10.1016/S0003-9861(03)00029-8)
- Lemaire, G., De Sousa, G., & Rahmani, R. (2004). A PXR reporter gene assay in a stable cell culture system: CYP3A4 and CYP2B6 induction by pesticides. *Biochemical Pharmacology*, 68(12), 2347–2358. <https://doi.org/10.1016/j.bcp.2004.07.041>
- Liang, Y., Zhan, J., Liu, D., Luo, M., Han, J., Liu, X., Liu, C., Cheng, Z., Zhou, Z., & Wang, P. (2019). Organophosphorus pesticide chlorpyrifos intake promotes obesity and insulin resistance through impacting gut and gut microbiota. *Microbiome*, 7(1), 1–15. <https://doi.org/10.1186/s40168-019-0635-4>
- Liguori, M. J., Lee, C. H., Liu, H., Ciurlionis, R., Ditewig, A. C., Doktor, S., Andracki, M. E., Gagne,

- G. D., Waring, J. F., Marsh, K. C., Gopalakrishnan, M., Blomme, E. A. G., & Yang, Y. (2012). AhR activation underlies the CYP1A autoinduction by A-998679 in rats. *Frontiers in Genetics*, 3(OCT), 1–13. <https://doi.org/10.3389/fgene.2012.00213>
- Lin, J. (2004). Sustainable Aquaculture. In *Journal of Environment Quality* (Vol. 33, Issue 2). <https://doi.org/10.2134/jeq2004.0796>
- Loretz, C. A. (1995). Electrophysiology of Ion Transport in Teleost Intestinal Cells. *Fish Physiology*, 14(C), 25–56. [https://doi.org/10.1016/S1546-5098\(08\)60241-1](https://doi.org/10.1016/S1546-5098(08)60241-1)
- Lundeberg, H., & Leifsdatter Grønlund, A. (2017). *From Brazilian fields to Norwegian farms*. 1–34.
- Ma J, Liu Y, Niu D, Li X. Effects of chlorpyrifos on the transcription of CYP3A cDNA, activity of acetylcholinesterase, and oxidative stress response of goldfish (*Carassius auratus*). *Toxicol.* 2015 Apr;30(4):422-9. doi: 10.1002/tox.21918. Epub 2013 Nov 4. PMID: 24190793
- Maage, A., Hove, H., & Julshamn, K. (2008). Monitoring and surveillance to improve farmed fish safety. *Improving Farmed Fish Quality and Safety*, 547–564. <https://doi.org/10.1533/9781845694920.3.547>
- Mahmood, H. (2014). Intestinal Lipid Absorption and Lipoprotein Formation. *Current Opinion in Lipidology*, 25(3), 200–206. <https://doi.org/10.1097/MOL.0000000000000084>.
- Makkar, H. P. S., Blümmel, M., & Becker, K. (1995). In vitro effects of and interactions between tannins and saponins and fate of tannins in the rumen. *Journal of the Science of Food and Agriculture*, 69(4), 481–493. <https://doi.org/10.1002/jsfa.2740690413>
- Martin, S. A. M., Dehler, C. E., & Król, E. (2016). Transcriptomic responses in the fish intestine. *Developmental and Comparative Immunology*, 64(March), 103–117. <https://doi.org/10.1016/j.dci.2016.03.014>
- Mateer, S. W., Cardona, J., Marks, E., Goggin, B. J., Hua, S., & Keely, S. (2016). Ex vivo intestinal sacs to assess mucosal permeability in models of gastrointestinal disease. *Journal of Visualized Experiments*, 2016(108), 1–7. <https://doi.org/10.3791/53250>
- Menoyo, D., López-Bote, C. J., Obach, A., & Bautista, J. M. (2005). Effect of dietary fish oil substitution with linseed oil on the performance, tissue fatty acid profile, metabolism, and oxidative stability of Atlantic salmon. *Journal of Animal Science*, 83(12), 2853–2862. <https://doi.org/10.2527/2005.83122853x>
- Meucci, V., & Arukwe, A. (2006). The xenoestrogen 4-nonylphenol modulates hepatic gene expression of pregnane X receptor, aryl hydrocarbon receptor, CYP3A and CYP1A1 in juvenile Atlantic salmon (*Salmo salar*). *Comparative Biochemistry and Physiology - C Toxicology and Pharmacology*, 142(1–2), 142–150. <https://doi.org/10.1016/j.cbpc.2005.11.011>
- Minghetti, M., Drieschner, C., Bramaz, N., Schug, H., & Schirmer, K. (2017). A fish intestinal epithelial barrier model established from the rainbow trout (*Oncorhynchus mykiss*) cell line, RTgutGC. *Cell Biology and Toxicology*, 33(6), 539–555. <https://doi.org/10.1007/s10565-017-9385-x>
- Moran-Ramos, S., Tovar, A. R., & Torres, N. (2012). Diet: Friend or foe of enteroendocrine cells: How it interacts with enteroendocrine cells. *Advances in Nutrition*, 3(1), 8–20. <https://doi.org/10.3945/an.111.000976>
- National Institutes of Health, National Library of Medicine (NIH , NLM), ToxTutor (Learn Essential Principles of Toxicology) (ToxTutor (Learn Essential Principles of Toxicology)),2016 Available at: <https://toxxtutor.nlm.nih.gov/>

- Neal, R. A. (1980). Microsomal metabolism of thiono-sulfur compounds: Mechanisms and toxicological significance. *Rev. Biochem. Toxicol.*, 2, 131–171
- Nikinmaa, M. (2014). Detoxification. *An Introduction to Aquatic Toxicology*, 87–98. <https://doi.org/10.1016/b978-0-12-411574-3.00009-8>
- Okada, T., Narai, A., Matsunaga, S., Fusetani, N., & Shimizu, M. (2000). Assessment of the marine toxins by monitoring the integrity of human intestinal Caco-2 cell monolayers. *Toxicology in Vitro*, 14(3), 219–226. [https://doi.org/10.1016/S0887-2333\(00\)00014-X](https://doi.org/10.1016/S0887-2333(00)00014-X)
- Olli, J. J., Krogdahl, & Våbenø, A. (1995). Dehulled solvent-extracted soybean meal as a protein source in diets for Atlantic salmon, *Salmo salar* L. *Aquaculture Research*, 26(3), 167–174. <https://doi.org/10.1111/j.1365-2109.1995.tb00899.x>
- Olsvik P. A., Sjøfteland, L. (2020). Mixture toxicity of chlorpyrifos-methyl, pirimiphos-methyl, and nonylphenol in Atlantic salmon (*Salmo salar*) hepatocytes. *Toxicology Reports*, 7(December 2019), 547–558. <https://doi.org/10.1016/j.toxrep.2020.03.008>
- Olsvik, P. A., Hammer, S. K., Sanden, M., & Sjøfteland, L. (2019). Chlorpyrifos-induced dysfunction of lipid metabolism is not restored by supplementation of polyunsaturated fatty acids EPA and ARA in Atlantic salmon liver cells. *Toxicology in Vitro*, 61(September), 104655. <https://doi.org/10.1016/j.tiv.2019.104655>
- Olsvik, P. A., Larsen, A. K., Berntssen, M. H. G., Goksøyr, A., Karlsen, O. A., Yadetie, F., Sanden, M., & Kristensen, T. (2019). Effects of agricultural pesticides in aquafeeds on wild fish feeding on leftover pellets near fish farms. *Frontiers in Genetics*, 10(SEP), 1–18. <https://doi.org/10.3389/fgene.2019.00794>
- Olzmann, J. A., & Carvalho, P. (2019). Dynamics and functions of lipid droplets. *Nature Reviews Molecular Cell Biology*, 20(3), 137–155. <https://doi.org/10.1038/s41580-018-0085-z>
- Pang, G.-F. (2018). Pesticide Introduction. *Analytical Methods for Food Safety by Mass Spectrometry*, 1–9. <https://doi.org/10.1016/B978-0-12-814167-0.00001-6>
- Pawlak, M., Lefebvre, P., & Staels, B. (2015). Molecular mechanism of PPAR α action and its impact on lipid metabolism, inflammation and fibrosis in non-alcoholic fatty liver disease. *Journal of Hepatology*, 62(3), 720–733. <https://doi.org/10.1016/j.jhep.2014.10.039>
- Peterson, L. W., & Artis, D. (2014). Intestinal epithelial cells: Regulators of barrier function and immune homeostasis. *Nature Reviews Immunology*, 14(3), 141–153. <https://doi.org/10.1038/nri3608>
- Pettersson, A. (2010). Effects of Replacing Fish Oil with Vegetable Oils in Feed for Rainbow Trout (*Oncorhynchus mykiss*) and Arctic Charr (*Salvelinus alpinus*). In *Sciences-New York*.
- Racke, K., Simmons, N., & Tiu, C. (2002). *Is Chlorpyrifos a Persistent Organic Pollutant ?* 1–7.
- Relyea, R. A. (2009). A cocktail of contaminants: How mixtures of pesticides at low concentrations affect aquatic communities. *Oecologia*, 159(2), 363–376. <https://doi.org/10.1007/s00442-008-1213-9>
- Sabra, F., El-Deeb Mehana, E.-S., & Soliman Sabra, F. (2015). Pesticides Toxicity in Fish with Particular Reference to Insecticides. *Asian Journal of Agriculture and Food Sciences*, 03(01), 2321–1571. <https://www.researchgate.net/publication/272575872>
- Sæle, Ø., Rød, K. E. L., Quinlivan, V. H., Li, S., & Farber, S. A. (2018). A novel system to quantify intestinal lipid digestion and transport. *Biochimica et Biophysica Acta - Molecular and Cell Biology of Lipids*, 1863(9), 948–957. <https://doi.org/10.1016/j.bbalip.2018.05.006>
- Sahlmann, C., Gu, J., Kortner, T. M., Lein, I., Krogdahl, Å., & Bakke, A. M. (2015). Ontogeny of the

- digestive system of Atlantic salmon (*Salmo salar* L.) and effects of soybean meal from start-feeding. *PLoS ONE*, *10*(4), 1–23. <https://doi.org/10.1371/journal.pone.0124179>
- Sales, J., & Glencross, B. (2011). A meta-analysis of the effects of dietary marine oil replacement with vegetable oils on growth, feed conversion and muscle fatty acid composition of fish species. *Aquaculture Nutrition*, *17*(2). <https://doi.org/10.1111/j.1365-2095.2010.00761.x>
- Sams, C., Cocker, J., & Lennard, M. S. (2004). Biotransformation of chlorpyrifos and diazinon by human liver microsomes and recombinant human cytochrome P450s (CYP). *Xenobiotica*, *34*(10), 861–873. <https://doi.org/10.1080/00498250400017273>
- Samtiya, M., Aluko, R. E., & Dhewa, T. (2020). Plant food anti-nutritional factors and their reduction strategies: an overview. *Food Production, Processing and Nutrition*, *2*(1), 1–14. <https://doi.org/10.1186/s43014-020-0020-5>
- Schimmel, S. C., Garnas, R. L., Patrick, J. M., & Moore, J. C. (1983). Acute Toxicity , Bioconcentration , and Persistence of AC 222 , 705 , Benthocarb , Environment. *Society*, *1*, 104–113.
- Schlenk, D., Celander, M., Gallagher, E., George, S., James, M., Kullman, S., van den Hurk, P., & Willett, K. (2008). Biotransformation in Fishes. In *The Toxicology of Fishes* (Issue February). <https://doi.org/10.1201/9780203647295.ch4>
- Schug, H., Begnaud, F., Debonneville, C., Berthaud, F., Gimeno, S., & Schirmer, K. (2018). TransFER: a new device to measure the transfer of volatile and hydrophobic organic chemicals across an in vitro intestinal fish cell barrier. *Analytical Methods*, *10*(36), 4394–4403. <https://doi.org/10.1039/c8ay01253a>
- Segner, H. (1998). Fish cell lines as a tool in aquatic toxicology. *Exs*, *86*(1), 1–38. https://doi.org/10.1007/978-3-0348-8853-0_1
- Seiliez, I., Belghit, I., Gao, Y., Skiba-Cassy, S., Dias, K., Cluzeaud, M., Rémond, D., Hafnaoui, N., Salin, B., Camougrand, N., & Panserat, S. (2016). Looking at the metabolic consequences of the colchicine-based in vivo autophagic flux assay. *Autophagy*, *12*(2), 343–356. <https://doi.org/10.1080/15548627.2015.1117732>
- Seite, S., Pioche, T., Ory, N., Plagnes-Juan, E., Panserat, S., & Seiliez, I. (2019). The autophagic flux inhibitor bafilomycin A1 affects the expression of intermediary metabolism-related genes in trout hepatocytes. *Frontiers in Physiology*, *10*(MAR), 1–11. <https://doi.org/10.3389/fphys.2019.00263>
- Shuler, L., & Hickman, J. J. (2016). TEER measurements in cells. In *Journal of Laboratory Automation* (Vol. 20, Issue 2). <https://doi.org/10.1177/2211068214561025>
- Søfteland, L., Kirwan, J. A., Hori, T. S. F., Størseth, T. R., Sommer, U., Berntssen, M. H. G., Viant, M. R., Rise, M. L., Waagbø, R., Torstensen, B. E., Booman, M., & Olsvik, P. A. (2014). Toxicological effect of single contaminants and contaminant mixtures associated with plant ingredients in novel salmon feeds. *Food and Chemical Toxicology*, *73*, 157–174. <https://doi.org/10.1016/j.fct.2014.08.008>
- Sørensen, M., Berge, G. M., Thomassen, M., Ruyter, B., Hatlen, B., Ytrestøl, T., Aas, T. S., & Åsgård, T. (2011). Today's and tomorrow's feed ingredients in Norwegian aquaculture. In *68* (Issue December). www.nofima.no
- Sørensen, M., Penn, M., El-Mowafi, A., Storebakken, T., Chunfang, C., Øverland, M., & Krogdahl, Å. (2011). Effect of stachyose, raffinose and soya-saponins supplementation on nutrient digestibility, digestive enzymes, gut morphology and growth performance in Atlantic

- salmon (*Salmo salar*, L). *Aquaculture*, 314(1–4), 145–152.
<https://doi.org/10.1016/j.aquaculture.2011.02.013>
- Sparg, S. G., Light, M. E., & Van Staden, J. (2004). Biological activities and distribution of plant saponins. *Journal of Ethnopharmacology*, 94(2–3), 219–243.
<https://doi.org/10.1016/j.jep.2004.05.016>
- Spire, C., Rogue, A., Brun, M., Claude, N., & Guillouzo, A. (2010). Gene expression changes induced by PPAR gamma agonists in animal and human liver. *PPAR Research*, 2010.
<https://doi.org/10.1155/2010/325183>
- Srivastava, P., Singh, A., & Pandey, A. K. (2016). Pesticides toxicity in fishes: Biochemical, physiological and genotoxic aspects. *Biochemical and Cellular Archives*, 16(2), 199–218.
- Stalin, A., Suganthi, P., Mathivani, S., Paray, B. A., Al-Sadoon, M. K., Gokula, V., & Musthafa, M. S. (2019). Impact of chlorpyrifos on behavior and histopathological indices in different tissues of freshwater fish *Channa punctatus* (Bloch). *Environmental Science and Pollution Research*, 26(17), 17623–17631. <https://doi.org/10.1007/s11356-019-05165-3>
- Stanley, J., Preetha, G., Stanley, J., & Preetha, G. (2016). Pesticide Toxicity to Microorganisms: Exposure, Toxicity and Risk Assessment Methodologies. In *Pesticide Toxicity to Non-target Organisms*. https://doi.org/10.1007/978-94-017-7752-0_6
- Stewart, A. S., Pratt-Phillips, S., & Gonzalez, L. M. (2017). Alterations in Intestinal Permeability: The Role of the “Leaky Gut” in Health and Disease. *Journal of Equine Veterinary Science*, 52, 10–22. <https://doi.org/10.1016/j.jevs.2017.02.009>
- Sun, F., & Chen, H. S. (2008). Monitoring of pesticide chlorpyrifos residue in farmed fish: Investigation of possible sources. *Chemosphere*, 71(10), 1866–1869.
<https://doi.org/10.1016/j.chemosphere.2008.01.034>
- Sunanda, M., Chandra Sekhara Rao, J., Neelima, P., Govinda Rao, K., & Simhachalam, G. (2016). Effects of chlorpyrifos (An organophosphate pesticide) in fish. *International Journal of Pharmaceutical Sciences Review and Research*, 39(1), 299–305.
- Sundell, K., Jutfelt, F., Ágústsson, T., Olsen, R. E., Sandblom, E., Hansen, T., & Björnsson, B. T. (2003). Intestinal transport mechanisms and plasma cortisol levels during normal and out-of-season parr-smolt transformation of Atlantic salmon, *Salmo salar*. *Aquaculture*, 222(1–4), 265–285. [https://doi.org/10.1016/S0044-8486\(03\)00127-3](https://doi.org/10.1016/S0044-8486(03)00127-3)
- Sundell, K. S., & Sundh, H. (2012). Intestinal fluid absorption in anadromous salmonids: Importance of tight junctions and aquaporins. *Frontiers in Physiology*, 3 SEP(September), 1–13. <https://doi.org/10.3389/fphys.2012.00388>
- Sundh, H., & Sundell, K. S. (2015). Environmental impacts on fish mucosa. In *Mucosal Health in Aquaculture*. Elsevier Inc. <https://doi.org/10.1016/B978-0-12-417186-2.00007-8>
- Takeuchi, S., Matsuda, T., Kobayashi, S., Takahashi, T., & Kojima, H. (2006). In vitro screening of 200 pesticides for agonistic activity via mouse peroxisome proliferator-activated receptor (PPAR) α and PPAR γ and quantitative analysis of in vivo induction pathway. *Toxicology and Applied Pharmacology*, 217(3), 235–244. <https://doi.org/10.1016/j.taap.2006.08.011>
- Tang, J., Cao, Y., Rose, R. L., Brimfield, A. A., Dai, D., Goldstein, J. A., & Hodgson, E. (2001). Metabolism of Chlorpyrifos by Human Cytochrome P450 Isoforms and Human, Mouse, and Rat Liver Microsomes. *Drug Metabolism and Disposition*, 29(9), 1201 LP – 1204.
<http://dmd.aspetjournals.org/content/29/9/1201.abstract>
- Tang, J., Cao, Y., Rose, R. L., & Hodgson, E. (2002). In vitro metabolism of carbaryl by human

- cytochrome P450 and its inhibition by chlorpyrifos. *Chemico-Biological Interactions*, 141(3), 229–241. [https://doi.org/10.1016/S0009-2797\(02\)00074-1](https://doi.org/10.1016/S0009-2797(02)00074-1)
- Taxvig, C., Dreisig, K., Boberg, J., Nellemann, C., Schelde, A. B., Pedersen, D., Boergesen, M., Mandrup, S., & Vinggaard, A. M. (2012). Differential effects of environmental chemicals and food contaminants on adipogenesis, biomarker release and PPAR γ activation. *Molecular and Cellular Endocrinology*, 361(1–2), 106–115. <https://doi.org/10.1016/j.mce.2012.03.021>
- Tinant, G., Neefs, I., Das, K., Rees, J. F., Larondelle, Y., & Debier, C. (2020). Methylmercury displays pro-adipogenic properties in rainbow trout preadipocytes. *Chemosphere*, 263, 127917. <https://doi.org/10.1016/j.chemosphere.2020.127917>
- Tirelli, V., Catone, T., Turco, L., Di Consiglio, E., Testai, E., & De Angelis, I. (2007). Effects of the pesticide clorpyrifos on an in vitro model of intestinal barrier. *Toxicology in Vitro*, 21(2), 308–313. <https://doi.org/10.1016/j.tiv.2006.08.015>
- Tocher, D. R. (2003). Metabolism and functions of lipids and fatty acids in teleost fish. *Reviews in Fisheries Science*, 11(2), 107–184. <https://doi.org/10.1080/713610925>
- Topic Popovic, N., Howell, T., Babish, J. G., & Bowser, P. R. (2012). Cross-sectional study of hepatic CYP1A and CYP3A enzymes in hybrid striped bass, channel catfish and Nile tilapia following oxytetracycline treatment. *Research in Veterinary Science*, 92(2), 283–291. <https://doi.org/10.1016/j.rvsc.2011.03.003>
- Trapani, G., Franco, M., Trapani, A., Lopedota, A., Latrofa, A., Gallucci, E., Micelli, S., & Liso, G. (2004). Frog intestinal Sac: A new in vitro method for the assessment of intestinal permeability. *Journal of Pharmaceutical Sciences*, 93(12), 2909–2919. <https://doi.org/10.1002/jps.20180>
- van den Ingh, T. S. G. A. M., Krogdahl, Å., Olli, J. J., Hendriks, H. G. C. J. M., & Koninkx, J. G. J. F. (1991). Effects of soybean-containing diets on the proximal and distal intestine in Atlantic salmon (*Salmo salar*): a morphological study. *Aquaculture*, 94(4), 297–305. [https://doi.org/10.1016/0044-8486\(91\)90174-6](https://doi.org/10.1016/0044-8486(91)90174-6)
- Varó, I., Serrano, R., Pitarch, E., Amat, F., López, F. J., & Navarro, J. C. (2002). Bioaccumulation of chlorpyrifos through an experimental food chain: Study of protein HSP70 as biomarker of sublethal stress in fish. *Archives of Environmental Contamination and Toxicology*, 42(2), 229–235. <https://doi.org/10.1007/s00244-001-0013-6>
- Wang, C. W. (2016). Lipid droplets, lipophagy, and beyond. *Biochimica et Biophysica Acta - Molecular and Cell Biology of Lipids*, 1861(8), 793–805. <https://doi.org/10.1016/j.bbalip.2015.12.010>
- Wang, J., Lei, P., Gamil, A. A. A., Lagos, L., Yue, Y., Schirmer, K., Mydland, L. T., Øverland, M., Krogdahl, Å., & Kortner, T. M. (2019). Rainbow trout (*Oncorhynchus mykiss*) intestinal epithelial cells as a model for studying gut immune function and effects of functional feed ingredients. *Frontiers in Immunology*, 10(FEB), 1–17. <https://doi.org/10.3389/fimmu.2019.00152>
- Welte, M. A., & Gould, A. P. (2017). Lipid droplet functions beyond energy storage. *Biochimica et Biophysica Acta - Molecular and Cell Biology of Lipids*, 1862(10), 1260–1272. <https://doi.org/10.1016/j.bbalip.2017.07.006>
- Whittamore, J. M., Genz, J., Grosell, M., & Wilson, R. W. (2016). Measuring intestinal fluid transport in vitro: Gravimetric method versus non-absorbable marker. *Comparative*

- Biochemistry and Physiology -Part A : Molecular and Integrative Physiology*, 194, 27–36.
<https://doi.org/10.1016/j.cbpa.2016.01.004>
- Willson, T. M., & Kliewer, S. A. (2002). PXR, car and drug metabolism. *Nature Reviews Drug Discovery*, 1(4), 259–266. <https://doi.org/10.1038/nrd753>
- Xing, H., Liu, T., Zhang, Z., Wang, X., & Xu, S. (2015). Acute and subchronic toxic effects of atrazine and chlorpyrifos on common carp (*Cyprinus carpio* L.): Immunotoxicity assessments. *Fish and Shellfish Immunology*, 45(2), 327–333.
<https://doi.org/10.1016/j.fsi.2015.04.016>
- Xing, H., Wang, X., Sun, G., Gao, X., Xu, S., & Wang, X. (2012). Effects of atrazine and chlorpyrifos on activity and transcription of glutathione S-transferase in common carp (*Cyprinus carpio* L.). *Environmental Toxicology and Pharmacology*, 33(2), 233–244.
<https://doi.org/10.1016/j.etap.2011.12.014>
- Xing, H., Zhang, Z., Yao, H., Liu, T., Wang, L., Xu, S., & Li, S. (2014). Effects of atrazine and chlorpyrifos on cytochrome P450 in common carp liver. *Chemosphere*, 104, 244–250.
<https://doi.org/10.1016/j.chemosphere.2014.01.002>
- Ye, H., Xu, M., Liu, Q., Sun, Z., Zou, C., Chen, L., Su, N., & Ye, C. (2019). Effects of replacing fish meal with soybean meal on growth performance, feed utilization and physiological status of juvenile obscure puffer, *Takifugu obscurus*. *Comparative Biochemistry and Physiology Part - C: Toxicology and Pharmacology*, 216(September 2018), 75–81.
<https://doi.org/10.1016/j.cbpc.2018.11.006>
- Yen, J., Donerly, S., Levin, E. D., & Linney, E. A. (2011). Differential acetylcholinesterase inhibition of chlorpyrifos, diazinon and parathion in larval zebrafish. *Neurotoxicology and Teratology*, 33(6), 735–741. <https://doi.org/10.1016/j.ntt.2011.10.004>
- Yıldız, M., Eroldoğan, T. O., Ofori-Mensah, S., Engin, K., & Baltacı, M. A. (2018). The effects of fish oil replacement by vegetable oils on growth performance and fatty acid profile of rainbow trout: Re-feeding with fish oil finishing diet improved the fatty acid composition. *Aquaculture*, 488(December 2017), 123–133.
<https://doi.org/10.1016/j.aquaculture.2017.12.030>
- Ytrestøyl, T., Aas, T. S., & Åsgård, T. (2015). Utilisation of feed resources in production of Atlantic salmon (*Salmo salar*) in Norway. *Aquaculture*, 448, 365–374.
<https://doi.org/10.1016/j.aquaculture.2015.06.023>
- Zhao, Y., Zhang, Y., Wang, G., Han, R., & Xie, X. (2016). Effects of chlorpyrifos on the gut microbiome and urine metabolome in mouse (*Mus musculus*). *Chemosphere*, 153, 287–293. <https://doi.org/10.1016/j.chemosphere.2016.03.055>

10. Appendix

Table 10.1: Composition of diets

Ingredient	Control %	SBM %
Fish meal NA	40	5
Corn gluten		
Hi Pro Soy bean meal		30
pea meal NTC17267		
Wheat gluten	20	21
Faba bean dehulled	5	5
SPC	12.2	12.5
Fish oil NA	8.533	9.634
Rapeseed oil	8	9.032
Wheat	6.064	6.35
Astaxanthin 10%	0.01	0.01
VitC	0.01	0.01
Vitamin premix	0.1	0.1
MinMix	0.1	0.1
Other micro ingredients	0.736	3.077
Estimated content	Control %	SBM %
Dry matter	93	93
Moisture	7	7
Crude Protein	52.6	44.1
Crude fat	22.9	22
Ash	7.1	5.2

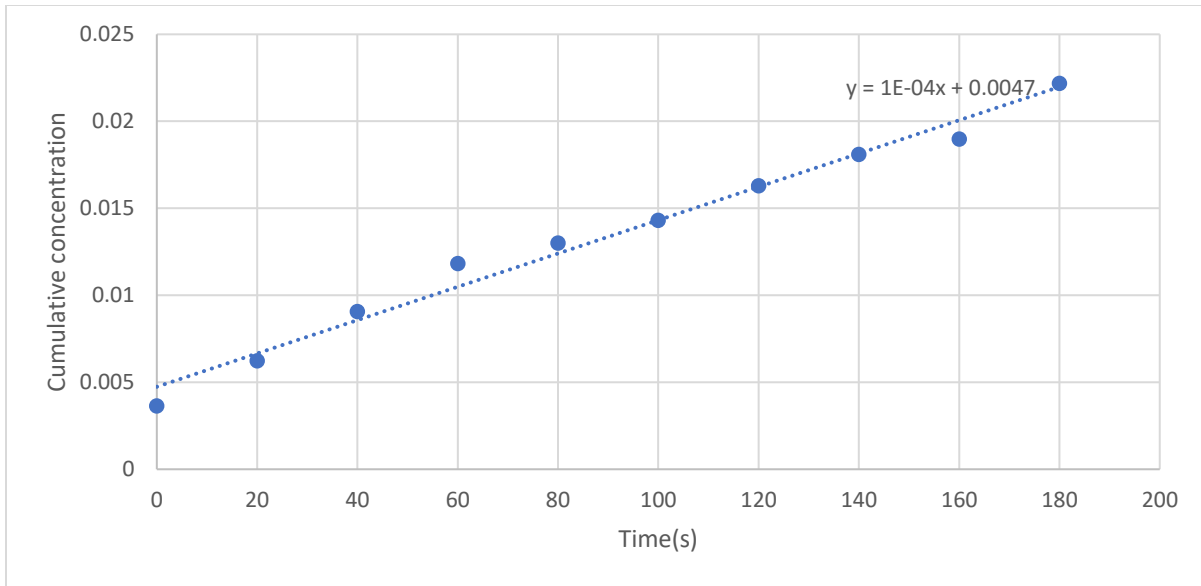


Figure 10.1 Cumulative concentration of FITC-D in the intestinal sac of fish 3 fed with SBM.

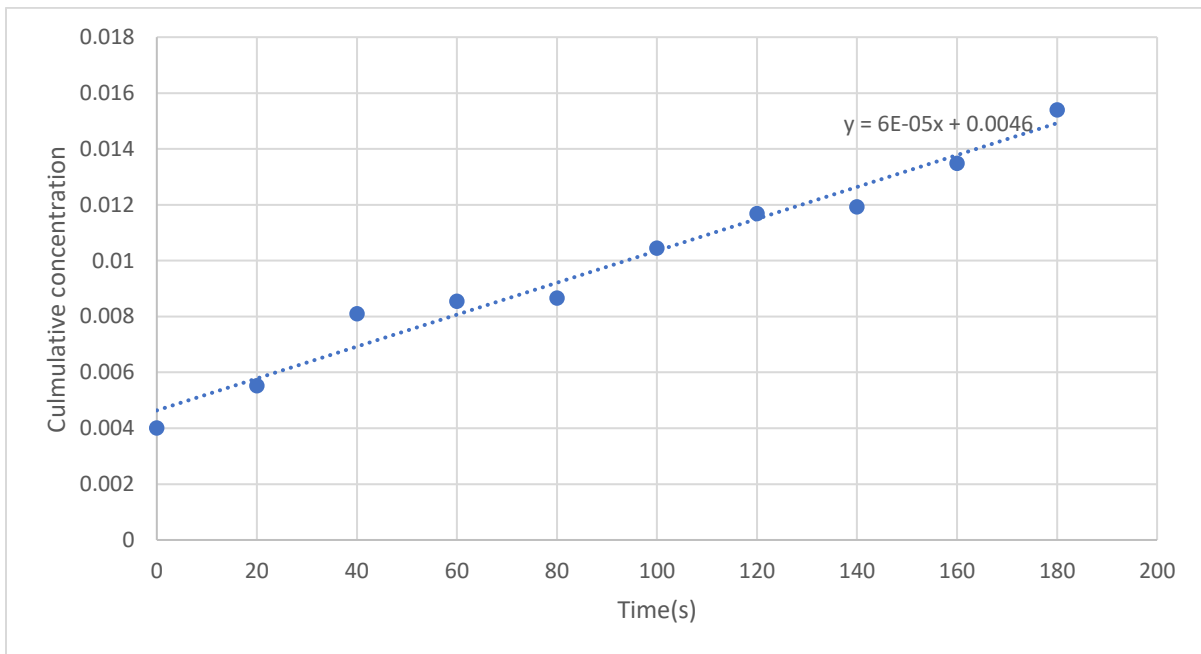


Figure 10.2 Cumulative concentration of FITC-D in the intestinal sac of fish 3 fed with FM and later filled with 500 μ M CPF.

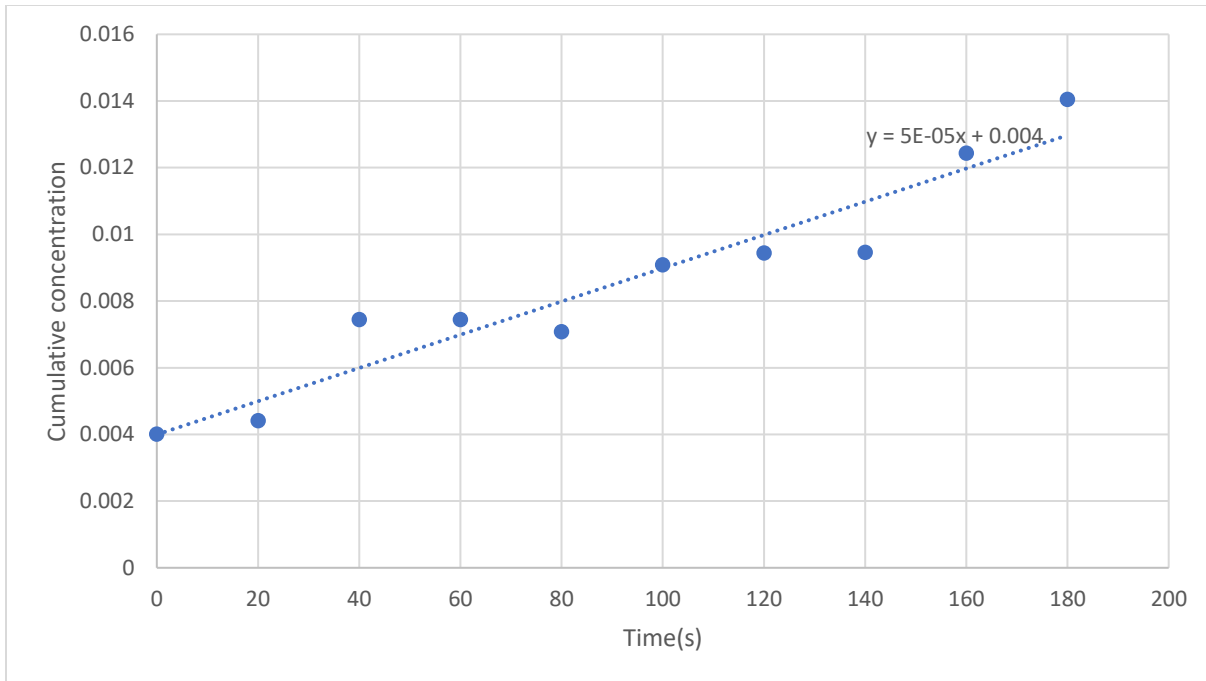


Figure 10.3 Cumulative concentration of FITC-D in the intestinal sac of fish 4 fed with FM.

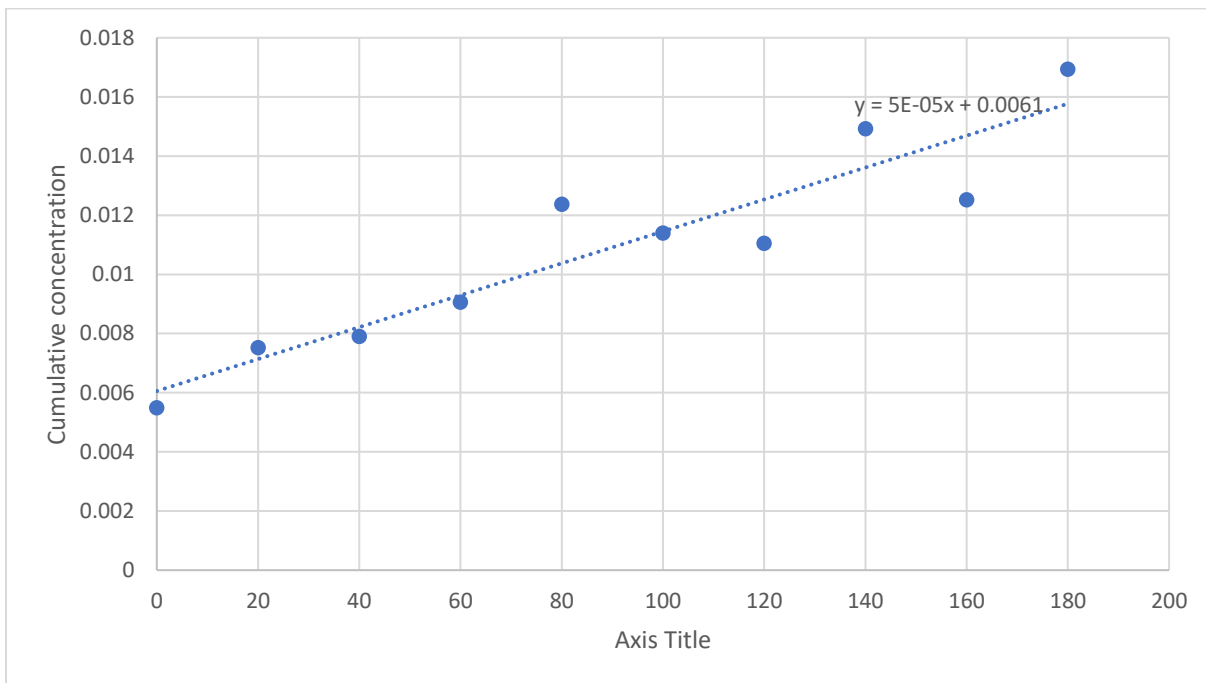


Figure 10.4 Cumulative concentration of FITC-D in the intestinal sac of fish 5 fed with SBM and later filled with 500 μM CPF.

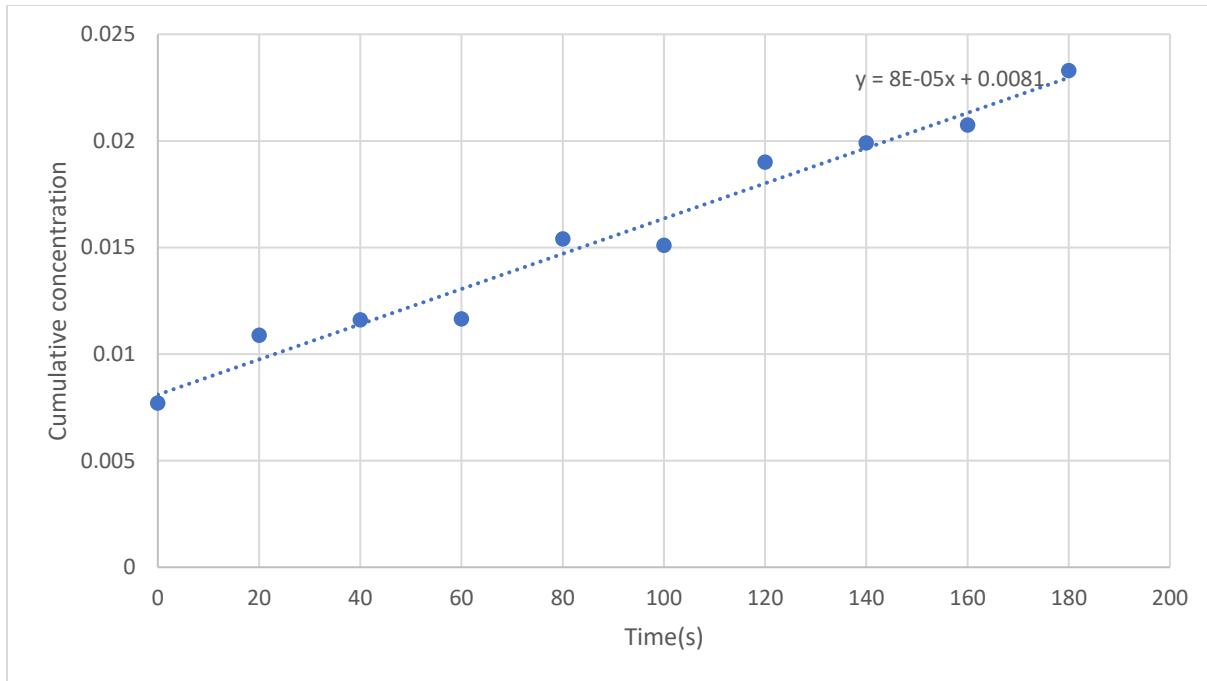


Figure 10.5 Cumulative concentration of FITC-D in the intestinal sac of fish 6 fed with FM and later filled with 500 μ M CPF.

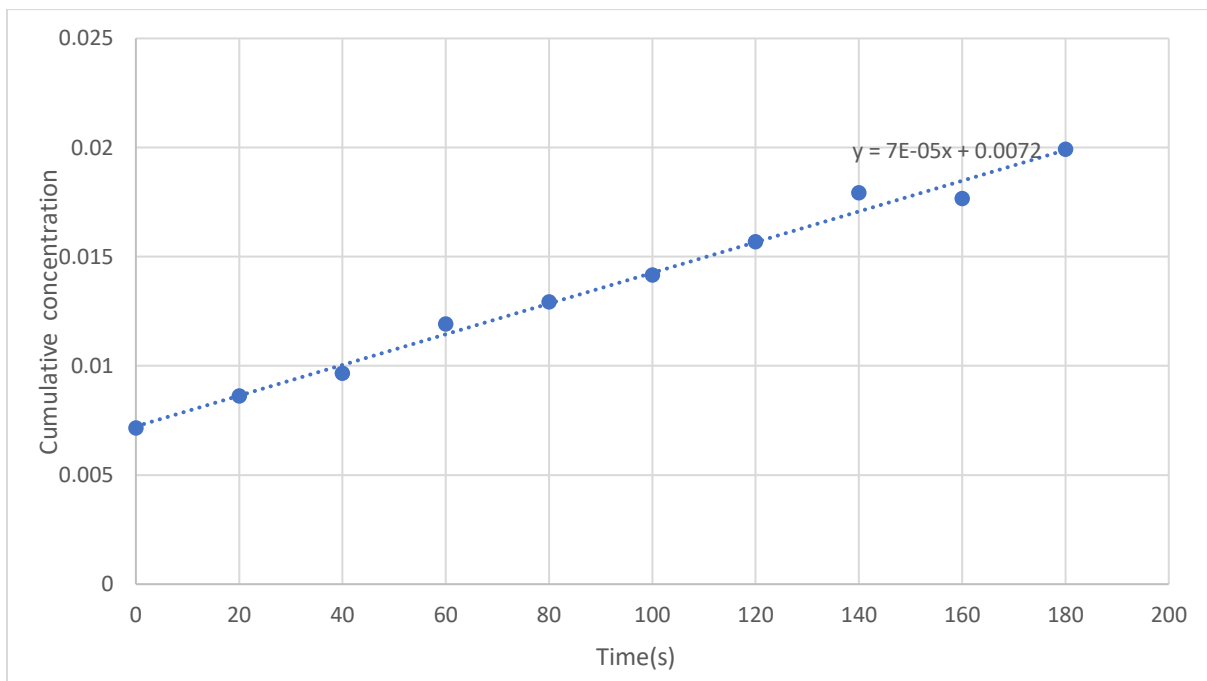


Figure 10.6 Cumulative concentration of FITC-D in the intestinal sac of fish 7 fed with FM and later filled with 500 μ M CPF.

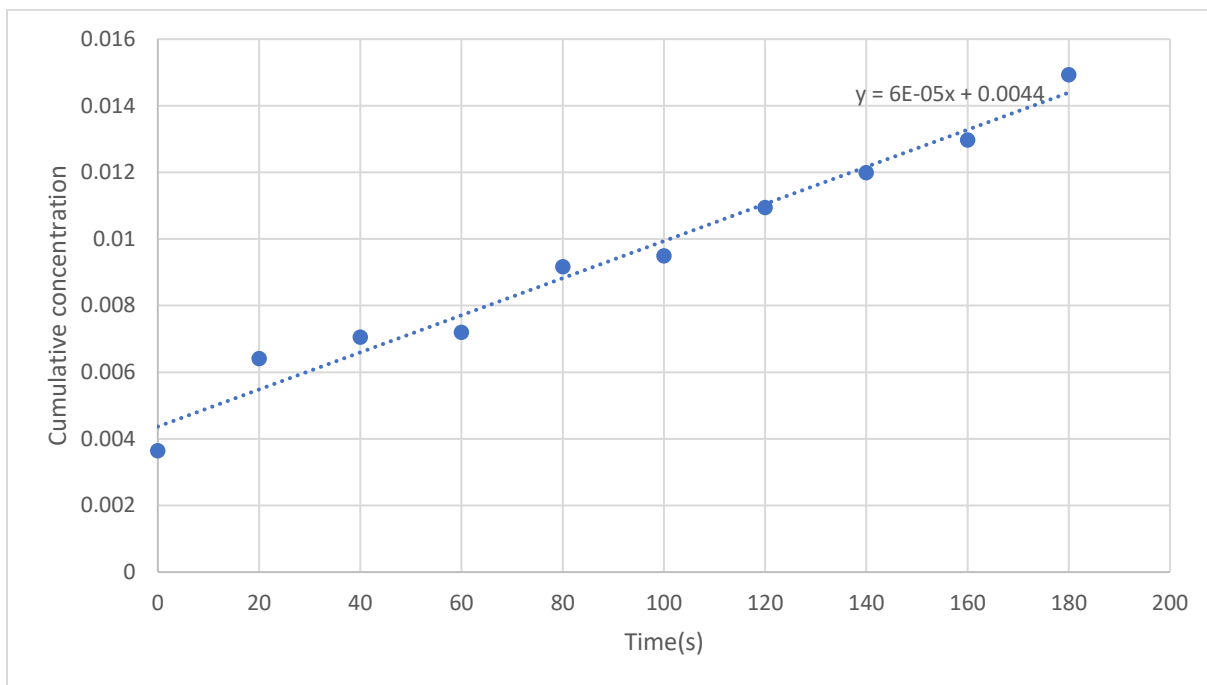


Figure 10.7 Cumulative concentration of FITC-D in the intestinal sac of fish 8 fed with SBM.

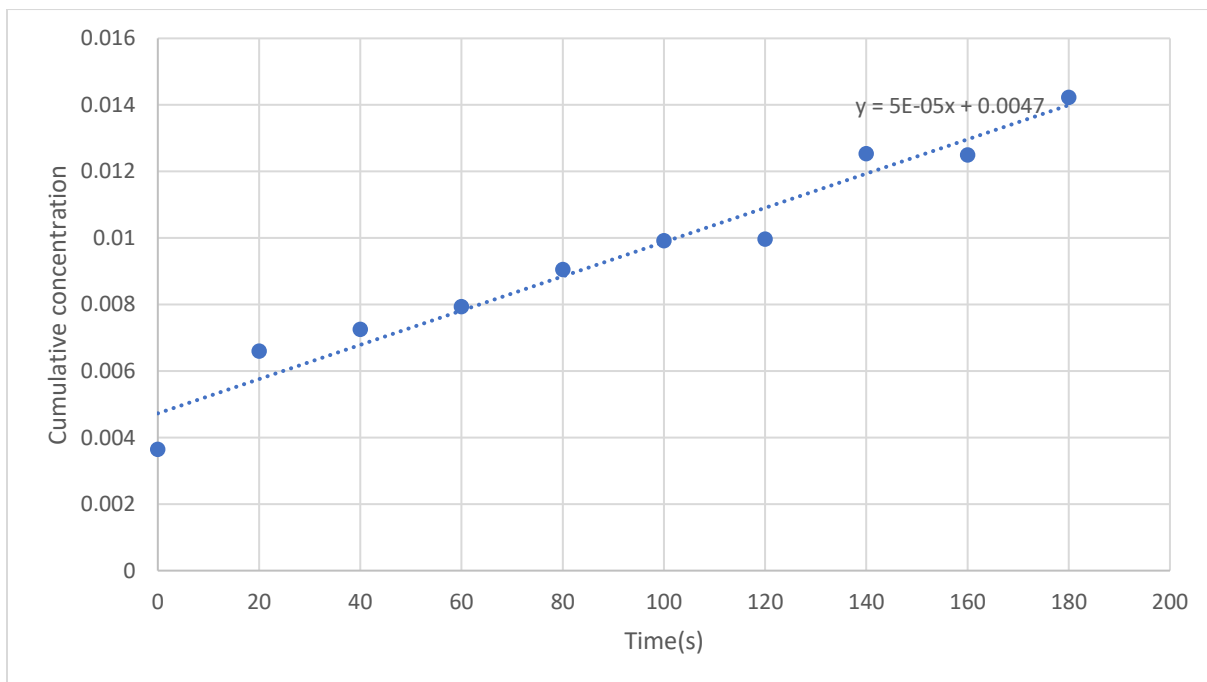


Figure 10.8 Cumulative concentration of FITC-D in the intestinal sac of fish 9 fed with SBM and later filled with 500 μ M CPF.

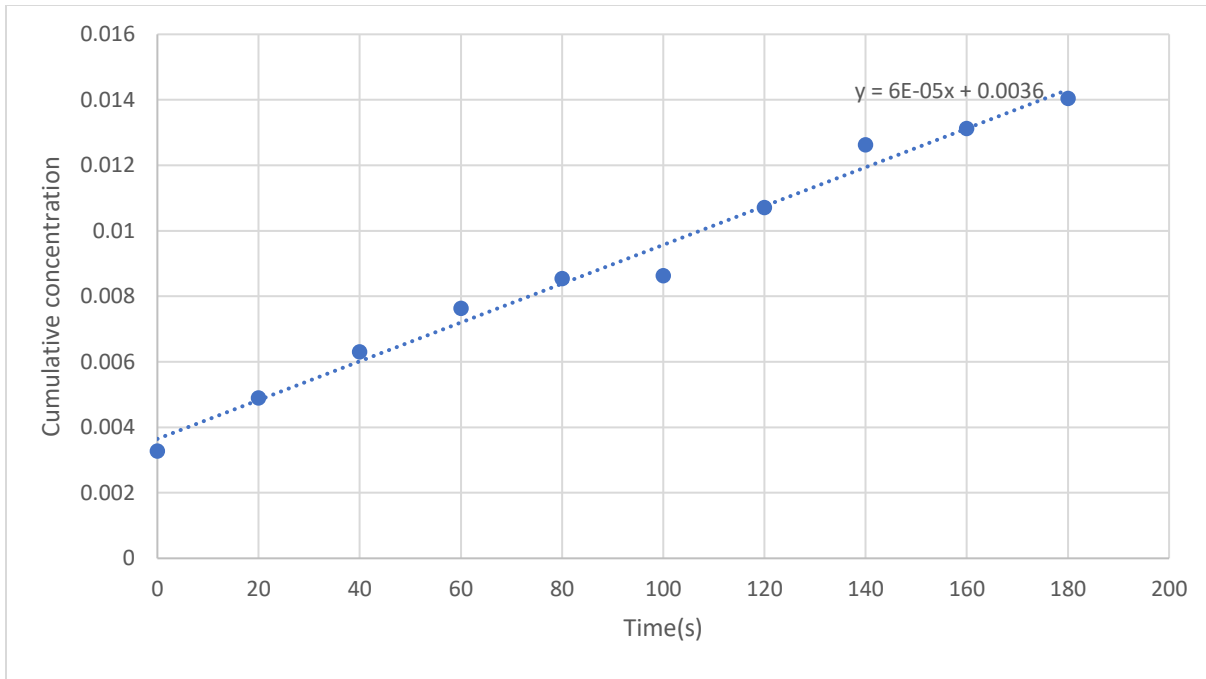


Figure 10.9 Cumulative concentration of FITC-D in the intestinal sac of fish 10 fed with FM.

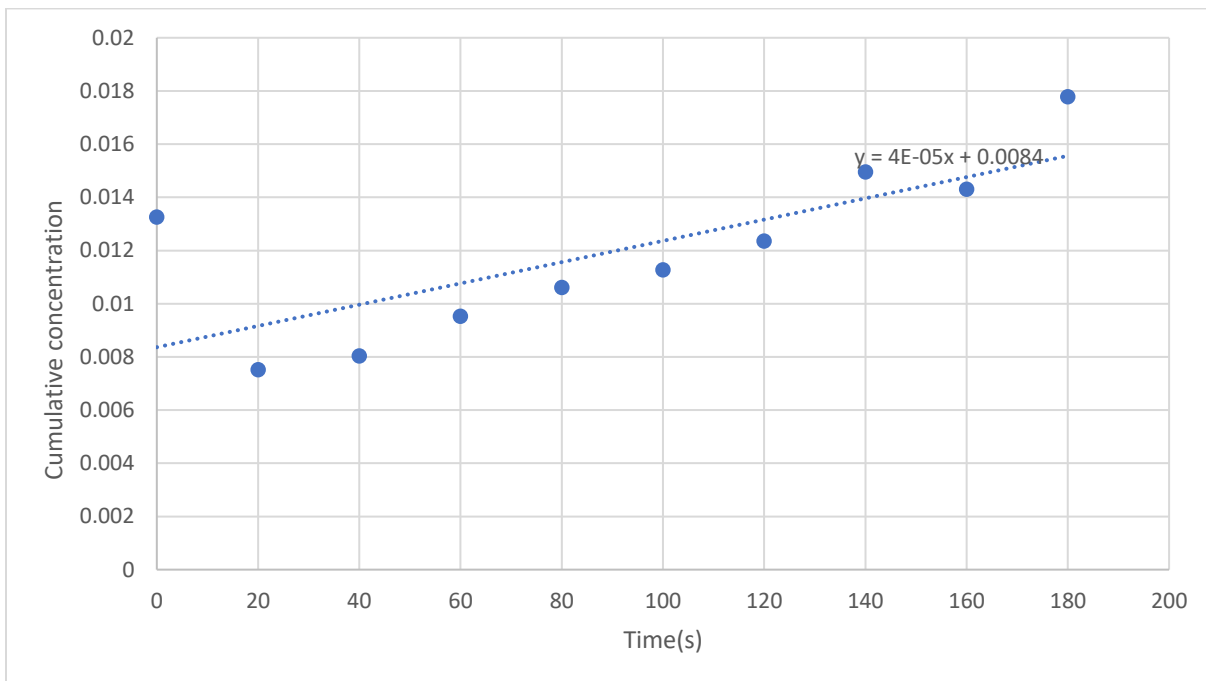


Figure 10.10 Cumulative concentration of FITC-D in the intestinal sac of fish 11 fed with SBM.

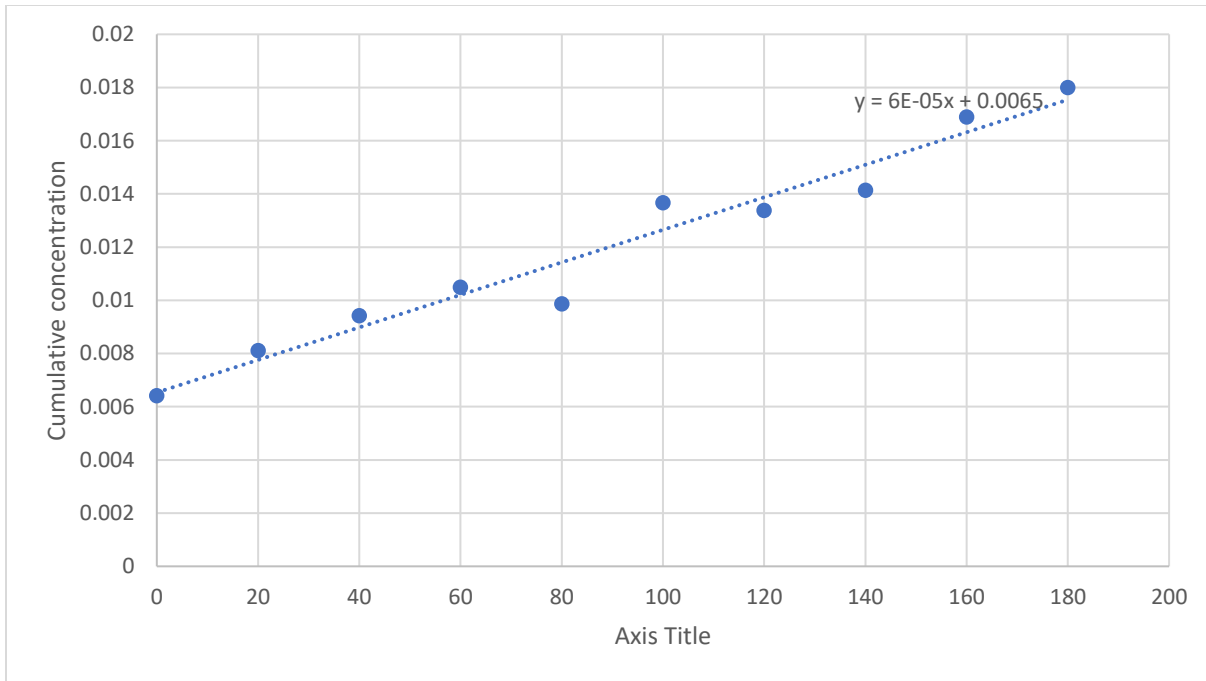


Figure 10.11 Cumulative concentration of FITC-D in the intestinal sac of fish 12 fed with FM.

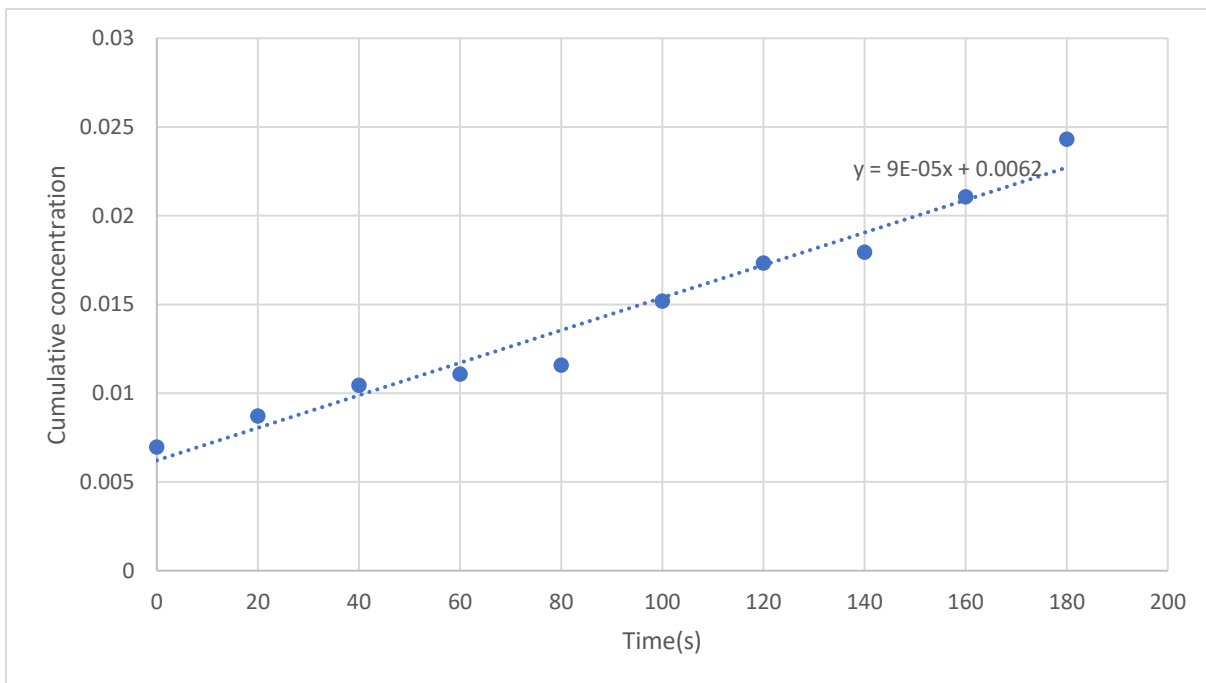


Figure 10.12 Cumulative concentration of FITC-D in the intestinal sac of fish 13 fed with SBM and later filled with 500 μM CPF.

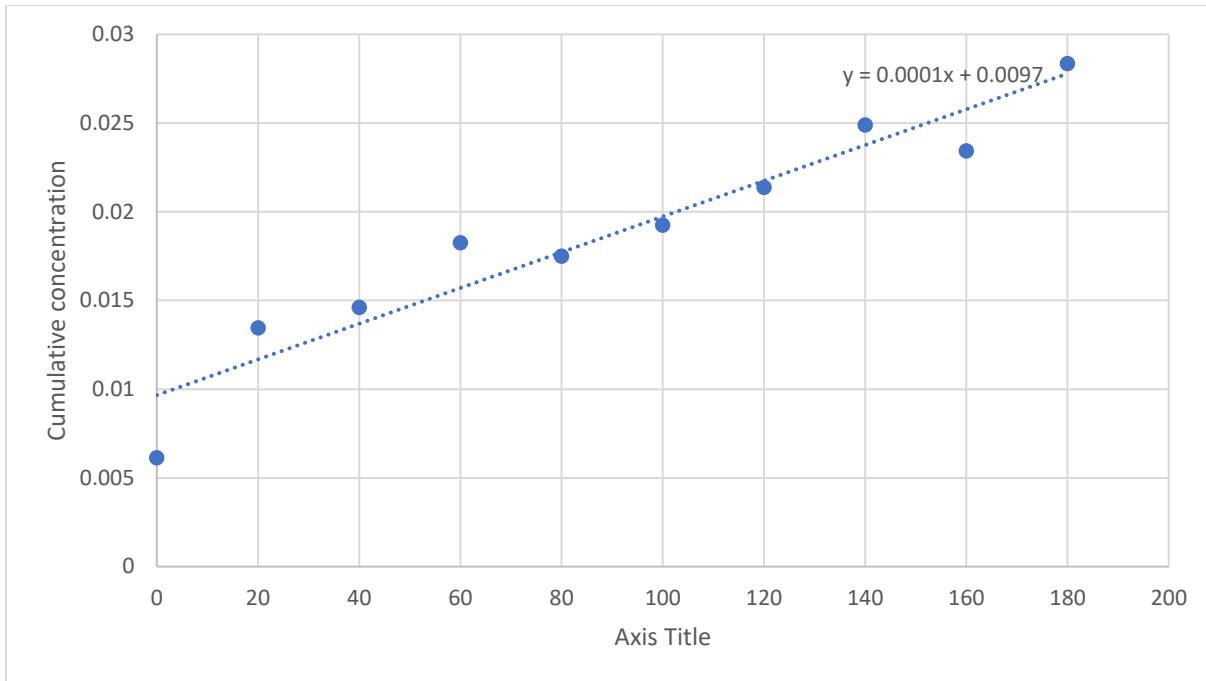


Figure 10.13 Cumulative concentration of FITC-D in the intestinal sac of fish 14 fed with FM.

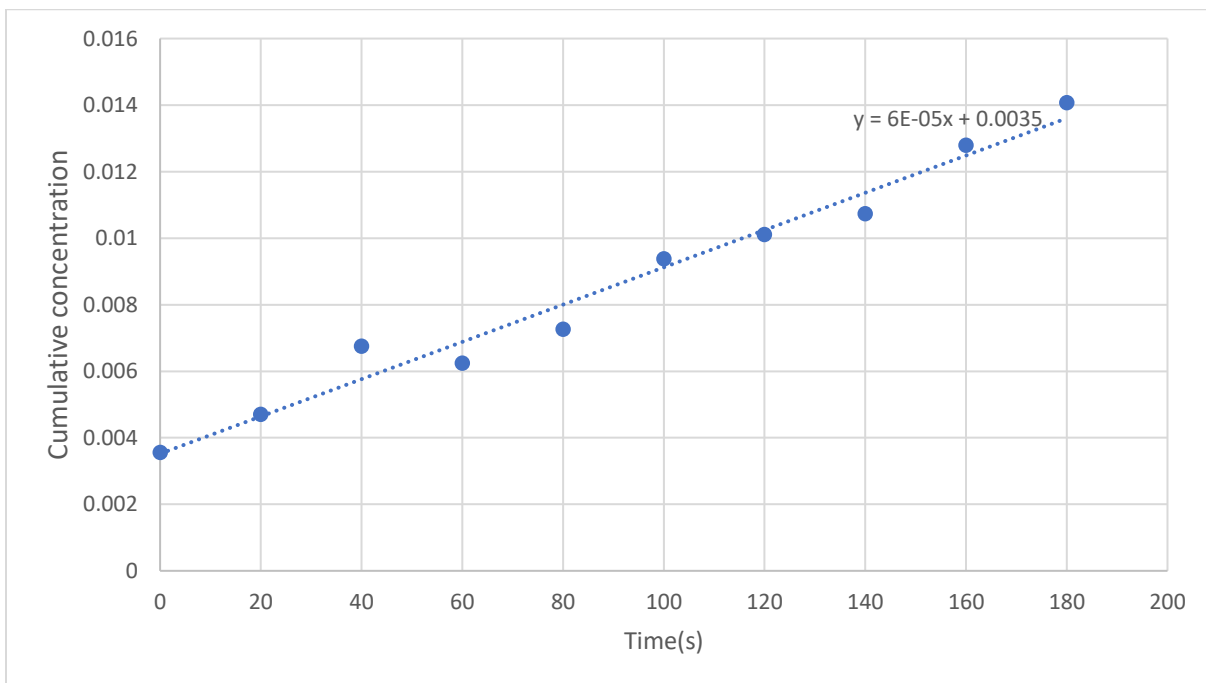


Figure 10.14 Cumulative concentration of FITC-D in the intestinal sac of fish 15 fed with FM and later filled with 500 μ M CPF.

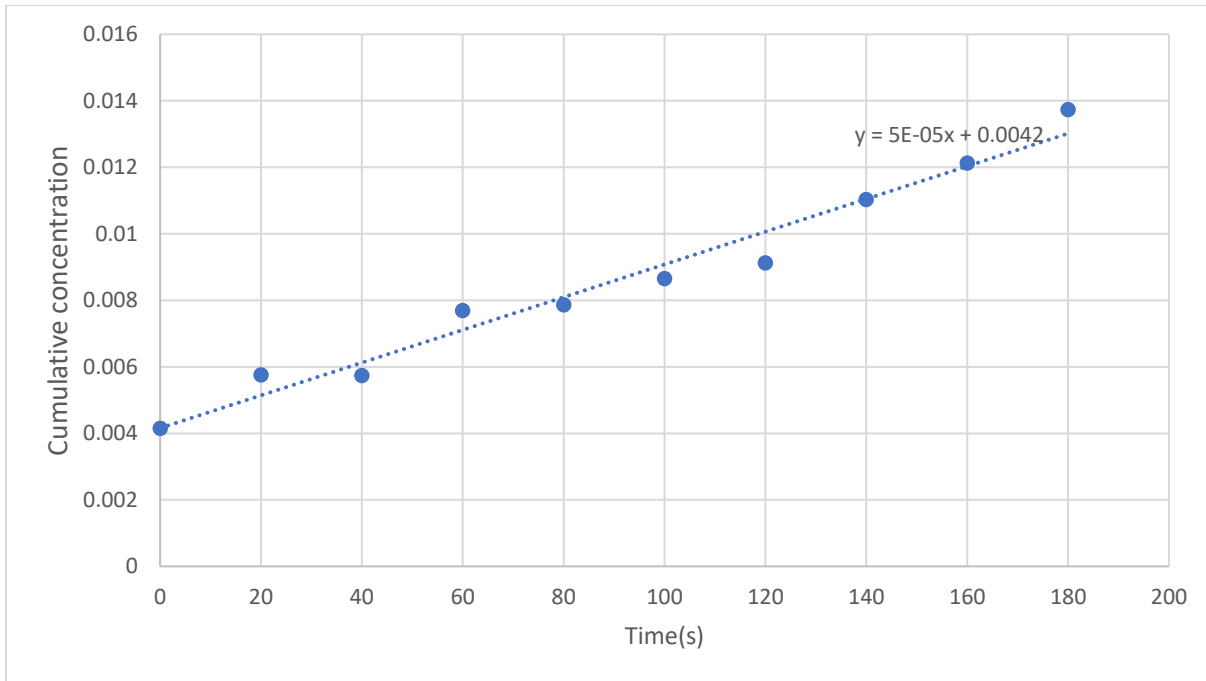


Figure 10.15 Cumulative concentration of FITC-D in the intestinal sac of fish 16 fed with SBM.

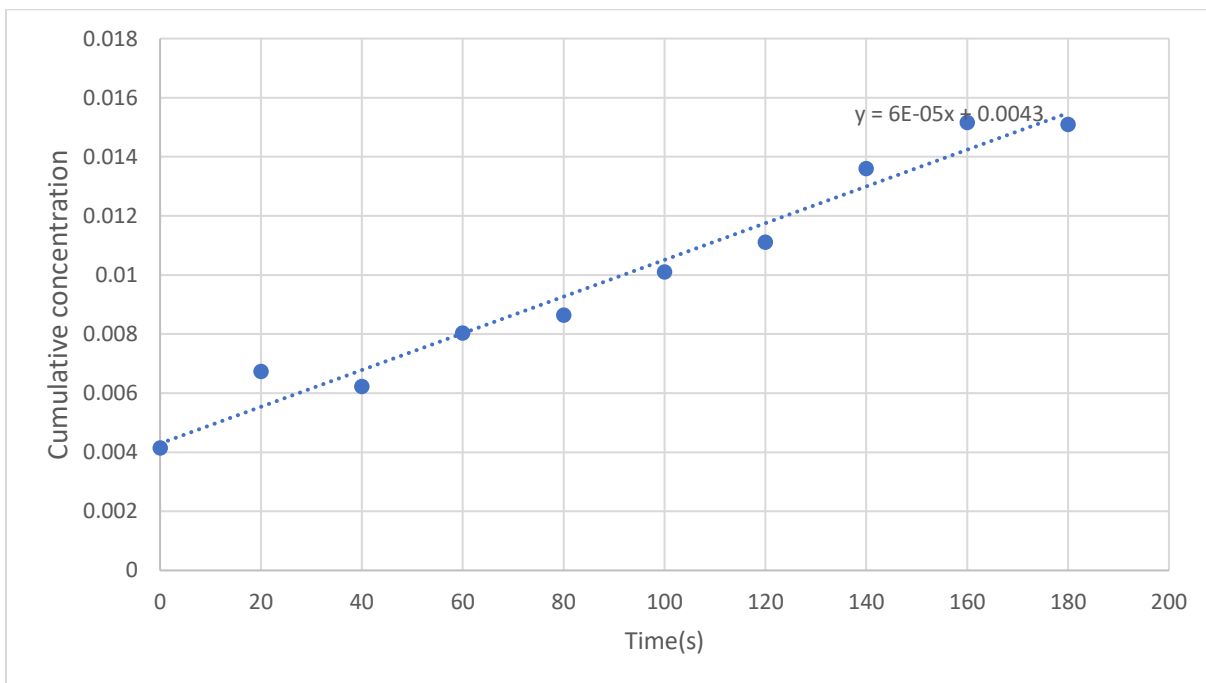


Figure 10.16 Cumulative concentration of FITC-D in the intestinal sac of fish 17 fed with SBM and later filled with 500 μ M CPF.

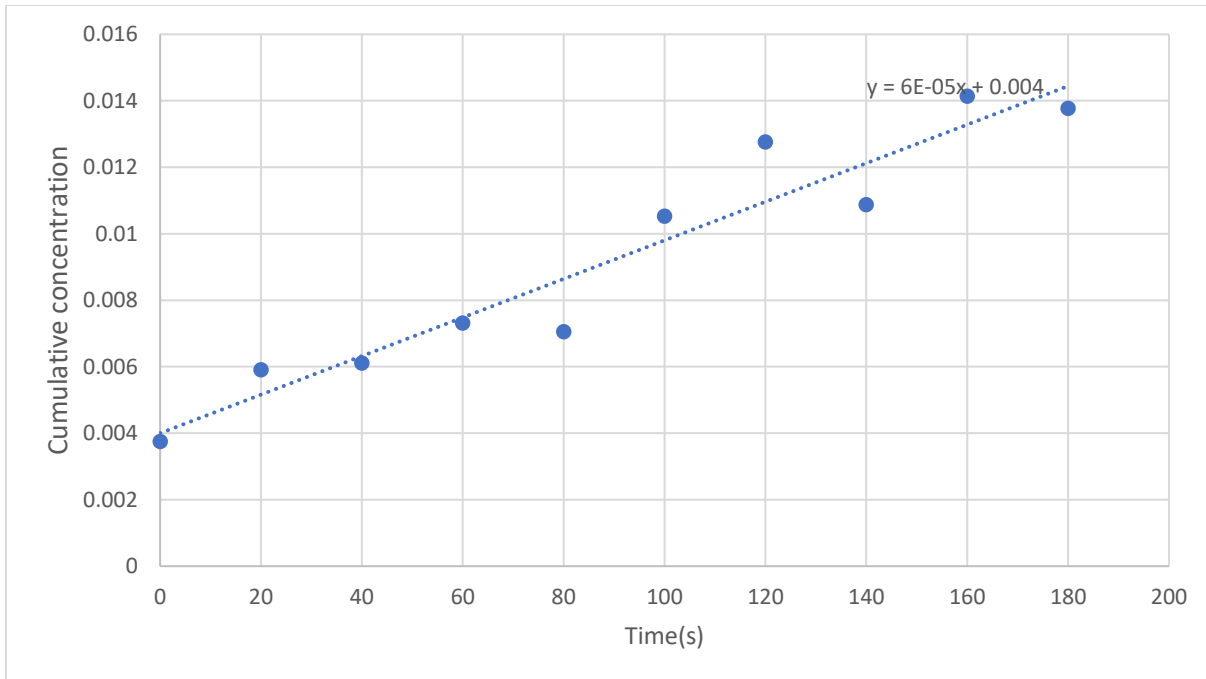


Figure 10.17 Cumulative concentration of FITC-D in the intestinal sac of fish 18 fed with FM and later filled with 500 μ M CPF.

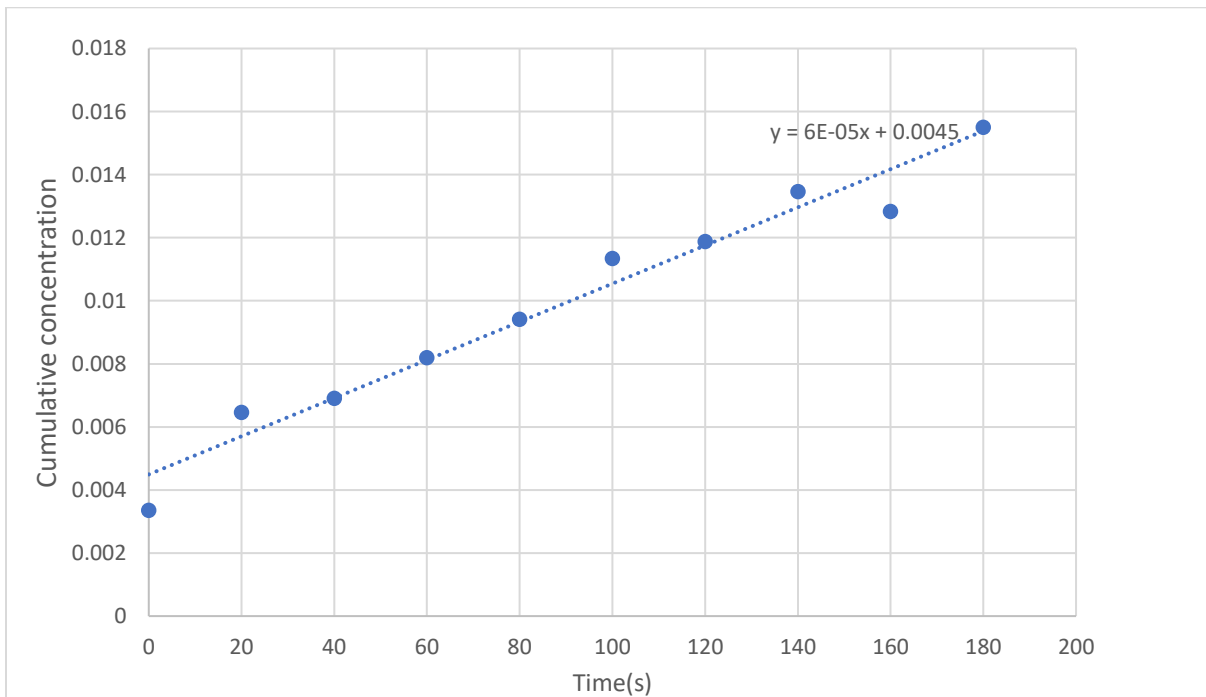


Figure 10.18 Cumulative concentration of FITC-D in the intestinal sac of fish 19 fed with SBM and later filled with 500 μ M CPF.

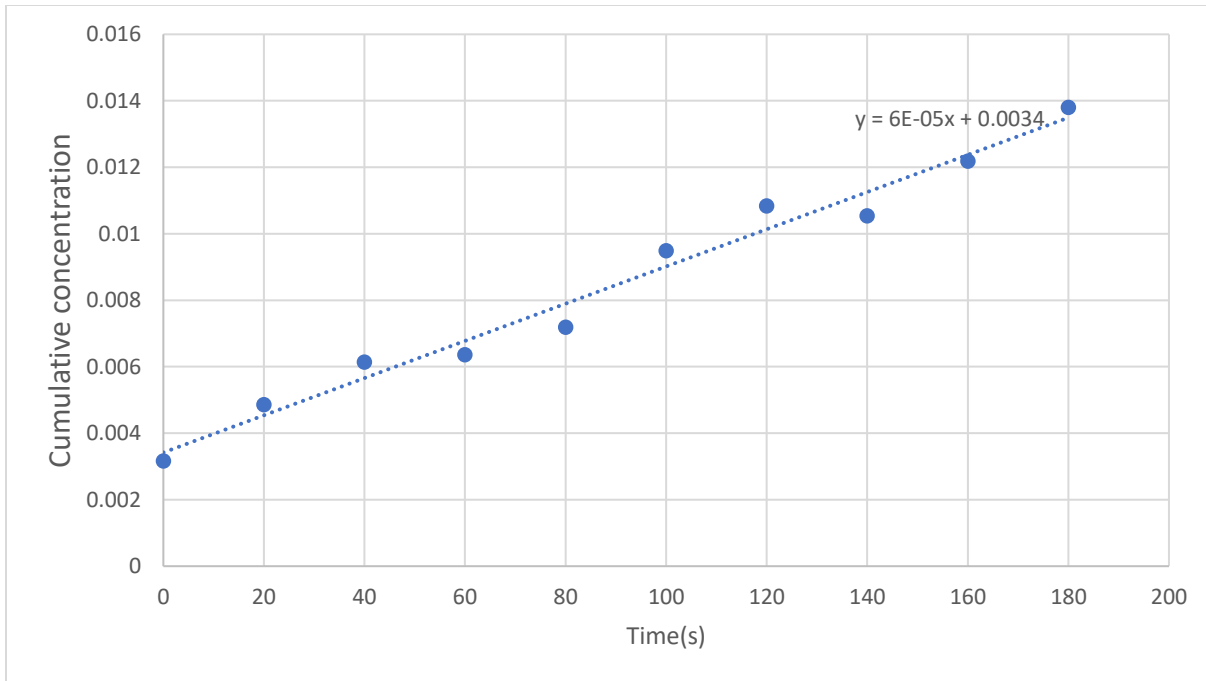


Figure 10.19 Cumulative concentration of FITC-D in the intestinal sac of fish 20 fed with SBM.

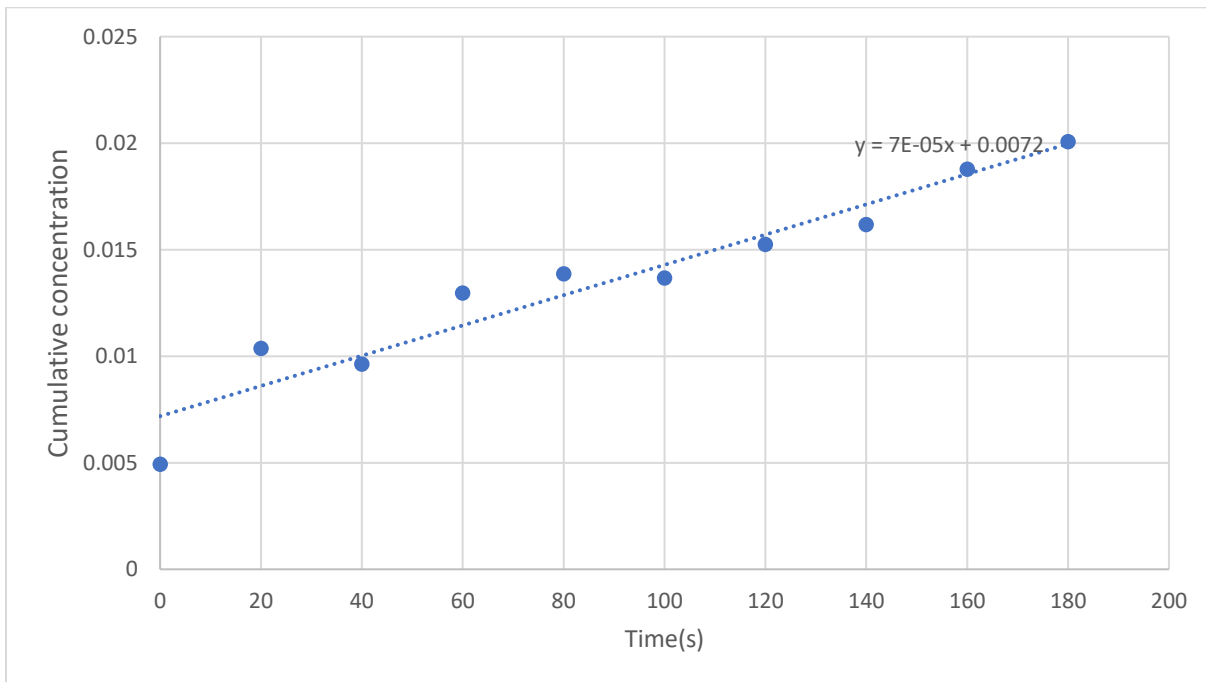


Figure 10.20 Cumulative concentration of FITC-D in the intestinal sac of fish 21 fed with FM.

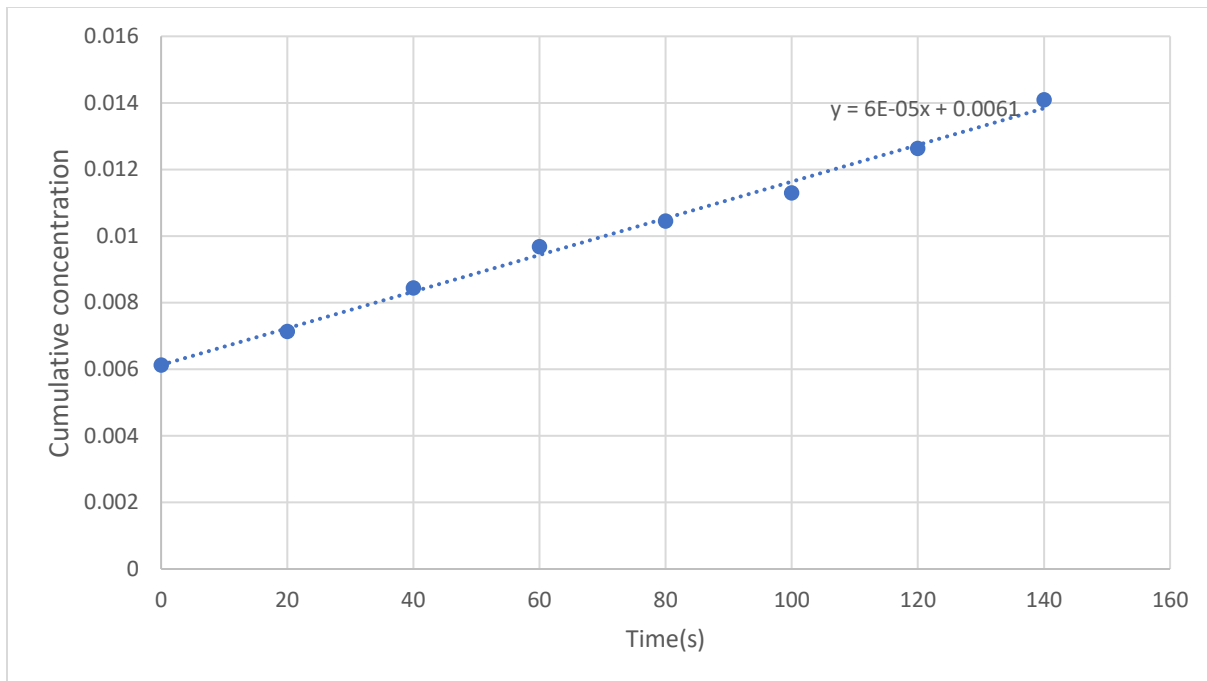


Figure 10.21 Cumulative concentration of FITC-D in the intestinal sac of fish 22 fed with FM and later filled with 500 μ M CPF.

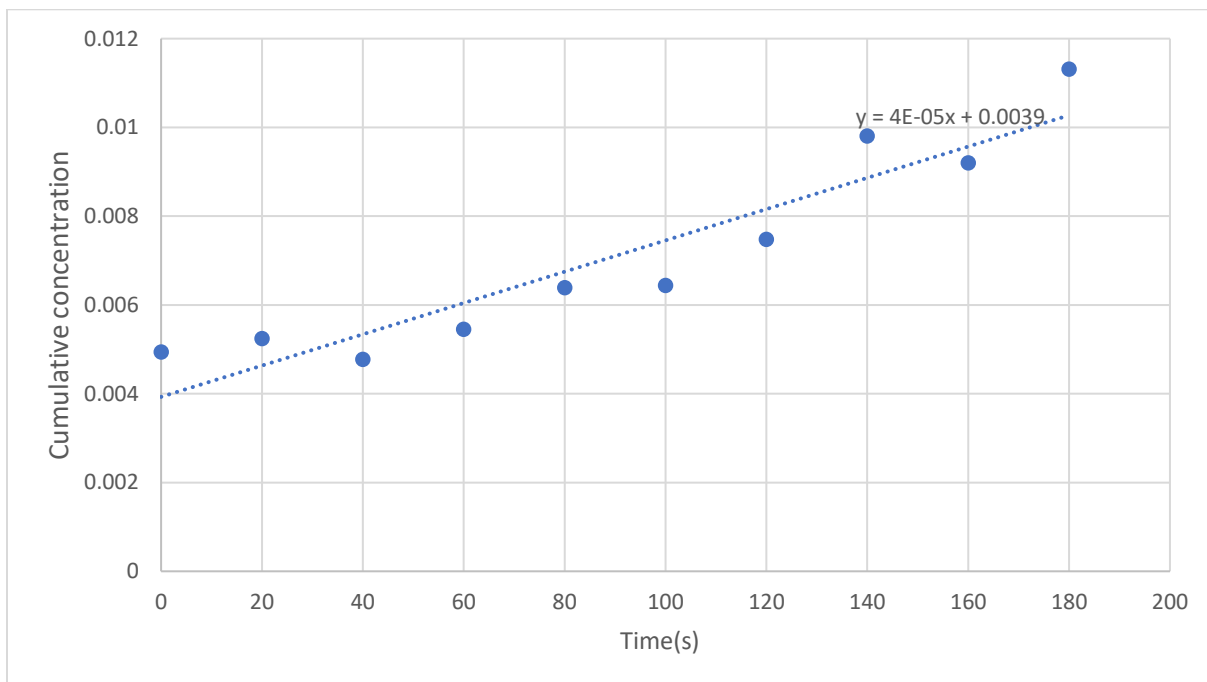


Figure 10.22 Cumulative concentration of FITC-D in the intestinal sac of fish 23 fed with SBM and later filled with 500 μ M CPF.

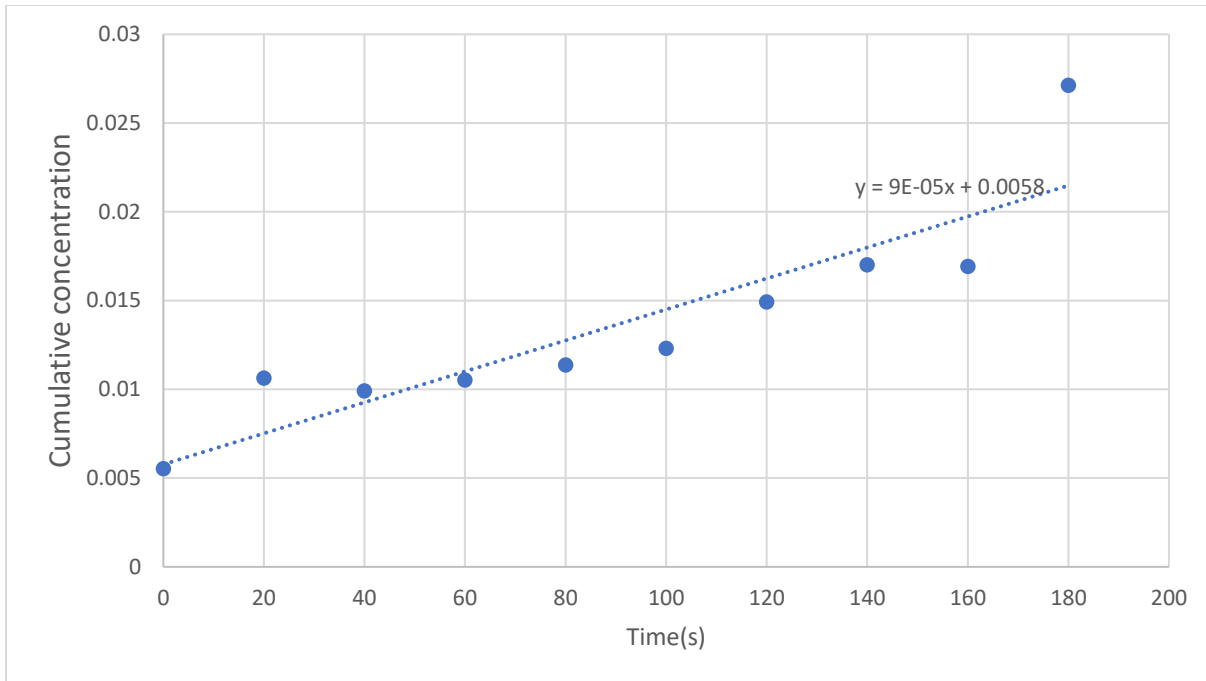


Figure 10.23 Cumulative concentration of FITC-D in the intestinal sac of fish 24 fed with FM.

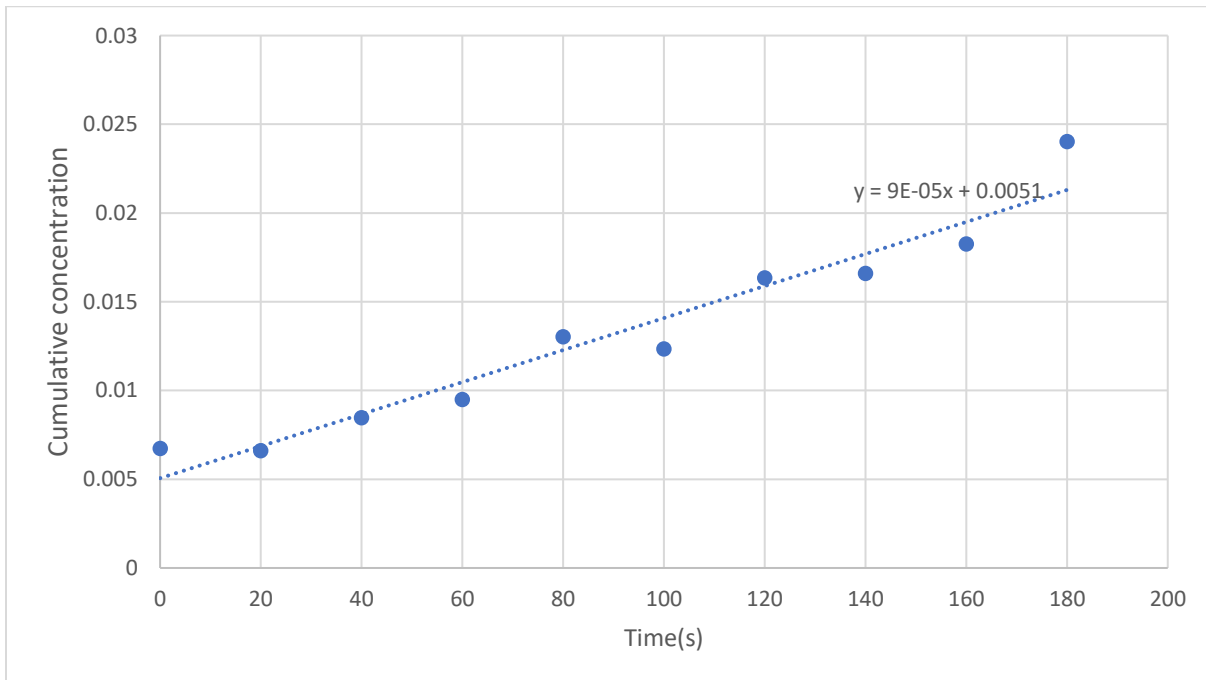


Figure 10.24 Cumulative concentration of FITC-D in the intestinal sac of fish 25 fed with SBM.

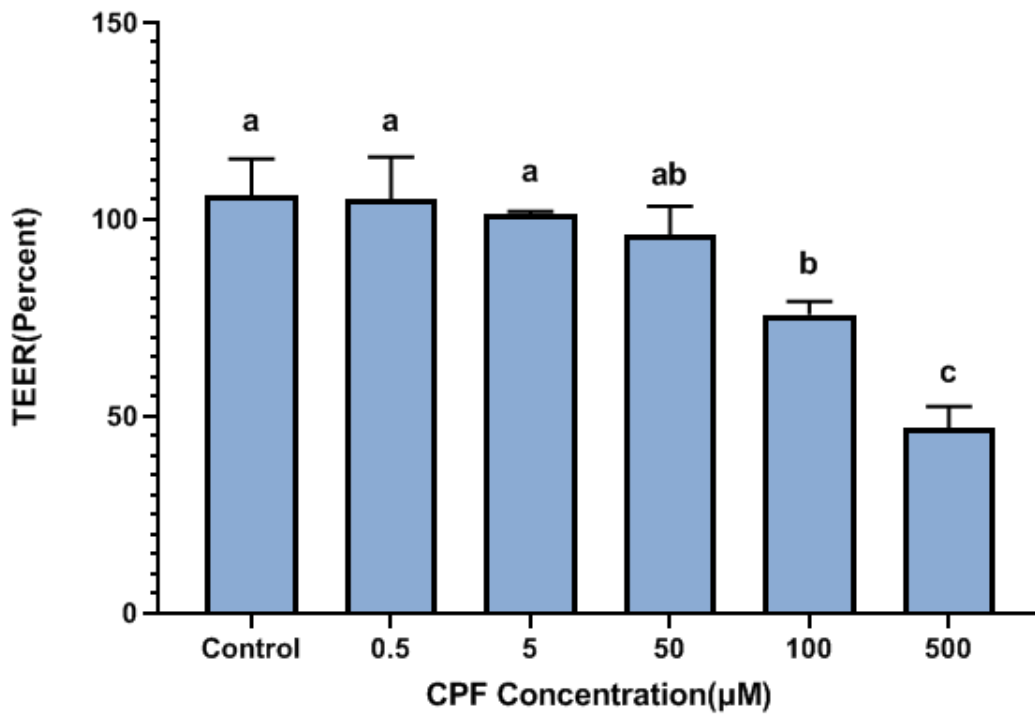


Figure 10.25: Transepithelial electrical resistance (TEER) values in RTgutGC cells after treatment with different concentrations of chlorpyrifos (CPF) for 48 hours compared with the initial value. Results are expressed as the mean \pm SD of three independent experiments. Different letters (a,b,c) indicate significant differences in TEER (One - way ANOVA, $p < 0.05$).

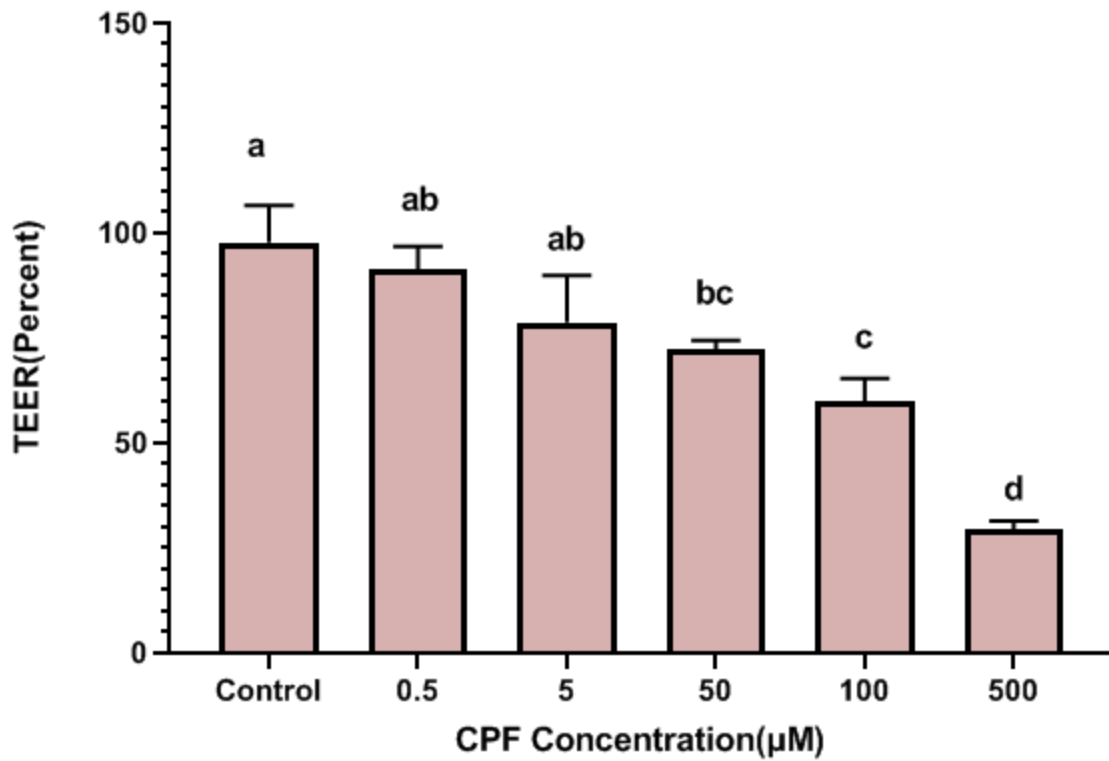


Figure 10.26 Transepithelial electrical resistance (TEER) values in RTgutGC cells after treatment with different concentrations of chlorpyrifos (CPF) for six days compared with the initial value. Results are expressed as the mean \pm SD of three independent experiments. Different letters (a,b,c) indicate significant differences in TEER (One - way ANOVA, $p < 0.05$).

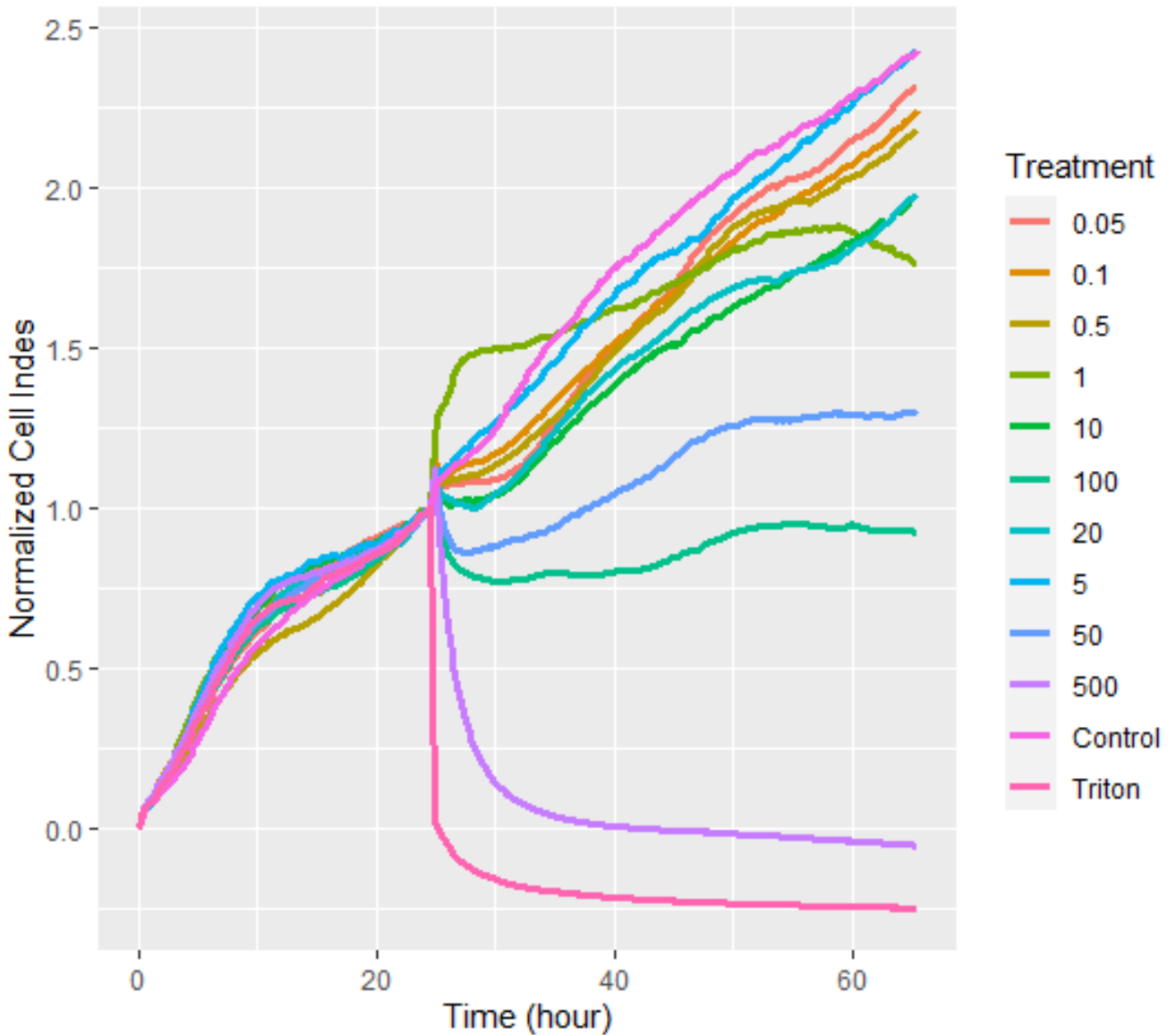


Figure 10.27 Analysis of xCELLigence cell adhesion. xCELLigence data shows cell adhesion as mean cell index against time. Here, time point 0 denotes the point at which the E-plate 96 was first scanned after cell addition. CPF was added 24 hours after seeding cells and the cell index was normalized prior to CPF addition.

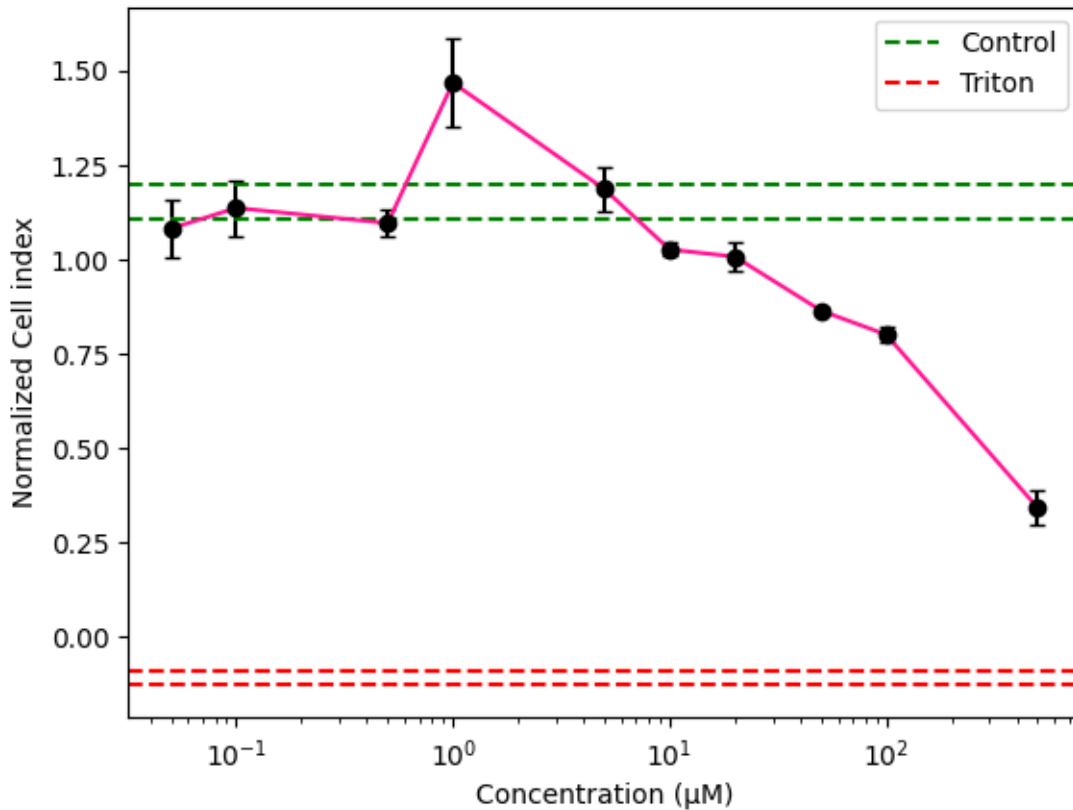


Figure 10.28 Response curve of the cell index of RTgutGC cells upon CPF exposure. Cells were seeded at a density of 20,000 cells/well in a 96-well E-plate allowing the cells to adhere and proliferate for 24 hours. Cells were then exposed to CPF in the dose range of 0.05 – 500 µM for 3 h using an xCELLigence system. xCELLigence data shows cell adhesion as mean cell index ± SD of three replicates., Green lines = ± SD interval of the Control, Red lines = ± SD interval of the Triton 20%,

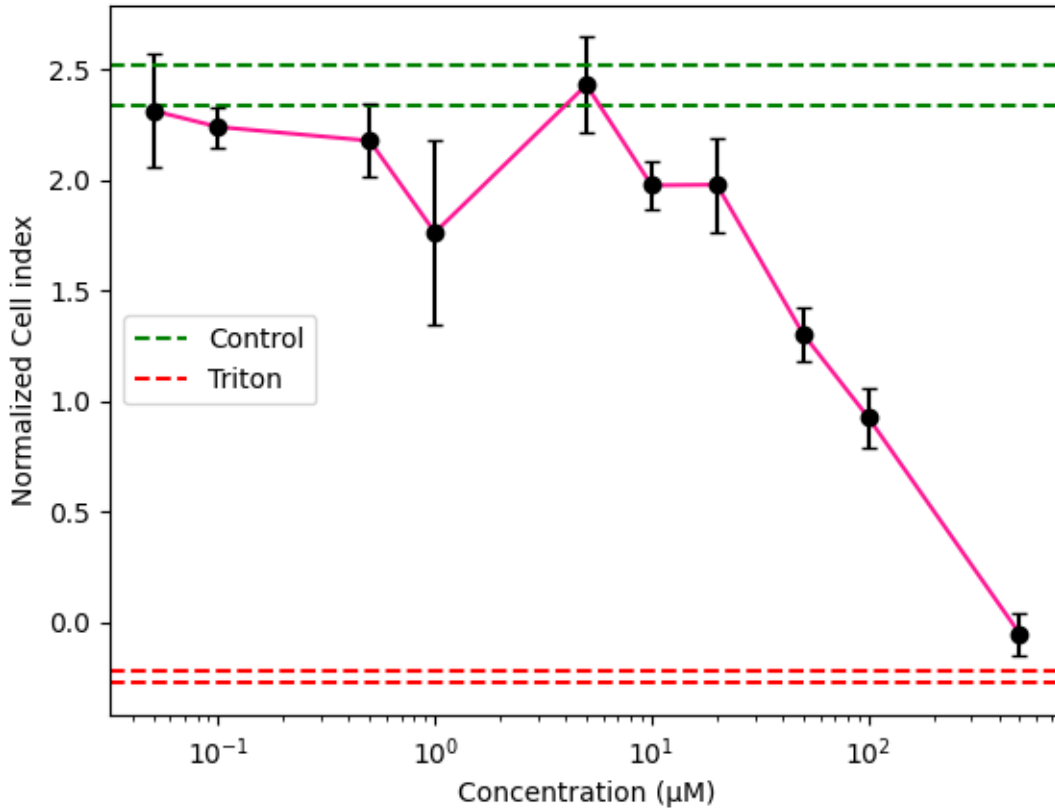


Figure 10.29 Response curve of the cell index of RTgutGC cells upon CPF exposure. Cells were seeded at a density of 20,000 cells/well in a 96-well E-plate allowing the cells to adhere and proliferate for 24 hours. Cells were then exposed to CPF in the dose range of 0.05 – 500 µM for 41 h using an xCELLigence system. xCELLigence data shows cell adhesion as mean cell index ± SD of three replicates., Green lines = ± SD interval of the Control, Red lines = ± SD interval of the Triton 20%,